Max-Planck Institut für Biochemie

Abteilung Zelluläre Biochemie

Characterisation of Tpr2, a Novel Regulator of the Hsp70/Hsp90 Multichaperone Complex

Alexander Brychzy

Vollständiger Abdruck der von der Fakultät für Chemie der Technischen Universität München zur Erlangung des akademischen Grades eines Doktors der Naturwissenschaften (Dr. rer. nat.) genehmigten Dissertation.

Vorsitzender: Univ.-Prof. Dr. Johannes Buchner

Prüfer der Dissertation:

                  1. apl. Prof. Dr. Wolfgang Baumeister

                  2. Hon.-Prof. Dr. Franz-Ulrich Hartl,
                     Ludwig-Maximilians-Universität München

                  3. Univ.-Prof. Dr. Sevil Weinkauf

Die Dissertation wurde am 27.01.2004 bei der Technischen Universität München eingereicht und durch die Fakultät für Chemie am 23.03.2004 angenommen.

Und jedem Anfang wohnt ein Zauber inne,
Der uns beschützt und der uns hilft, zu leben.

Herrmann Hesse
Das Glasperlenspiel

1 Introduction

1.1 *Protein folding and the chaperone concept*

Proteins form the central framework of all biological processes. Enzymes catalyse substrate conversions in metabolic pathways, other proteins participate in transport and sorting events, maintenance of cellular structures and can even trigger cell death. To perform their tasks, proteins have to interact with one another, as well as with target substrates. This is accomplished through contact sites determined in the protein's three-dimensional structure. In theory the newly synthesised linear polypeptide chains could adopt a variety of completely divergent final conformations but the native three-dimensional structure of the protein is usually very well defined and is encoded in the primary amino-acid sequence. Whereas for some proteins the information contained in the primary sequence is sufficient to fold correctly, others need assisting proteins. Those helper proteins are called molecular chaperones. In addition to preventing misfolding and aggregation by promoting accurate protein folding, chaperones also play a role in the functional regulation of signalling proteins and in the regulation of protein degradation. It is the goal of the research on molecular chaperones to unravel the mechanisms behind these processes.

1.1.1 Protein folding *in vitro*

The Levinthal paradox describes the problem that the acquisition of a protein's native fold by means of a random search through all possible conformations results in a timescale that is inappropriate for biological processes (Zwanzig et al. 1992). For an arbitrary protein of 100 amino acids, a theoretical folding time of 10^{11} years is needed to test all possible conformations, if the folding occurs unbiased by energetic considerations. This calculation assumes that changes in the main-chain conformation occur at the physical rate limit of 10^{11} conversions per second (Dinner et al. 2000). In contrast to these mathematical calculations, protein folding *in vivo* usually occurs within seconds (Sali et al. 1994). In the 1960s Anfinsen and co-workers already reported an experimental proof for this finding. They demonstrated the refolding of heat-denatured Ribonuclease A from *Staphylococcus* in *in vitro* experiments (Taniuchi and Anfinsen 1969). This reaction occurred spontaneously and did not require

additional factors (Anfinsen 1972; Anfinsen 1973). Moreover, the refolding happened within seconds (Schechter et al. 1970). Together this demonstrated that the native three-dimensional structure of a protein is determined by its amino-acid sequence and in many cases this is sufficient for the protein to fold correctly, at least under conditions *in vitro*.

Mathematical calculations for a simplified lattice model led to a thermodynamic description of the folding process (Onuchic et al. 1997; Pande and Rokhsar 1999). The folding of a protein can be described by an energy landscape, where the native state has the lowest free energy (Dobson and Karplus 1999). This model resembles a funnel-like structure with multiple downhill pathways and the native protein-structure at the bottom of the funnel (Schultz 2000). A number of local energy minima may be present along the vectorial folding pathways. They correspond to transient folding intermediates and kinetically trapped/misfolded configurations (Pande et al. 1998). For proteins with a more complex structure the model predicts two fast folding steps. The first one is the collapse from a random-coil to a molten globule state. This is followed by a slow search for a transition conformation and a second fast folding step to the native state (Dinner et al. 2000). The availability of only a limited number of thermodynamically favoured intermediate conformers is sufficient to lower the timescale for spontaneous protein-folding to the range of seconds and thereby solving the Levinthal paradox.

1.1.2 Protein folding *in vivo*

Compared to the test tube, the *in vivo* conditions differ significantly. A concentration of up to 300 g/l protein in the cytoplasm has been reported (Cayley et al. 1991; Zimmerman and Trach 1991). The biophysical consequences of such a dense environment are altered binding kinetics, as well as increased association constants (Minton 1983; Zimmerman and Minton 1993). Besides this effect, which is known as molecular crowding, other variables like temperature, pH value or ionic strength can diverge from the optimal conditions for spontaneous folding *in vivo*. While *in vitro* experiments mainly focus on the "posttranslational" refolding of a complete polypeptide chain, the *in vivo* situation also includes cotranslational folding and membrane transport events (Neupert 1997; Netzer and Hartl 1998). During the translation process the rate of folding (within seconds) is much faster than the rate of translation (4-20 amino-acids per second). This increases the possibility of

non-productive inter- and intra-molecular interactions due to exposed hydrophobic amino acid residues, which are otherwise buried in the native fold (Dobson et al. 1998). Translating polypeptide chains represent aggregation-prone folding intermediates. Similar aggregation-sensitive intermediates occur during the membrane passage of proteins through translocation machines. In summary, the *in vivo* conditions favour off-pathway reactions, which result in irreversible aggregation.

To overcome this situation, cells utilize molecular chaperones. Chaperone proteins represent several different structural families but share some common features (Ellis and Hartl 1999). Chaperones do not change the native conformation of a protein, nor are they part of the native structure. Unlike enzymes (for example isomerases) they typically do not change the folding rates of substrate proteins. Their main mode of action is to transiently shield aggregation-prone surfaces from improper interactions, until the protein is capable of reaching its native fold (Agashe and Hartl 2000). This is typically achieved by multiple rounds of binding and release of substrate polypeptide in an ATP-regulated manner. Thus, chaperones provide an environment in which the folding equilibrium is shifted away from unintended off-pathway reactions towards productive folding (Feldman and Frydman 2000).

Folding efficiency becomes even more important when the organism is exposed to severe stress conditions such as extreme temperature or pH shifts. Here, the native conformation of already folded proteins is destabilized and they begin to display aggregation-prone hydrophobic stretches. To deal with the increased number of substrates, the expression of some chaperones is upregulated (Lindquist 1986; Morimoto 1998). On the basis of this finding, which was described after temperature stress, the term Hsp (heat-shock protein) was coined, which is still largely a synonym for chaperones. Hsps sequester these partially unfolded proteins, protect them from aggregation and stabilize them until the conditions permit proper refolding. While the function of chaperones generally help the cell to prevent the accumulation of protein aggregates, some disease related proteins, like the Prion protein or Huntingtin, can escape these quality control mechanism. Their misfolding and aggregation are then thought to cause a number of neurodegenerative disorders (Wickner et al. 2000; Soti and Csermely 2002).

1.1.3 Regulated folding networks

The preceding paragraphs have already indicated that chaperones take on a diverse set of functions in the cell. To handle these, different families of chaperones have evolved, acting at different stages of protein folding. Despite their functional and structural differences, they form a cooperative, complementary network that guides substrates from the ribosome to their native conformations (Beissinger and Buchner 1998; Frydman 2001). This already suggests a high degree of regulation, which is achieved by a great variety of chaperone-associated cofactors and co-chaperones. Those proteins can fine-tune the repetitive binding and release cycles of the chaperones, as well as the transition of client proteins between different chaperone families. Although the occurrence of Hsps and their cofactors differ amongst the three kingdoms of life (see Table 1 for summary) similar folding pathways exist in both bacteria and eukaryotes (Hartl and Hayer-Hartl 2002). Since on average eukaryotic proteins are larger and have a higher content of independent folding-domains, one can observe a higher degree of cotranslational folding compared to bacteria (Netzer and Hartl 1997). At present the available information about chaperones is still growing and not all functions or substrates are known yet. Figure 1 gives a schematic overview of the folding pathways, which will be introduced in the next paragraphs.
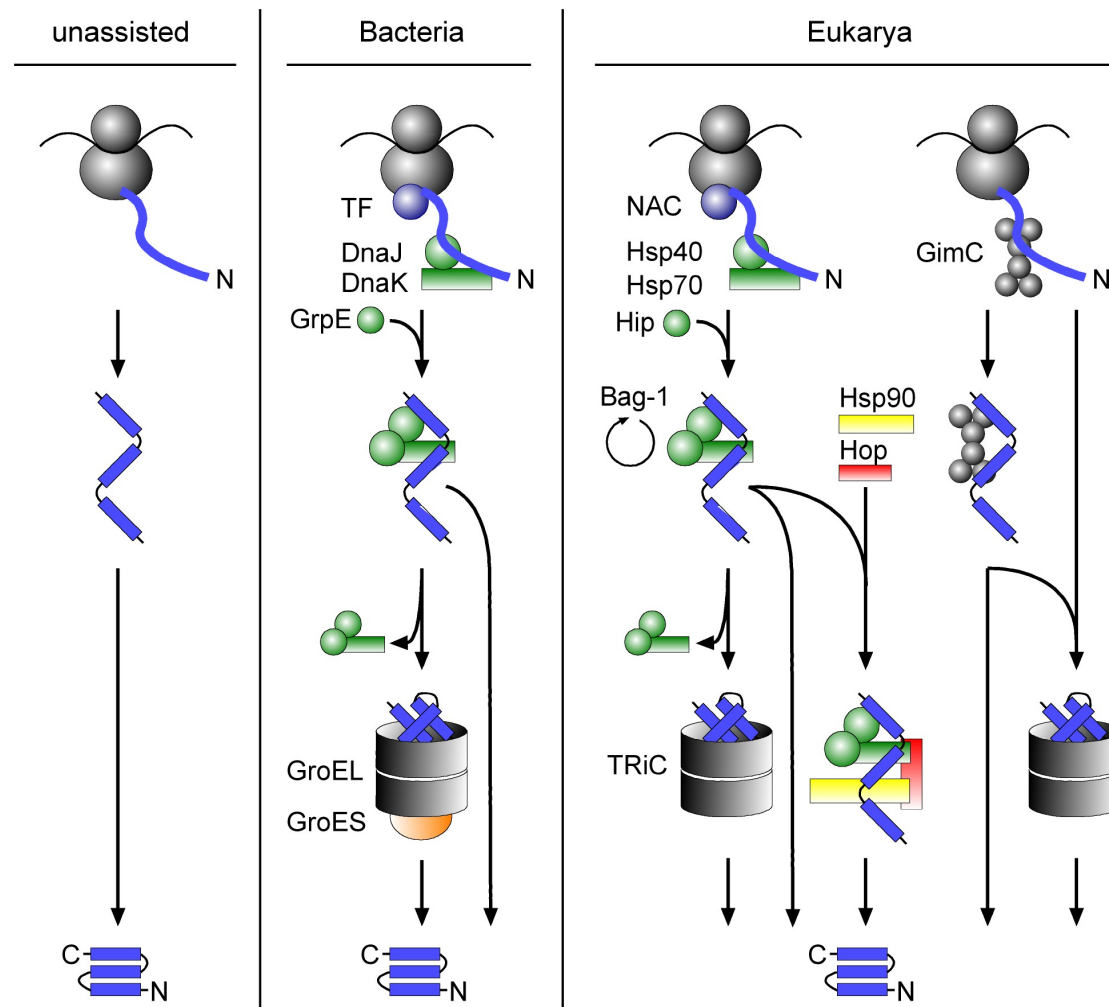
Figure 1   **Protein folding pathways**

Comparative overview of possible folding pathways. **Bacteria**: TF: trigger factor. **Eukarya**: BAG-1: Bcl-2 binding athanogene, NAC: nascent chain associated complex, GimC: genes involved in microtubule biogenesis or Prefoldin, TRiC: TCP-1 containing ring complex or CCT.

Generally the first interaction between a client protein and chaperones happens at the stage when the nascent polypeptide chain first emerges from the ribosome exit tunnel. Trigger factor (in *E. coli*) is directly bound to the L23 ribosomal protein subunit, which forms part of the exit pore and is the first contact partner in the chaperone network (Bukau et al. 2000; Kramer et al. 2002). In yeast and higher eukaryotes this function maybe conducted by the Nascent Chain Associated Complex (NAC, (Pfund et al. 1998; Reimann et al. 1999).

The next interaction partners are chaperones from the Hsp70 family, like the bacterial DnaK (Teter et al. 1999). They recognize exposed hydrophobic stretches and shield these from unproductive interactions by iterative cycles of binding and release (Blond-Elguindi et

al. 1993; Rudiger et al. 1997). For some, mostly smaller proteins, this assistance is sufficient to reach their native fold (Netzer and Hartl 1998). For others, the possible folding pathways branch from here. Some proteins are stabilized in this state and translocated across membranes. Others are handed over to the second major chaperone class, the chaperonins (GroEL in *E. coli*) (Hartl 1996; Bukau et al. 2000).

In contrast to the monomeric Hsp70, chaperonins are homo- or hetero-oligomers. Chaperonins (Hsp60 in mitochondria, TriC in the eukaryotic cytosol, Thermosome in archaea) are characterised by a barrel shaped protein structure, which contains a central cavity (Xu et al. 1997; Ditzel et al. 1998). For some of them, the interaction with a cofactor (GroES in *E. coli*, Hsp10 in mitochondria) is required for proper function (Mayhew and Hartl 1996). Under normal conditions about 10-15% of all cellular proteins take this folding route, at least in bacteria. They are characterised by a statistically significant high amount of $\alpha\beta$-folds (Houry et al. 1999). The chaperonins recognise the substrates as collapsed protein structures, known as molten globules, and bind them inside their hydrophilic cavities (Martin et al. 1991; Hayer-Hartl et al. 1994; Robinson et al. 1994). The binding of the cofactor leads to a complete encapsulation of the client protein in a sequestered environment. This process is accompanied by a substantial enlargement of the cavity and the inwards release of the substrate. The protein can now fold, isolated from effects of the crowded cytosol (Martin et al. 1993; Mayhew et al. 1996; Leroux and Hartl 2000).

Other proteins proceed from Hsp70 to Hsp90 (HtpG in *E. coli*, Grp94 in the endoplasmic reticulum and TRAP75 in mitochondria) (Smith et al. 1992). The best studied of these homologs, Hsp90 in the eukaryotic cytosol, is characterized by a relatively narrow substrate range. Most known clients belong to the group of signal-transduction or cell-cycle regulating proteins (Pratt 1998; Picard 2002). Hsp90 acts at a late stage in the folding pathway and recognizes mostly native like structures (Jakob et al. 1995). The handing-over of substrates from Hsp70 involves a transition through intermediate complexes, characterised by a changing subset of cofactors (Smith 1993; Hutchison et al. 1994; Hutchison et al. 1994; Johnson and Craig 1997). While bound to Hsp90, substrate proteins obtain their native fold and are released in an ATP dependent manner. It is characteristic for some Hsp90 substrates that their mature conformation is only temporarily stable and they need to re-enter the folding-cycle by binding to Hsp70 (Hutchison et al. 1994).

The complete chaperone network contributes to various cellular processes, including antigen presentation, quality control mechanisms, membrane transport and the disassembly of aggregates. These topics will be described in more detail in the following paragraphs. Table 1 presents an overview of molecular chaperone families.

Table 1   Summary of chaperone classes and cofactors

family	organism	location	name	cofactor	reference
small Hsps	bacteria	cytoplasm	lbpA, lbpB	none	(Clark and Muchowski 2000)
	eukarya	cytoplasm	Hsp12-Hsp42, α-crystallin		(Haslbeck et al. 1999; Vijayalakshmi et al. 2001)
Hsp100	bacteria	cytoplasm	Clps (A, B, C, P, X)	other Clps	(Wawrzynow et al. 1996; Glover and Tkach 2001)
	yeast	mitochondrial cytoplasm	Clp homologs, Hsp104		(Glover and Lindquist 1998)
	plants	chloroplast	Clp homologs		(Sokolenko et al. 1998; Adam and Clarke 2002)
Hsp70	bacteria	cytoplasm	DnaK	DnaJ, GrpE	(Zhu et al. 1996; Rudiger et al. 2001)
			Hsc62/HscC	Hsc56, GrpE	(Yoshimune et al. 2002)
			Hsc66/HscA	Hsc20	(Agashe and Hartl 2000; Cupp-Vickery and Vickery 2000)
	yeast	cytoplasm	SSA1-4, SSB1 and SSB2, Sse1/Hsp110	YDJ1, SIS1	(Morano et al. 1998; Pfund et al. 1998)
		mitochondria	SSC1	MDJ1, TIM44, mGrpE	(Neupert 1997)
		endoplasmatic reticulum	BiP/Kar2	SCJ1, Sec63	(Morano et al. 1998)
	higher eukaryotes	cytoplasm	Hsp73/Hsc70 (constitutive), Hsp72/Hsp70 (inducible)	Hsp40, Hdj2, BAG-1, Hop, CHIP, Hip, Tpr2	(Minami et al. 1996; Hohfeld 1998)
		mitochondria	mHsp70	TIM44	(Neupert 1997)
		endoplasmatic reticulum	BiP	Sec63	(Haas and Wabl 1983; Blond-Elguindi et al. 1993)
Chaperonin Typ I	bacteria	cytoplasm	GroEL	GroES	(Martin et al. 1993; Xu et al. 1997)
	bacteria, plants	mitochondria	Hsp60	Hsp10	(Cloney et al. 1992)
Chaperonin Typ II	eukaryotes	cytoplasm	TRiC	GimC/Prefoldin	(Ditzel et al. 1998; Leroux and Hartl 2000)

family	organism	location	name	cofactor	reference
Hsp90	bacteria	cytoplasm	HtpG		(Schulz et al. 1997)
	yeast	cytoplasm	Hsp82	Hop/p60/Sti1, p23, immunophilins, PP5, CDC37, CHIP, TOM34, Tpr2, BAG-1	(Chang and Lindquist 1994; Liu et al. 1999)
	higher eukaryotes	cytoplasm	Hsp90α, Hsp90β	see above	(Pearl and Prodromou 2000)
		mitochondria	Hsp75/TRAP1		(Felts et al. 2000)
		endoplasmatic reticulum	Grp96/Gp94		(Meunier et al. 2002)

1.2 Chaperone families

In this chapter the chaperone families are introduced in more detail. An overview of known structure/domain information, the mechanistic aspects of chaperone function, regulatory cofactors and substrate specificity will be presented. The focus will be on ATP driven chaperones, which go through cycles of ATP binding and hydrolysis to make regulated contacts with their substrates. Although some chaperones are not ATPases, they share the ability to prevent proteins from aggregation. In addition many chaperones are inducible under stress. Cells often contain several isoforms of a chaperone, which are either constitutively expressed or are regulated by a stress inducible promoter.

1.2.1 Small heat shock proteins

Small heat shock proteins (sHsps) are a ubiquitous and diverse class of ATP independent chaperones. They have a molecular mass between 15 and 42 kDa but tend to form dynamic, oligomeric complexes, which vary from 150 kDa up to 800 kDa. It has been suggested that these structures reorganize into smaller, active complexes when the organism is exposed to stress conditions (Haslbeck et al. 1999). Several non-native substrates are then bound by one sHsp-complex at the same time. A productive refolding of the proteins is only achieved in cooperation with other chaperones. The best known member of the sHsp class is alpha-crystalline. It is a major component of the eye-lens where aggregated proteins cause haziness and lead to loss of sight (Clark and Muchowski 2000).

1.2.2 Hsp100

Members of the Hsp100 chaperone class (Clp in bacteria) participate in a number of diverse cellular functions such as DNA replication, gene expression, modulation of protein aggregates or in degradation processes (Wawrzynow et al. 1996; Glover and Lindquist 1998; Zolkiewski 1999; Glover and Tkach 2001). They possess an ATPase activity and can interact with each other. ClpA and ClpX target recognition sequences in misfolded proteins and degrade them with the help of a proteolytic fragment (ClpAP, ClpXP) (Porankiewicz et al. 1999). ClpB forms a cooperative chaperone network with the Hsp70 system to solubilize protein aggregates (Mogk et al. 1999; Motohashi et al. 1999). However, because they appear to act in the unfolding, rather than in the folding of proteins, they are not chaperones in the classical sense.

1.2.3 Chaperonins

Chaperonins are multimeric barrel-shaped chaperone complexes with a unique folding strategy (Xu et al. 1997; Ditzel et al. 1998). They act at a later stage of protein folding and recognize substrates, which have already adopted a partially collapsed state, known as the molten globule form. At this stage, folding intermediates are characterized by a substantial amount of secondary structure, a relatively compact size but a significant amount of exposed hydrophobic surface areas (Martin et al. 1991; Hayer-Hartl et al. 1994; Robinson et al. 1994). The functional principle of chaperonins is to encapsulate a substrate polypeptide and thereby isolate it from the crowded cellular environment. This allows the protein to fold protected from nonproductive protein-protein interactions, which can lead to irreversible aggregation (Martin et al. 1993; Mayhew et al. 1996; Leroux and Hartl 2000). Based on an evolutionary classification, chaperonin-families can be divided into two groups.

Group 1 comprises chaperonins found in bacteria and eukaryotic organelles (Hemmingsen et al. 1988), best characterized by the cytosolic *E.coli* GroEL. Its cylindrical structure is formed by two stacked homo-oligomeric 7mer rings, which enclose two central cavities (Figure 2 D, E). The monomeric subunit is about 60 kDa and encodes 3 domains. With regard to their position in the double ring, they are termed equatorial, intermediate and apical (Figure 2 F). Substrate binding to hydrophobic patches in the apical domains occurs

only to one ring at a time (Fenton et al. 1994; Hartl 1996). This so-called cis-ring has 7 ATP molecules bound to its equatorial domains. Interaction with the GroES cofactor completes the substrate encapsulation. This homomeric 7mer protein (~ 10 kDa per subunit) binds to the apical-domains of the cis-ring and induces major conformational changes that almost double the volume of the cavity (compare Figure 2 F left: no GroES bound and right: GroES bound) (Braig et al. 1994; Roseman et al. 1996; Xu et al. 1997). As a consequence thereof, the substrate-binding patches in the apical domain are removed from substrate interactions, releasing the protein into the hydrophilic cavity (Bukau and Horwich 1998). This so called Anfinsen-cage mimics an infinite dilution and provides an aggregation-free environment for substrate refinement (Anfinsen 1973). It is still controversially discussed if the movement of the apical domains induces a forceful unfolding of the substrate, which can be used to overcome thermodynamically trapped folding intermediates (Fenton and Horwich 1997). After ATP hydrolysis (10-15 sec) and binding of ATP to the opposite (trans) ring, GroES and the substrate are released from the chaperonin (Hayer-Hartl et al. 1995; Rye et al. 1997). If the protein has not yet reached its native fold, it can rebind to GroEL and undergo additional rounds of folding. Under normal growth conditions about 10-15% of the cytoplasmatic proteins interact with GroEL (Ewalt et al. 1997), a process essential for the cell, since the deletion of GroEL is lethal (Horwich et al. 1993). Homologs of GroEL/GroES exist in mitochondria (Hsp60/Hsp10) and in chloroplasts (cpn60/cpn10).

Group 2 hetero-oligomeric chaperonins can be found in the eukaryotic cytosol (TriC, TCP-1 ring complex, also known as CCT, cytosolic chaperonin containing TCP-1, with TCP-1 standing for tailless complex polypeptide 1) and in archaea (thermosome) (Trent et al. 1991; Gao et al. 1992; Lewis et al. 1992). The *in vivo* substrates and the mechanistic aspects of their folding cycle are much less characterized compared to the distantly related group 1 chaperonins. TriC is a large, about 900 kDa, heteromeric complex consisting of two rings with 8 different subunits in each (Figure 2 A, B). It is required for the folding of actin and tubulin and interacts with the von-Hippel-Lindau tumor suppressor protein before it is assembled into an ubiquitin-ligase complex (Sternlicht et al. 1993; Feldman et al. 1999; Llorca et al. 2001). An increase in the folding rate of actin was observed in the presence of the heteromeric 6-mer protein GimC (prefoldin), suggesting that GimC acts cooperatively with TriC as a downstream cofactor in the folding process (Vainberg et al. 1998; Hansen et al. 1999; Siegers et al. 1999). Although GimC exists in some archaeal species it has not been shown to function with the archaeal thermosome. Though the ATP-driven folding cycle of

TriC appears to be similar to that in GroEL, the encapsulation of substrate is solely achieved by rearrangements of α-helical extensions in the apical domains (Figure 2 C) (Klumpp et al. 1997; Ditzel et al. 1998; Llorca et al. 2001). Group 2 chaperonins can bind substrates cotranslationally (Frydman et al. 1994), but it is not clear if such nascent polypeptides can be encapsulated.
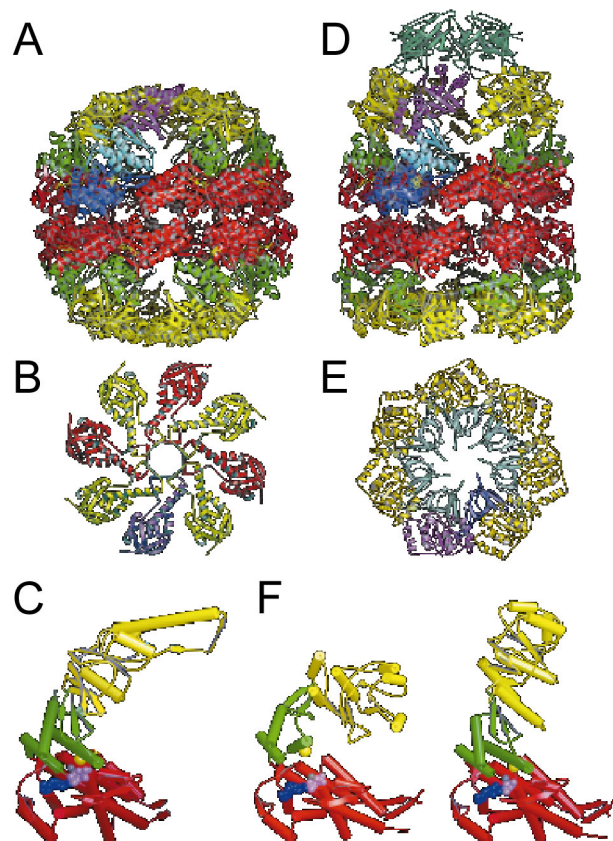
Figure 2   Chaperonin crystal structures

A: side view of the thermosome (Ditzel et al. 1998). **B**: thermosome top view, α-subunits (red/violet) and β-subunits (yellow). **C**: single thermosome subunit, red equatorial-, green middle-, yellow apical-domain. **D**: side view of the asymmetric GroEL/ES/(ADP)$_7$ complex (Xu et al. 1997). **E**: GroEL/ES/(ADP)$_7$ complex top view. **F**: single GroEL domain in the absence (left) or presence (right) of GroES, red equatorial-, green middle-, yellow apical-domain.

1.2.4 Hsp70

The main Hsp70 homolog of bacteria is DnaK and the mammalian cytosol has a stress-inducible (70 kDa heat shock protein, Hsp70) and constitutively expressed form (70 kDa heat shock cognate protein, Hsc70). Because Hsc70 and Hsp70 are thought to function similarly, they will be termed Hsp70 for simplicity.

Hsp70 chaperones act during the *de novo* folding of proteins and assist the refolding of denatured substrates (Hartl and Hayer-Hartl 2002). An increasing number of publications indicate that mammalian cytosolic Hsp70 is also involved in other cellular processes like degradation, antigen-presentation or modulation of disease-related aggregation (Nicchitta 2000; Dougan et al. 2002; Sakahira et al. 2002). To adapt to these different functions, a set of cofactors and co-chaperones interacts with Hsp70, modulating its ATPase activity or connecting it with other cellular structures.

1.2.4.1   Hsp70 function

Hsp70 can bind cotranslationally to nascent polypeptide chains (Pfund et al. 1998). Cytosolic proteins can be folded by Hsp70 co- or post-translationally or are stabilized until they are handed over to downstream chaperones (Frydman et al. 1994). Also, substrates which need to be transported to a target organelle, are kept in a translocation-competent state by Hsp70. Until they reach the appropriate receptor pore, Hsp70 shields them from aggregation and collapse (Zimmermann 1998). After the substrate has passed through the biomembrane barrier, organelle specific Hsp70 homologs in the mitochondria and ER receive the polypeptide and help it fold or pass it on in the chaperone network (Stuart et al. 1994).

The role of Hsp70 in protein folding is also coupled to a quality control mechanism. The ubiquitin-domain containing cofactor BAG-1 (BCL2-associated athanogene) associates with the 26S proteasome and forms a physical link between Hsp70 and the degradation machinery (Luders et al. 2000). BAG-1 also interacts with CHIP (carboxyl terminus of Hsc70-interacting protein), an E3 ubiquitin-ligase for chaperone substrates (Luders et al. 2000; Wiederkehr et al. 2002). In combination, these cofactors modulate the Hsp70 activity

and may facilitate proteasomal degradation if the substrate is not foldable (Demand et al. 2001).

Another aspect of the protein folding function of Hsp70 is its ability to modulate the aggregation of proteins. This has been established for models of Huntington's disease (Krobitsch and Lindquist 2000; Muchowski et al. 2000). This syndrome is characterized by the appearance of protein aggregate deposits in neurons. They can only form when the N-terminal poly-glutamine (polyQ) tract of the huntingtin (htt) protein exceeds a certain length and the protein is partially degraded. *In vitro*, these aggregates have an amyloid-like fibrillar structure and are characterized by their resistance to detergents. When the Hsp70 chaperone system is active during the period of aggregate formation, the shape and the solubility change towards amorphous, detergent-soluble aggregates (Muchowski et al. 2000).

1.2.4.2   Hsp70 mechanism

The atomic-structure of Hsp70 has been partially solved and revealed two separate domains. Amino acids 1 to 385 of human Hsc70 form the N-terminal ATPase domain, which is highly conserved from bacteria to mammals. It possesses an overall fold similar to actin and a central nucleotide-binding cleft (Figure 3, A) (Flaherty et al. 1991). The C-terminal peptide-binding domain (aa 393-607 of human Hsc70) is less conserved but shows two distinct structural features. A β-sandwich structure provides a binding cleft for an extended hydrophobic peptide and an α-helical sub-domain forms a lid structure, which can close over the cleft (Figure 3, B) (Zhu et al. 1996; Mayer et al. 2000; Rudiger et al. 2000). Biochemical data show that the N- and C-terminal domain work in a cooperative manner. It would therefore be of particular interest to obtain the structure of full-length Hsp70.

A

B
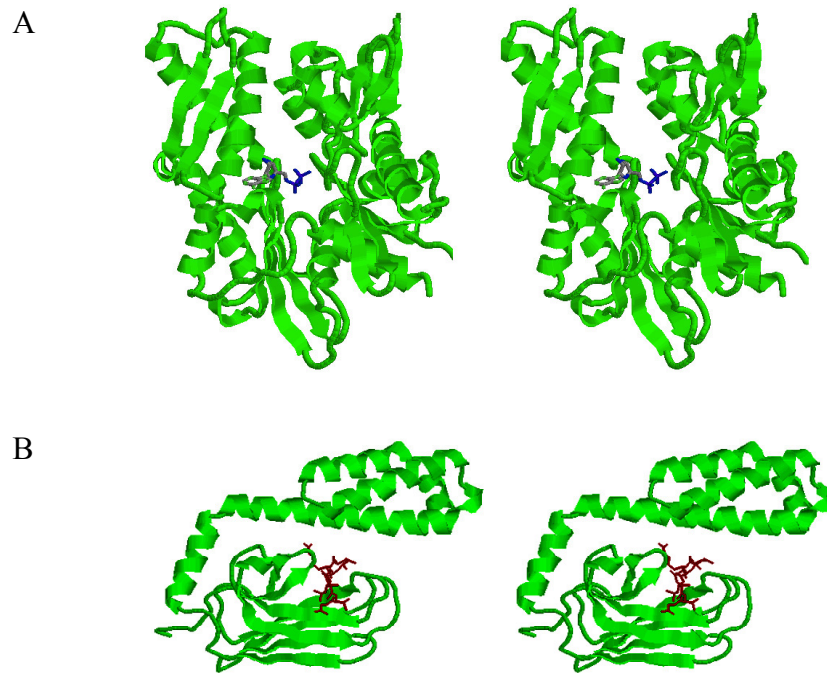
Figure 3   Stereo view of Hsp70 domains

(A) Stereo view of the N-terminal Hsp70 ATPase domain with ADP bound (PDB code 1HJO). (B) Stereo view of the C-terminal Hsp70 peptide-binding domain with a seven amino acid peptide (PDB code 1DKX).

The functional principle of Hsp70, as understood at the moment, is a repetitive binding and release to exposed hydrophobic stretches in substrate proteins. The folding state of the substrate can range from completely unstructured, like in the case of nascent polypeptide chains to partially native structures in the case of hormone receptors. Most of the experimental data come from the bacterial homolog DnaK, but also apply to the mammalian system. The binding cycles are coordinated by regulated ATP hydrolysis (Buchberger et al. 1994; Ha and McKay 1994; Theyssen et al. 1996). This in turn is organized by a set of cofactors (Szabo et al. 1994). In its ATP-bound form the peptide-binding cleft is open and Hsp70 has fast on and off rates for substrate. ATP hydrolysis triggers the closure of the cleft and decreases the dissociation rate, thus stabilizing the Hsp70-substrate interaction in the ADP bound state. The nucleotide turnover is the rate-limiting step in this process (Gao et al. 1993; Schmid et al. 1994; McCarty et al. 1995). The low, basal ATPase activity of Hsp70 is stimulated by substrate peptides and regulated by a set of cofactors (Flynn et al. 1989; Liberek et al. 1991).

1.2.4.3 Hsp70 cofactors

The co-chaperone Hsp40 (DnaJ in bacteria) stimulates the ATP hydrolysis step in the Hsp70 binding cycle (for an overview of the Hsp70 cycle, see Figure 4). The required structural feature for this action is the J-domain. It can be found in a number of otherwise divergent proteins, all sharing the ability to stimulate the ATPase rate of Hsp70. The J-domain is about 80 amino acids long and comprises a three-helix bundle. The loop between helix two and three contains the functionally essential HPD motif. A single point mutation in this sequence abolishes the stimulatory effect of the J-domain (Wall et al. 1994; Karzai and McMacken 1996; Pellecchia et al. 1996). Although some J-domain containing proteins contact Hsp70 in the C-terminal region, the stimulatory effect is conducted by interaction of the J-domain with the ATPase domain. Bacterial Hsp40 (DnaJ) possesses an ATP independent intrinsic chaperone activity and binds directly to substrates, therefore preventing their aggregation. The intrinsic chaperone activity of mammalian Hsp40 is significantly weaker (Minami et al. 1996; Szabo et al. 1996; Nagata et al. 1998).
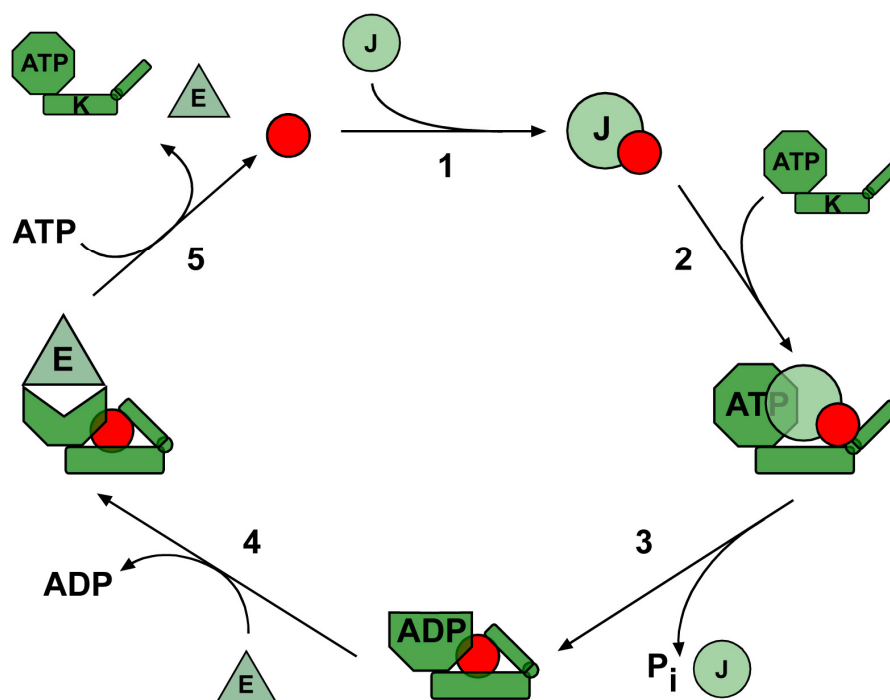

Figure 4   Model of the DnaK chaperone cycle

1: fast, transient association of DnaJ (J) with substrate (red circle). **2**: substrate transfer to DnaK (K), low affinity binding with fast exchange rates. **3**: DnaJ stimulated ATP hydrolysis and stable substrate binding. **4**: GrpE (E) association releases nucleotide. **5**: ATP binding to DnaK and complex disassembly

It was shown in *in vitro* experiments that the combination of bacterial DnaK/J is sufficient to bind denatured model substrates. Polypeptide folding can be further stimulated in the additional presence of bacterial GrpE, which facilitates the exchange from ADP to ATP and thereby enhances the overall ATPase/refolding activity of DnaK (Figure 4) (Liberek et al. 1991; Langer et al. 1992; Schroder et al. 1993). Mammalian BAG-1 is a functional but not structural homolog of GrpE (Hohfeld and Jentsch 1997; Bimston et al. 1998). A number of BAG homologs generally interact via their C-terminal α-helical BAG-domain (about 110 aa) with the Hsp70 ATPase domain (Sondermann et al. 2001). BAG-1 exists in different isoforms, distinguished by the length of their N-terminus. Most of them stimulate the ADP-ATP exchange on Hsp70 (Hohfeld and Jentsch 1997; Yang et al. 1998). Many BAG proteins contain an additional ubiquitin-like domain and are substrates for the CHIP ubiquitin ligase.

CHIP, together with Hop and a number of other cofactors, is characterized by a TPR (tetratricopeptide repeat) protein-protein interaction-motif. A TPR domain is composed of at least 3 TPR motifs, which are highly degenerated 34 amino-acid repeats. Each single TPR motif forms a helix-turn-helix structure, which packs with adjacent TPRs into a regular series of anti-parallel helixes (Figure 5 A). The three dimensional fold is characterized by a groove that provides a binding cleft for the recognition of a linear polypeptide (Figure 5 B). The identification of the binding partner depends on the variable size and hydrophobicity of amino acids at defined positions in the TPR domain (Sikorski et al. 1990). A subgroup of TPR-domains, which interacts specifically with the C-termini of Hsp70 and/or Hsp90 (both ending in EEVD), forms a two-carboxylate clamp anchor (a so-called TPR-clamp). This contact requires five conserved amino acids in the TPR-domain, which contribute to interactions both with the carboxyl group of the protein main-chain and with the carboxyl group of the last aspartate. Based on biochemical observations, the TPR-clamps fall into two groups. The first clearly distinguishes between Hsp70 and Hsp90 and the second binds to both chaperone families. The selectivity is obtained from interactions with a larger and divergent portion of the chaperone C-termini, as shown in the crystal structure of the Hop TPR-domains. In accordance with these finding, the deletion of the EEVD motif from the chaperones abolishes the interaction with TPR-clamp cofactors in general (Scheufler et al. 2000; Brinker et al. 2002).
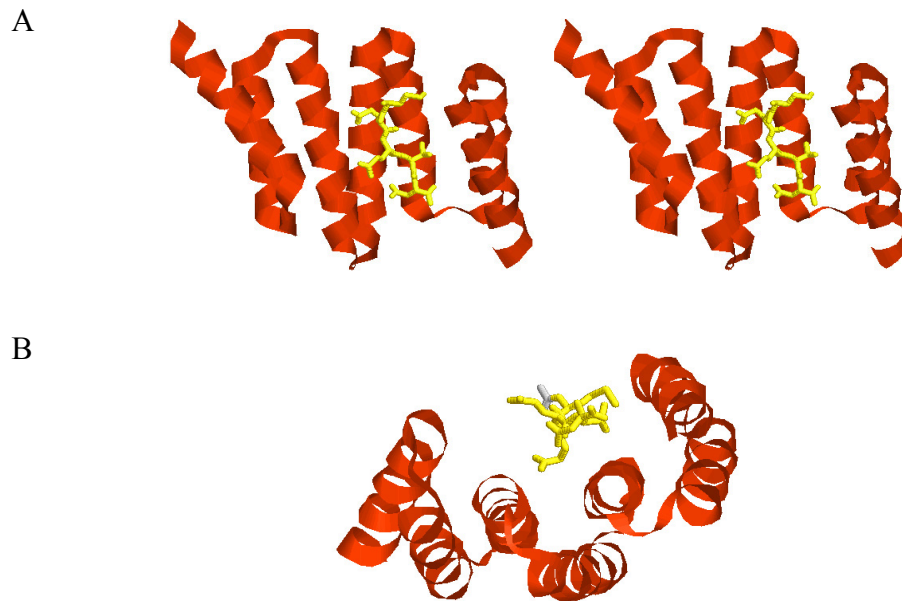
Figure 5 **Crystal structure of the Hop-TPR2A complex.**

A: stereo picture of TPR2A side view with Hsp90 peptide MEEVD (PDB code1ELR). **B**: top view of TPR2A with MEEVD-peptide.

CHIP (carboxyl terminus of Hsc70-interacting protein) is a TPR-clamp cofactor of Hsp70 that binds to the C-terminus of Hsp70 - and also to Hsp90 - and slows down the Hsp70 ATPase cycle at the stage of the ATP-complex, thus favoring fast substrate on- and off-rates (Ballinger et al. 1999). It attaches atypical poly-ubiquitin chains (moieties linked through lysine 11) to BAG-1, which stimulates the association of the chaperone complex with the proteasome. This assembly is dependent on the integral ubiquitin domain of BAG-1 (Luders et al. 2000; Alberti et al. 2002). It was suggested that the physical link of Hsp70 to the proteasome is an important contribution to protein quality control and facilitates the degradation of unfoldable substrates (Wiederkehr et al. 2002).

The binding of Hip (Hsc70 interacting protein) to the Hsp70 ATPase domain competes with BAG-1 binding. Hip stabilizes the ADP-bound form of Hsp70 and thereby prolongs the time of tight substrate binding. Although the TPR-domain in Hip is essential for the interaction with the chaperone, this region does not resemble a TPR-clamp domain and hence does not interact with the Hsp70 C-terminus (Hohfeld et al. 1995; Frydman and Hohfeld 1997).

Hop (heat shock protein organizing protein) functions as a scaffold protein on which both Hsp70- and Hsp90-class chaperones can associate via two selective TPR-clamp sites. It has been suggested that this configuration allows the passage of substrate from Hsp70 to Hsp90 (Chen and Smith 1998; Johnson et al. 1998; Morishima et al. 2000). Together all of these cofactors cooperate in fine-tuning the Hsp70 activity *in vivo*.

1.2.5 Hsp90

1.2.5.1   Hsp90 function

Hsp90 represents one of the most abundant proteins in the cytoplasm, comprising about 1-2% of all cellular proteins, even under permissive conditions (Welch and Feramisco 1982). It acts at a late stage of protein folding and is essential in eukaryotes under all conditions (Parsell and Lindquist 1993; Jakob et al. 1995; Louvion et al. 1996; Nathan et al. 1997). Contrary to that, the bacterial homolog (HtpG) is dispensable during normal growth but improves the stress tolerance in Cyanobacteria and *Bacillus subtilis* (Bardwell and Craig 1988; Tanaka and Nakamoto 1999; Versteeg et al. 1999). Grp94/gp96, the mammalian paralog of the endoplasmatic reticulum, was reported to be involved in the presentation of antigens (Little et al. 1994; Argon and Simen 1999; Nicchitta 2000). So far little is known about TRAP1 (Hsp75), an Hsp90 species which resides in the mitochondrial matrix of higher eukaryotes (Felts et al. 2000). Most of the functional and structural information on Hsp90 was gained from the mammalian protein (α and β isoform) or its yeast homologs (Hsp82, Hsc82), all referred to as Hsp90 for simplicity (Borkovich et al. 1989; Gupta and Golding 1996). Under permissive conditions Hsp90 is characterized by a narrow, but growing range of substrates. Most known Hsp90 substrates belong to classes of signal-transduction molecules (e.g. steroid hormone receptors (SHR) such as glucocorticoid receptor or growth factor receptors such as erb B2) or are involved in cell-cycle regulation (signaling kinases such as v-src, Wee-1, Cdk4 or Raf) (Xu and Lindquist 1993; Aligue et al. 1994; Stepanova et al. 1996; van der Straten et al. 1997; Picard 2002). Hsp90 substrates are thought to exhibit an native-like conformation and to be loaded via an Hsp70 dependent mechanism (Smith et al. 1992; Smith 1993; Hutchison et al. 1994). The chaperone undergoes regulated cycles of ATP binding and hydrolysis and finally releases the native protein (Prodromou et al. 1997;

Obermann et al. 1998; Panaretou et al. 1998). Under stress conditions Hsp90 loses its substrate selectivity and adopts the role of a general storage compartment for unfolded proteins. It stabilizes substrates until they can be refolded by other chaperones (Freeman and Morimoto 1996). This "holding" mechanism may be ATP independent (Buchner 1999).

1.2.5.2 Hsp90 mechanism

Limited proteolysis of Hsp90 revealed three separate domains (Figure 6 B, (Stebbins et al. 1997). Sequence analysis demonstrated that the N- and C-terminal domains are very conserved amongst Hsp90 homologs and both were reported to be involved in substrate recognition and ATP binding (Lindquist and Craig 1988; Young et al. 1997; Scheibel et al. 1998). A short stretch between the N- and middle-domain (aa 220-291 of human Hsp90α) is quite variable and even absent in HtpG and TRAP1. It acts as a flexible linker without being directly involved in substrate contacts (Song et al. 1995; Buchner 1999). The crystallographic structure of the N-terminal domain (N90, aa 1-236 of human Hsp90) has been solved (Prodromou et al. 1997; Stebbins et al. 1997). The N90 domain contains an ATP binding pocket, which does not share homology with the classical Walker motif. It rather resembles the fold found in the topoisomerase GyraseB, and in the DNA repair enzyme MutL (Bergerat et al. 1997; Dutta and Inouye 2000). The base of the structure is formed by eight antiparallel β-sheets on which nine α-helixes are packed, generating the 1.5 nm deep ATP binding pocket (Figure 6 A). In contrast to the extended conformation of ATP bound to Hsp70, the Hsp90 binding pocket forces the nucleotide to adopt a crooked shape (Prodromou et al. 1997; Stebbins et al. 1997). This characteristic structure is mimicked by the benzoquinone ansamycin antibiotics Geldanamycin (GA) or Radicicol (RA) (Whitesell et al. 1994), which compete for ATP binding. The antibiotics block Hsp90 function and lead to release of substrates followed by degradation *in vivo*. The C-terminal domain (C90, aa 629-732) is needed for dimerisation and contains the docking site for TPR-clamp cofactors (Minami et al. 1991; Minami et al. 1994; Young et al. 1998; Scheufler et al. 2000), whereas the middle domain (M90, aa 272-617) has been suggested to confer protein-protein contacts (Fontana et al. 2002). The assembled Hsp90 dimer displays a tail-to-tail alignment with the N-termini pointing outwards. In the presence of ATP the amino-termini contact each other, allowing the chaperone dimer to form a ring-like structure (Maruya et al. 1999; Dutta and Inouye 2000). The contact of the N-termini is probably a prerequisite for ATP hydrolysis, which precedes

the transition back to the open conformation (Young and Hartl 2000). Recent data suggest that a lid structure shields the N-terminal dimerisation site. After nucleotide binding the lid flips and contacts structures in the middle domain. This stabilizes the substrate bound, ring-like conformation of Hsp90 and repositions certain residues of the M90 domain which are implicated in the ATPase activity of the N-domain (Meyer et al. 2003). In analogy to DNA gyrase it was suggested that the ATP-regulated molecular clamp mechanism of the Hsp90 dimer allows the temporary holding of substrate (Berger et al. 1996; Ban et al. 1999). How this contributes to folding remains to be resolved (Young et al. 2001).

A
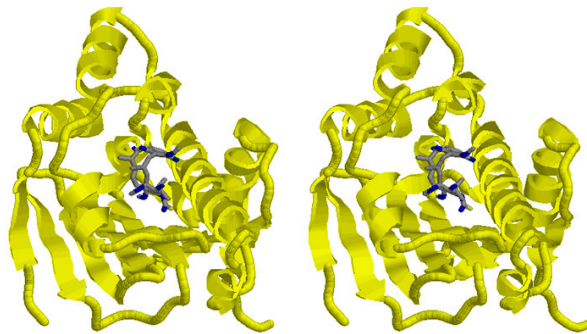
B
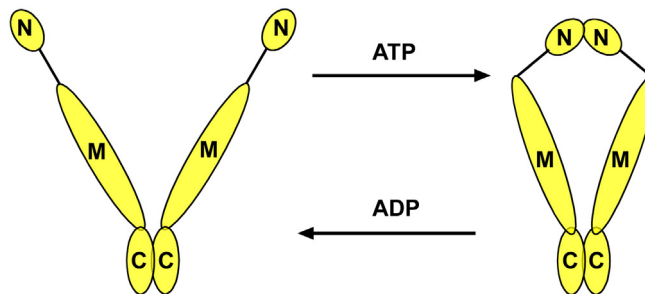
Figure 6   **Structural and mechanistically aspects of Hsp90**

A: stereo view of the Hsp90 N-terminal ATPase domain in complex with Geldanamycin (PDB code 1A4H). **B**: schematic clamp model of conformational changes of the Hsp90 dimer upon nucleotide binding.

1.2.5.3   Hsp90 cofactors

During its ATP-driven folding cycle Hsp90 interacts with a set of cofactors. Many of them possess TPR-clamp domains and compete for binding to the COOH-terminus of the chaperone. In addition to the Hsp90 interaction site the cofactors contain functional domains,

whereby optional enzymatic activities are recruited to the chaperone. The large immunophilins Cyp40, FKBP52, FKBP51 contribute a peptidyl-prolyl cis/trans isomerase activity, whereas PP5 is a serine-threonine protein phosphatase (Johnson and Toft 1994; Chen et al. 1996).

Other cofactors are localized to cellular structures and act as docking partners for the chaperones. It was shown recently that Tom70, the import receptor in the outer mitochondrial membrane, recognizes Hsp70 and Hsp90 through its TPR-clamps, thus facilitating the subsequent translocation of preproteins (Young et al. 2003). CHIP (carboxy-terminus of Hsc70 interacting protein) was also shown to bind to Hsp90 via the same TPR-clamp site and thereby links both chaperones with the ubiquitination machinery, which controls proteasomal degradation (Connell et al. 2001).

Hop (heat shock protein organizing protein, also p60, Sti1 in yeast) is almost entirely composed of TPR domains (TPR1, TPR2A, TPR2B). The first two bind chaperones whereas the third one does not. Also, the TPR-clamps in Hop distinguish between Hsp70 and Hsp90. The crystal structure shows that TPR1 coordinates the last eight residues of Hsp70 (GPTIEEVD) and TPR2A positions the last five amino acids of Hsp90 (MEEVD). The isolated domains bind to the peptides with the same affinity as to the full-length proteins, suggesting that the crystal structure adequately explains the basis of the selectivity (Scheufler et al. 2000; Brinker et al. 2002). Hop works as a scaffold protein and builds a ternary complex with Hsp70 and Hsp90 (Chen and Smith 1998; Johnson et al. 1998). This spatial coordination is a prerequisite for the substrate transfer between the chaperones. In addition Hop inhibits the ATPase activity of Hsp90 by blocking the access to the nucleotide binding-pocket. This maintains the chaperone dimer in an open conformation, ready to take up substrate (Prodromou et al. 1999). After binding of ATP the Hop/Hsp70 complex is displaced and the Hsp90-dimer clamp can tightly close around the substrate. Although this mechanism remains to be demonstrated in detail, the chronology of the complex composition was already established by co-precipitation experiments (Smith et al. 1992; Smith 1993; Hutchison et al. 1994) and will be described in more detail in chapter 1.3.

Hsp90 also interacts with cofactors lacking TPR-clamps. p23 (Sba1 in yeast) is a major component in the mature Hsp90-substrate complex. It specifically recognizes the ATP-bound state of Hsp90 and binds to the dimerised N-terminal domains (Johnson and Toft 1994;

Sullivan et al. 1997; Fang et al. 1998). p23 stimulates the ATP hydrolysis dependent release of substrate without changing the ATPase activity itself. It was suggested that the co-chaperone enhances conformational changes, which are associated with ATP hydrolysis and lead to substrate dissociation (Young and Hartl 2000). p23 can act as a molecular chaperone itself and bind to denatured polypeptides (Bose et al. 1996; Freeman et al. 1996). This could be the driving force for the recently demonstrated, p23 induced, disassembly of transcriptional regulatory complexes, which are activated by intracellular hormone receptors (Freeman et al. 2000).

Cdc37 (p50) is proposed to target Hsp90 to protein-kinase substrates and might contribute a certain chaperone activity itself (Dai et al. 1996; Stepanova et al. 1996). The proteasome activator PA28 binds to Hsp90 and stimulates the Hsp70 mediated refolding of luciferase *in vitro* (Minami et al. 2000). The ubiquitous stress-regulated cofactor Aha1 (activator of Hsp90 ATPase activity) and its shorter homolog Hch1 are reported to bind to the middle domain of Hsp90 and stimulate the low, intrinsic ATPase activity (Mayer et al. 2002; Panaretou et al. 2002; Lotz et al. 2003). It is reasonable to expect that more cofactors will be reported, which have been overlooked so far due to their substochiometric or transient appearance on Hsp90.

1.3 Multichaperone machinery

The term multichaperone machinery has been coined for the coordinated interaction of Hsp90 and Hsp70 type chaperones in concert with their cofactors and client protein (Figure 7). This cooperativity is crucial for the maturation of some Hsp90 dependent substrates, since they need to be loaded onto Hsp90 in an Hsp70 dependent step. Most of the information about the complex composition was obtained from experiments using the progesterone receptor or the glucocorticoid receptor as stringent Hsp90 substrates. Following the protein composition, as determined by immuno-precipitations, it was possible to suggest a timeline for the complex assembly (Smith et al. 1992; Smith 1993; Hutchison et al. 1994; Hutchison et al. 1994).
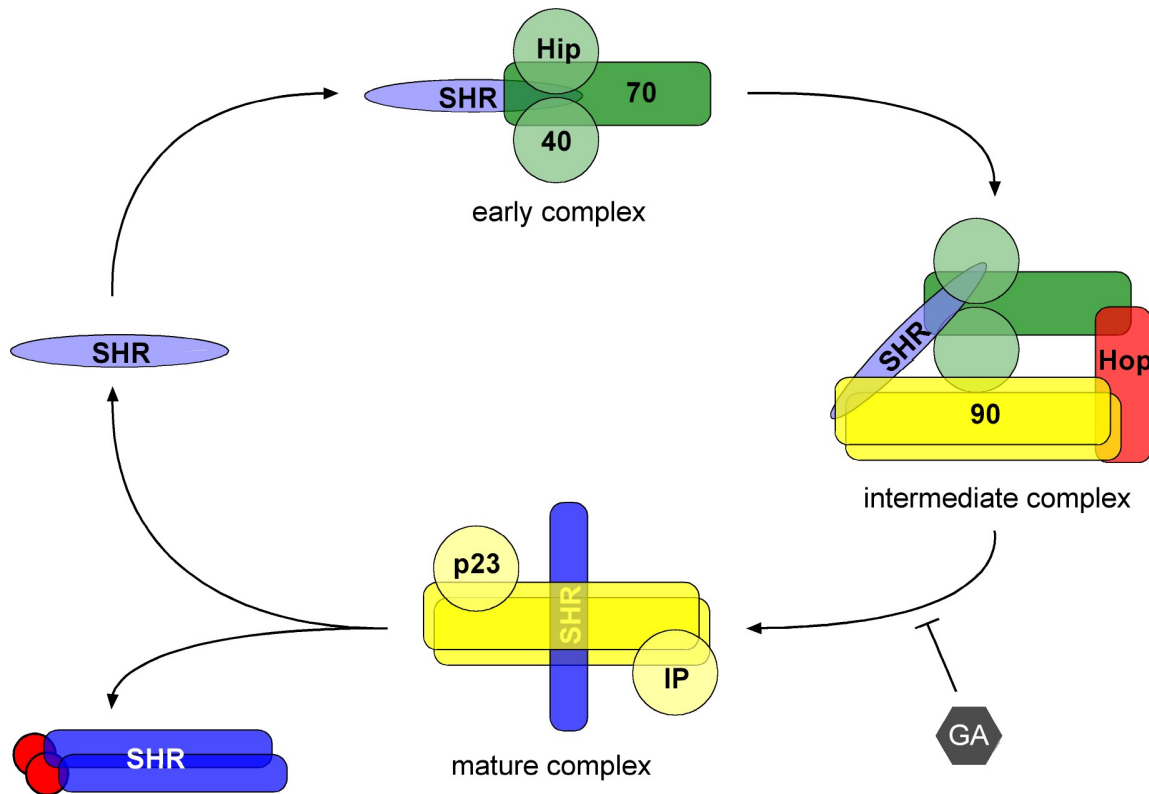
Figure 7   Multichaperone machinery

Early complex: steroid hormone receptor (SHR) is recognized and bound by the Hsp70 chaperone system (70: Hsp70. 40: Hsp40. BAG: BAG-1). **Intermediate complex**: Hsp90 (90) dimer connects via the scaffold protein Hop with the Hsp70 system. Substrate is passed over to Hsp90. Progression of the chaperone cycle can be inhibited by Geldanamycin (GA). **Mature complex**: immunophilin cofactors (IP) replace Hsp70/Hop. ATP hydrolysis and p23 binding release the SHR. **Free receptor**: activated SHR can interact with hormone (red circle) or re-enter the folding cycle via Hsp70.

early complex - At this initial stage, Hsp90 is not yet assembled into the complex and Hsp70 is the major chaperone component. The binding of Hsp70 to the substrate can already occur during its translation. Hsp40 induced ATP hydrolysis triggers the high affinity chaperone-client interaction. This state can be further prolonged by Hip, which stabilizes the ADP-bound conformation of the chaperone. The early complex is characterized by a partially folded substrate intermediate, which needs to be transferred to Hsp90 to reach its native conformation.

intermediate complex -The substrate transfer is facilitated by the spatial coordination of Hsp70 and Hsp90 on the scaffold protein Hop. Specific TPR-clamp interactions dock the C-termini of both chaperones to Hop. Hop also inhibits the ATPase activity of Hsp90 and stabilizes the nucleotide free, open conformation of the chaperone dimer. In this conformation

the substrate can efficiently be loaded on Hsp90. So far it is not clear, how exactly the transition occurs. Ansamycin inhibitors of the Hsp90 ATPase can inhibit the multichaperone machinery at this stage and cause degradation of the client protein (Smith et al. 1995).

mature complex - In progression to the final stage, the Hsp70 system and Hop are displaced by immunophilins. This happens by competitive binding to the Hsp90 C-terminus via TPR-clamp interaction. Depending on the substrate, only one species of the large immunophilins (Cyp-40, FKBP51, FKBP52) is assembled into the complex, suggesting an additional selectivity mechanism. The complete maturation of the substrate requires its ATP dependent activation by Hsp90. After nucleotide is hydrolyzed, p23 helps the release of client protein. The mature substrate can now interact with its target or return to the folding machinery through Hsp70.

In the case of SHR the target molecule is the respective hormone. It is recognized by the C-terminal ligand binding domain (LBD) of the receptor. The native fold of the LBD seems to be only metastable and the conformation of the hormone binding cleft needs to be maintained by recurrent rounds through the multichaperone machinery (Smith 1993; Young et al. 2001). After the SHRs are activated by hormone, the receptors dimerise and enter the nucleus. It remains to be resolved how and if chaperones are involved in transport events. In the nucleus, the receptors bind to other co-activators and dock to response elements in the DNA, triggering the transcription of downstream genes (Freedman 1999; McKenna and O'Malley 2002). After their task is completed, they are degraded by the proteasome (Wallace and Cidlowski 2001). Recent work suggests an active contribution to the disassembly of receptor-transcription complexes mainly by p23 and to some extent by Hsp90, providing a fast method for down-regulating gene activation after withdrawal of the hormone (Freeman and Yamamoto 2002).

Although the folding of SHRs was thoroughly investigated, it is less clear what the contributions of the single components of the multichaperone are on the folding, maintenance or other downstream events of the growing number of Hsp70/Hsp90 dependent substrates. These include helix-loop-helix transcription factors, tumor suppressor genes (p53), reverse transcriptase, telomerase and viral kinases (Buchner 1999). In addition new proteins have been reported that interact with the chaperones in a non-substrate manner and could contribute

regulatory functions. Amongst these is the protein Tpr2, which is the subject of research in this thesis and will be introduced in the next section.

1.4 Tpr2, a potential chaperone cofactor

Tpr2 together with Tpr1 was first identified in a chaperone-unrelated yeast two-hybrid screen as a binding partner of a truncated version of neurofibromin (Murthy et al. 1996). This tumor suppressor is a regulator of the GTPase activity of p21/Ras and stimulates the transition to the inactive GDP-bound form (Johnson et al. 1994; Gitler et al. 2003). Mutations in the NF1 gene cause Neurofibromatosis 1, which is characterized by an increased predisposition for diseases of the nervous system. These include peripheral nerve sheath tumors (neurofibromas), optic pathway glioma, vascular abnormalities and learning disability (Lynch and Gutmann 2002).

A sequence analysis of the isolated cDNAs revealed that Tpr1 and Tpr2 contain multiple TPR repeats. In addition, Tpr2 displays a J-domain towards its C-terminus. The complete domain prediction is shown in Figure 8. Although TPR clusters are potential protein-protein interaction sites, the binding sites of the bait-prey contact were not characterized in this study. The authors showed that the gene localizes to position 17q11.2-23 in the human genome. It encodes for a 2.2 kb transcript, which is constitutively transcribed in all tested adult and fetal tissues, as demonstrated by northern blot.
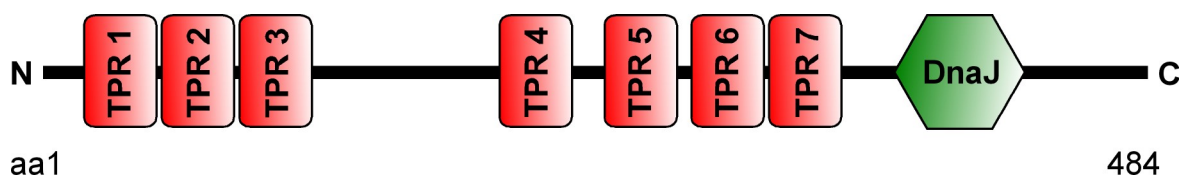
Figure 8   Domain prediction for Tpr2
The domain prediction was carried out with the SMART program at the EMBL Heidelberg. TPR: tetratricopeptide repeat. DnaJ: sequence is homologous to the J-domain of DnaJ. The size of the proteins is indicated in amino-acids (aa).

Tpr2, together with other TPR-motif containing proteins, was found in a separate yeast two-hybrid screen as an interaction partner of full-length Hsp70 or its 30 kDa C-terminal domain (C70) (Liu et al. 1999). Deletion mutants of Hsp70 or C70 were used to demonstrate

the specificity of this interaction. They lacked the carboxyterminal EEVD sequence and did not interact with Tpr2. This suggests that the TPR motifs could fulfill the criteria for a two-carboxylate clamp. Moreover, it was unlikely that Tpr2 is recognized by Hsp70 as a substrate. The authors of this study tried to narrow down the interaction sites using truncation mutants of the protein. For Tpr2, the results obtained with different experimental setups, were partially conflicting. This could be due to technical limitations of the assays or to possible misfolding or destabilization in the deletion mutants. In summary, the authors showed that the complete TPR-region (mutant 1-356, excluding the J-domain), the first three TPR-motifs (mutant 1-158) and a C-terminal deletion (mutant 103-484, lacking the first three TPR-motifs) are capable of interacting with C70, dependent on the EEVD motif. The strength of the interaction varied and was not comparable due to different experimental setups. It was not conclusively shown if and which additional sequences in Tpr2 were needed to promote the interaction with Hsp70 or C70. At least, this screen clearly identified a TPR-clamp dependent binding of Tpr2 to the C-terminus of Hsp70, which is independent of a possible J-domain interaction.

An interesting hint to the function of the J-domain in Tpr2 came from a Drosophila screen. The experiment set out to identify modifiers of a degeneration of the fly eye, which was caused by over-expression of polyglutamine tracts (Kazemi-Esfarjani and Benzer 2002). These expansions are a hallmark of a set of severe neurodegenerative diseases like Huntington's disease (HD), spinocerebellar ataxia (SCA) or spinobulbar muscular atrophy (Kim and Tanzi 1998). The disorders are dominantly inherited and characterised by a late onset. During the life span of the patient the uninterrupted CAG-repeats, which encode the polyglutamine tract (polyQ), expand until they reach a pathogenic threshold. The consequences of the diseases are neuronal cell loss and decline in motor and cognitive functions (Menalled and Chesselet 2002). *In vitro* experiments showed that the expanded polyQ-peptides are deposited as detergent-insoluble aggregates, consisting of amyloid-like fibrils. The presence of chaperones, especially Hsp70/Hsp40, during the aggregation period prevents fibrilisation and generates amorphous, detergent-soluble aggregates (Muchowski et al. 2000). Moreover, overexpression of chaperones in a Drosophila model was sufficient to suppress polyQ-mediated neuronal degeneration (Warrick et al. 1999; Fernandez-Funez et al. 2000). In the original Drosophila screen, Kazemi-Esfarjani *et al.* expressed a synthetic 127mer polyQ-peptide (127Q) in the Drosophila eye, which caused an easily detectable collapse of the eye structure and showed aggregate formation (Figure 9 compare A: wild type

and B 127Q). The screen yielded a set of 59 modifiers of this phenotype with the Drosophila homolog of Hsp40 (dhdJ1) and Tpr2 (dtpr2) being reported to be suppressors of the malformation (Figure 9 C and D). Since the only common structural feature in these two proteins is the J-domain, it was tempting to speculate that J-domain induced stimulation of Hsp70 is responsible for the rescue phenotype. However, unrelated effects of Tpr2 overexpression could not be excluded.
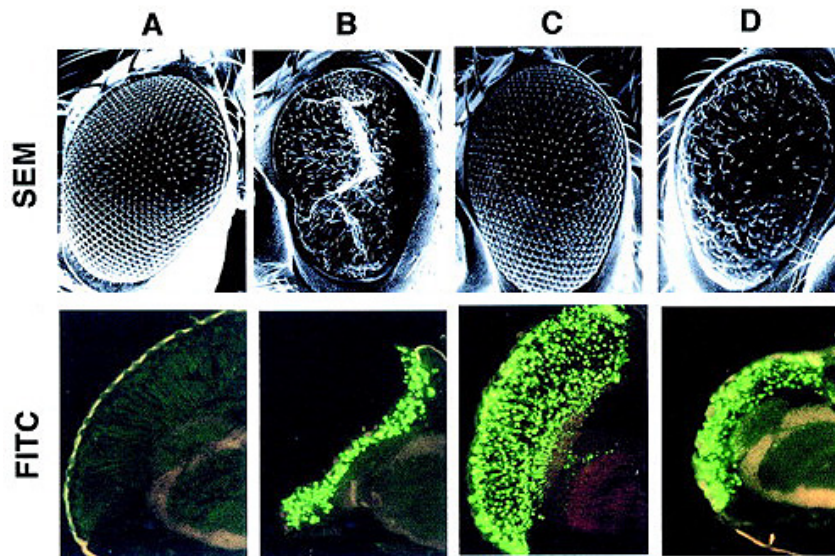
Figure 9   **Rescue of polyQ-induced malformation of the Drosophila eye**
Figure modified from (Kazemi-Esfarjani and Benzer 2002). SEM: scanning electron microscope. FITC: immunofluorescence detection of polyQ aggregates. **A**: wild type eye. **B**: collapsed eye after expression of 127 polyQ tract (127Q). **C**: co-expression of 127Q and dhdJ1. **D**: co-expression of 127Q and dtpr2.

In another yeast two-hybrid screen, which preceded this thesis, novel interaction partners of Hsp90 were searched for. A C-terminal fragment of human Hsp90 (aa 629-731) was expressed as a bait and Tpr2 was identified amongst other proteins as a positive binding partner (Brychzy et al. 2003). The re-screening of the library with the Tpr2 full-length sequence as a bait revealed interactions with both Hsp70 and Hsp90. This confirmed the already reported interactions and further extended them to the Hsp90 chaperone-class.

1.5 Aim of the project

The cumulative data indicated that Tpr2 could interact with both Hsp70 and Hsp90, but the biological relevance of this observation remained unresolved. The aim of this work was to characterise the functional aspects of these interactions in more detail.

Since both interactions partners are major components in the multichaperone machinery and the J-domain is a potential regulator of the Hsp70 activity, it was speculated that Tpr2 might be an up to now overlooked cofactor of this multi-protein system. Therefore, the first part of this work concentrates on the effects of Tpr2 on the folding of a stringent Hsp70/Hsp90 substrate in a physiological relevant *in vivo* context. The glucocorticoid receptor was chosen as a model substrate because it is endogenously present in many cell lines and its chaperone dependency is well documented. Interestingly, the siRNA (small interfering RNA) method for protein knock-downs in mammalian cells became available at the time of this thesis. This opened the possibility to screen for effects, which occur after the depletion of Tpr2 within the usual time course of the *in vivo* experiments.

The second part of this work tries to address the question which domains of Tpr2 confer specific functions on Hsp70 or Hsp90. Since both the TPR-clamp domain and the J-domain are well understood in terms of their mode of interaction, only single point-mutants in Tpr2 were introduced to disrupt the respective domain activity. *In vitro* experiments were used which allowed dissection of domain-specific aspect of Tpr2 at a time. The J-domain function of Tpr2 was tested with respect to its stimulation of the Hsp70 ATPase activity, substrate binding- and refolding-activity. The TPR-clamp interactions were examined regarding their chaperone binding-specificity and implications on the folding of GR. Finally, a complex *in vitro* refolding system was established, which allowed a reproduction of the *in vivo* situation.

2 Material and Methods

2.1 Chemicals

All chemicals were of "pro analysis" quality. If not stated otherwise, they were purchased from Fluka (Buchs, Switzerland), Merck (Darmstadt, Germany) or Sigma-Aldrich (Steinheim, Germany). Solutions were prepared with the indicated buffer or with deionised, double-destilled and autoclaved water. Concentrations in percent of liquids are given as volume per volume (v/v) and of solid chemicals as weight per volume (w/v).

Amersham (Buckinghamshire, England): α^{32}P-ATP, [1,2,4,5,7-^{3}H]Dexamethasone

Boehringer Ingelheim / Roche (Mannheim, Germany): ATP, Ampicillin.

Invitrogen / Life Technologies: cell culture media and supplements, LipofectAMINE PLUS system

Green Hectares (Wisconsin, USA): Rabbit reticulocyte lysate (RL).

New England Biolabs (NEB, Beverly, USA): E.coli strains DH5α and BL21pLysS, restriction enzymes and buffers, T4-DNA ligase, VENT DNA polymerase

Promega (Mannheim, Germany): TNT T7 Coupled Reticulocyte Lysate System, Luciferase Assay System, β-Galctosidase Enzym Assay System

Roche (Mannheim, Germany): Expand Long Template PCR Kit.

Stratagene (La Jolla, USA): QuickChange Site-Directed Mutagenesis Kit.

2.2 Instruments and materials

Beckman (Munich, Germany): Centrifuges J-6B, Anvanti J-25, GS-6R and Optima LE-80k ultracentrifuge, UV-VIS spectralphotometer DU640

BioRad (Hercules, USA): gel electrophoresis system for protein and DNA gels.

EG&G Berthold: Lumat LB9507

Eppendorf (Cologne, Germany): Centrifuges 5415C and 5417R.

Fuji (Stamford, USA): Phosphorimager Fuji Film FLA-2000.

Millipore (Eschborn, Germany): Amicon Centriprep concentrators, Milli-Qplus PF, sterile filters 0.22 μM Millex-HA

Misonix Inc. (New York, USA): Sonicator Ultrasonic Processor XL.

Packard (Dreieich, Germany): Liquid scintillation analyzer Tri-carb 1500.

Perkin Elmer (Weiterstadt, Germany): GenAmp 2400 thermocycler.

Pharmacia (Freiburg, Germany): FPLC system LKP, columns XXX

Qiagen (Hilden, Germany): Ni-NTA superflow matrix, Plasmid Midi kit, QIAprep Spin Mini prep kit, QIAquick PCR purification and gel extraction spin kit.

Rainin (Woburn, USA): Gilson pipettes.

Savant / Life Science Int. (Frankfurt, Germany): Slab gel dryer SGD 2000, DNA Speed Vac DNA100.

Schleicher&Schuell: Protran nitrocellulose transfer membrane

WTW (Weilheim, Germany): pH meter pH535.

Zeiss (Jena, Germany): Microscope Axiovert 200M.

2.3 Media and buffers

2.3.1 Media

Luria-Bertani (LB) medium: 10 g/l Bactotryptone
5 g/l Bactoyeast extract
5 g/l NaCl
for plates, medium was supplemented with 15 g/l agar

Terrific Broth (TB) medium: 12 g/l Bactotryptone
24 g/l Bactoyeast extract
8 ml/l glycerol
2.2 g/l KH_2PO_4
9.4 g/l K_2HPO_4

2.3.2 Buffers

ATPase buffer:	20 mM MOPS pH 7.6, 100 mM KCl, 5 mM MgAc$_2$
	prepared as 10x stock solution
Buffer B:	20 mM HEPES-KOH pH 7.5, 100 mM KAc, 5% glycerol
Buffer G:	20 mM HEPES-KOH pH 7.5, 100 mM KAc, 5 mM MgAc$_2$
Buffer C:	20 mM HEPES-KOH pH 7.5, 100 mM KAc, 1 % NP40, 1 % Na-deoxycholate, 0.1 % SDS
HBS:	10 mM HEPES pH 7.4, 150 mM NaCl, 3 mM EDTA, 0.05% Tween20
Laemmli buffer:	60 mM Tris-HCl pH 6.8, 10% glycerol, 2% SDS, 0.35 M 2-mercaptoethanol, 0.005% bromophenol blue
	prepare as 5x stock solution
Ni-NTA wash A:	50 mM KP$_i$ pH 8.0, 500 mM KCl, 20 mM imidazole
Ni-NTA wash B:	50 mM KP$_i$ pH 6.0, 500 mM KCl, 20 mM imidazole
Ni-NTA elution:	25 mM KP$_i$ pH 6.0, 250 mM KCl, 500 mM imidazole
PBS:	137 mM NaCl, 2.7 mM KCl, 8.4 mM Na$_2$HPO$_4$, 1.5 mM KH$_2$PO$_4$, pH 7.4, adjusted with HCl
	prepare as 10x stock solution
TB1:	100 mM RbCl$_2$, 50 mM MnCl$_2$, 30 mM KAc, 10 mM CaCl$_2$, 15 % glycerol; pH 5.8, adjusted with 0.2 M HOAc
TB2:	75 mM CaCl$_2$, 10 mM RbCl$_2$, 10 mM MOPS; 15 % glycerol, pH 6.5, adjusted with KOH
TBE:	89 mM Tris base; 89 mM boric acid; 20 mM EDTA
TEV-buffer:	50 mM Tris-HCl pH 8.0; 5 % glycerol; 20 mM NaCl
TLC running buffer:	0.5 M formic acid; 0.5 M LiCl

2.4 Bacterial strains, plasmids and primer

2.4.1 Bacterial strains

DH5αF'   (Novagen)

E. coli XL1-Blue (supercompetent)   (Stratagene)

BL21 DE3 pLysS   (Novagen)

2.4.2 Plasmids

The following plasmids were constructed to express recombinant proteins in *E.coli* Bl21 pLysS cells for further purification. Tpr2 was originally inserted into the EcoRI/SalI sites of pProEX HTa (Life Science):

pProEX-dT1   Tpr2 with point mutation in TPR-clamp 1 (R91A)

pProEX-dT2   Tpr2 with point mutation in TPR-clamp 2 (R323A)

pProEX-dT12   Tpr2 with point mutation in both TPR-clamps (R91A, R323A)

pProEX-dJ   Tpr2 with point mutation in the J-domain (H399A)

pProEX-dT12J   Tpr2 with triple point mutation (R91A, R323A, H399A)

Plasmid constructed for transfection of live cells: DNA sequence encoding Tpr2 was inserted into pcDNA3.1/MycHis(+)A (Invitrogen) in frame with the C-terminal myc-his-tag

pcDNA-Tpr2   Tpr2 in pcDNA3.1/MycHis(+)A

pcDNA-dT1   Tpr2 with point mutation in TPR-clamp 1 (R91A)

pcDNA-dT2   Tpr2 with point mutation in TPR-clamp 2 (R323A)

pcDNA-dT12   Tpr2 with point mutation in both TPR-clamps (R91A, R323A)

pcDNA-dJ   Tpr2 with point mutation in the J-domain (H399A)

pcDNA-dT12J   Tpr2 with triple point mutation (R91A, R323A, H399A)

The following constructs were obtained from the plasmid bank of the Department of Cellular Biochemistry, MPI for Biochemistry, Martinsried:

human Tpr2	pProEX-HTa	(Brychzy et al. 2003)
J-domain of human Tpr2	pProEX-HTa	(Obermann, unpublished data)
GR expression vector	pRK7-GR	(Rosenhagen et al. 2001)
p60/Hop	pET28a	(Young et al. 1998)
Hsp82	pProEX HTa	(Albrecht et al.)
C90	pET3d	(Young et al. 1997)
C70	pProEX HTa	(Brinker et al. 2002)
TEV protease		(Parks et al. 1994; Lucast et al. 2001)
β-Galactosidase reporter	pSV-β-Gal	Promega
GRE-luciferase reporter	pGRE-luc	Clontech

2.4.3 Primer

The following primers were used to introduce point mutations in Tpr2. Only the sense strand is listed. Underlined residues differ from the original Tpr2 sequence.

dT1 mutant, R91A	5'-GTCCGGGGACATCTA<u>GC</u>AGAGGGCAAGTGCCACC
dT2-mutant, R323A	5'-CACTTACATAAAAGCCTACTTG<u>GC</u>AAGAGCTCAGTG TTACATGGAC
dJ mutant, H399A	5'-GAAACGGGCCTTGATGCAC<u>GC</u>TCCAGATCGGCATAG TGGAG

For re-cloning the Tpr2 constructs into pcDNA3.1/MycHis(+)A mammalian expression vector (Invitrogen) the forward primer contained an *EcoRI* site and the backward primer contained an *XhoI* site. Restriction sites are underlined.

| pcDNA3.1 forward | 5'-GAGTGCGAT<u>GAATTC</u>ATGGCGGCGACCGAGCCGGAGCTG |
| pcDNA3.1 backward | 5'CCG<u>CTCGAG</u>GCCAAATTGAAAAAAGAAATTCCC |

2.5 Molecular biological methods

2.5.1 Competent *E. coli* cells using the rubidium chloride method

Cells were prepared as described (Hanahan 1983). 55 ml of LB medium was inoculated with a single colony of the required bacterial strain and grown to an OD_{600} of 0.5 at 37°C under shaking. After centrifugation for 20 min at 1000g at 4°C, cells were resuspended in 25 ml ice-cold TB1 buffer. After incubation on ice for 5 min, cells were centrifuged as described before and resuspended in 2 ml ice-cold buffer TB2. The cell suspension was kept on ice and aliquoted into pre-chilled tubes (250 µl/tube). Finally cells were shock frozen in liquid nitrogen and stored at −80°C.

2.5.2 Cloning, using polymerase chain reaction (PCR)

2.5.2.1 PCR

Plasmids were generated by using the PCR technique for amplification of inserts, followed by restriction digest and ligation. A standard PCR protocol is shown in Table 2.

Table 2   Standard protocol for PCR

Mixture
1.2 µg primer 1 (sense)
1.2 µg primer 2 (antisense)
5 µl 10x polymerase buffer
100 ng template DNA
250 µM dNTPs
1 µl DNA Polymerase
dd H_2O to 50 µl final volume

Reaction cycle		
cycle number	temperature	time
1	95°C	3 min
2-25	95°C	1 min
	50°C	30 sec
	72°C	1 min/kb
26	72°C	10 min
27	4°C	∞

Where no or inadequate amounts of PCR product were observed, the annealing temperature was decreased in 2°C steps.

2.5.2.2   PCR product purification

5 µl of the amplified products were analysed by agarose gel electrophoresis (1-2% agarose in TBE buffer, supplemented with 1 µg/ml ethidium bromide) at 50-100 volt. The remaining part of the sample was purified by anion exchange chromatography using the QIAquick PCR purification kit (Quiagen), resulting in 50 µl final volume.

2.5.2.3   Digestion of vector and insert

Purified PCR products and the respective target vector were digested for 1 hour at 37°C. The 50 µl reactions contained 5 µl of the appropriate 10x restriction buffer, 2µl of each restriction enzyme and 30 µl of the purified PCR product or 5-10 µg vector. Additionally the vector was dephosphorylated with 5 Units of calf intestinal phosphatase (CIP) for 1 hour. DNA fragments were resolved by preparative agarose gel electrophoresis and purified from agarose slices using anion exchange chromatography (QIAquick Gel extraction kit).

2.5.2.4   Ligation reaction.

Ligation reactions contained 50-100 ng (~1-2 µl) dephosphorylated vector DNA, 200-300 ng (~5-10 µl) insert, 2 µl 5x ligase buffer and 1 µl T4 ligase (100 units) in a volume of 20 µl. Samples were incubated for 1 hour at room temperature prior to transformation or storage at −20°C.

2.5.2.5   Transformation of chemical competent cells

Aliquots of 50 µl chemical competent cells were mixed with 1-2 µl of a ligation reaction or with 0.2 µg DNA from a plasmid preparation and kept on ice for 30 min. After a 60 sec heat shock at 42°C, the cells were transferred back on ice for 2 minutes. 1 ml LB medium was added, followed by 1 hour incubation at 37°C. Cells were pelleted at 20,000g for 15 sec and resuspended in 200 µl LB medium before plating on agar-dishes, containing the appropriate antibiotics. The plates were incubated at 37°C for 10-20 hours, until single bacterial colonies were clearly visible.

2.5.2.6   Plasmid recovery.

3 ml antibiotic-containing LB medium was inoculated with a single colony and incubated over night at 37°C under shaking. Plasmids were isolated from cell pellets using Qiagen Mini prep kit, following the manufacture's instructions. The plasmids were evaluated by restriction digestion and analytical agarose gel electrophoresis. When needed, the verified plasmids were re-transformed into *E. coli* cells and plasmid preparation was up-scaled using the amounts suggested for Qiagen Midi- or Maxi-prep kits, to yield high amounts of DNA.

2.5.2.7   DNA concentration

The amount of DNA was traced with adsorption measurement at 260 nm, assuming that 50 µg/ml double stranded DNA would give a readout of an $OD_{260} = 1$.

2.5.3 Site-directed mutagenesis

Site-directed mutagenesis was performed using the QuickChange System from Stratagene. It allows site-directed mutagenesis by using double-stranded DNA as a template in a single PCR reaction. The application of a complementary set of primers, which contain the desired mutation and span the respective region on the plasmid, generates a mutated, non methylated plasmid. Methylated, parental DNA is digested by treatment with the restriction enzyme DpnI (1 µl per PCR reaction, 1 hour at 37°C). Residual, mutated DNA was transformed into supercompetent *E.coli* cells (XL1-Blue) following the protocol as described above. Mutations were confirmed by DNA sequencing (Medigenomix, Munich, Germany). A standard protocol for site-directed PCR is given in Table 3.

Table 3   PCR protocol for site-directed mutagenesis

Reaction mixture		
125 ng mutagenic primer (sense)		
125 ng mutagenic primer (antisense)		
5 µl 10x reaction buffer		
25-100 ng template DNA		
250 µM dNTPs		
1 µl PFU turbo polymerase		
dd H$_2$O to 50 µl final volume		
Reaction cycle		
cycle number	temperature	time
1	95°C	3 min
2-17	95°C	30 sec
	55°C	1 min
	68°C	2 min/kb
18	68°C	20 min
19	4°C	∞

The mutations were verified by sequencing the plasmids using the Big Dye cycle sequencing kit (ABImed, Perkin-Elmer), following the manufacturer's instructions. The electrophoretic separation and fluorescence detection of the labelled DNA fragments was carried out at the Sequencing Service Facility at the MPI for Biochemistry or by Medigenomix (Martinsried).

2.6 Biochemical methods

2.6.1 SDS polyacrylamide gel-electrophoresis (SDS-PAGE)

SDS-PAGE allows the analysis of proteins under denaturing, reducing conditions (Laemmli 1970). 5x concentrated Laemmli sample buffer (final concentration: 2% SDS, 0.35M β-Mercaptoethanol, 60 mM Tris-HCl pH 6.8, 10% glycerol and 0.005% bromphenol blue) was added to the samples and incubated for 4 min at 95°C prior to loading of the gels. Stacking gels contained 5% polyacrylamide. The percentage of separation gels varied between 10 and 15 % acrylamide, depending on the desired resolution range. The accurate composition is listed in Table 4. Electrophoresis was carried out at a constant voltage of 200V in 50 mM Tris-HCl pH 8.3, 380 mM glycine, 0.1% (w/v) SDS.

Table 4   Preparation of SDS-PAGE gels

	resolving gel			stacking gel
% Acrylamide	10%	12%	15%	5%
H_2O [ml]	4.0	3.3	2.3	6.8
30% AA / 0.6% BisA mix [ml]	3.3	4.0	5.0	1.7
1.5 M Tris pH 8.8 [ml]	2.5	2.5	2.5	-
1 M Tris pH 6.8 [ml]	-	-	-	1.25
10% SDS [µl]	100	100	100	100
10% Ammoniumpersulfat [µl]	100	100	100	100
TEMED [µl]	4	4	4	10

2.6.2 Staining methods for protein gels

After electrophoresis, SDS-PAGE gels were stained with a Coomassie solution (0.1% Coomassie Brilliant Blue R-250, 30% methanol, 10% acetic acid) for 15 min and destained by incubation in fixing solution (30% methanol, 10% acetic acid) until unspecific stain was removed.

2.6.3 Protein expression and purification

All recombinant proteins were overexpressed in *E.coli* BL21pLysS cells (Novagen) in terrific broth (TB) medium, supplemented with antibiotics. Protein expression was induced by addition of 1 mM IPTG at an OD_{600} of 1. Depending on the solubility of the recombinant proteins, cells were incubated for 4 hours at 37°C or for 15 hours at 21°C. After that, cells were harvested by centrifugation for 4 min at 8.000g. Pellets were shock frozen in liquid nitrogen and stored at −80°C.

For cell lysis, pellets were resuspended in Ni-NTA wash buffer A, supplemented with protease inhibitors (Complete without EDTA, Roche), lysozyme (0.5 mg / ml) and Benzonase (Merck, 25 units/1l of induced cell culture). The suspension was kept at room temperature for about 20-30 min until it became fluid. The following purification steps were carried out on ice or at 4°C. The sample was sonicated for 2 min. Cell debris was removed by centrifugation at 10,000g for 15 min followed by an 80,000g spin for 30 min. The supernatant was incubated with Ni-NTA affinity matrix for 1 hour under gentle shaking. The resin was washed with 10 column volumes of Ni-NTA wash buffer A followed by 10 column volumes of Ni-NTA wash buffer B. The proteins were eluted from the matrix by incubation with Ni-NTA elution buffer. Samples were either shock frozen and stored at −80°C or desalted over a pre-packed PD10 column (Amersham), equilibrated with the desired buffer. For further removal of the His-tag, the buffer was exchanged to TEV cleavage buffer. The samples were incubated with tobacco etch virus (TEV) protease for 1 hour at room temperature followed by an overnight incubation at 4°C. The protein ratio between protease enzyme and target protein was adjusted to 1:40, based on a Bradford test. The cleaved His-tag and the uncleaved substrate was removed by incubation with Ni-NTA matrix. The cleaved protein was recovered in the flow-through. Fractions were analysed by SDS-PAGE and Coomassie Blue staining. Where necessary, proteins were subjected to size exclusion chromatography on a Superdex S200 column or desalted over a PD10 column into the desired buffer. Fractions containing the purified protein were pooled and concentrated using the Amicon Centriprep system (Pharmacia). Aliquots were shock frozen in liquid nitrogen and stored at −80°C.

2.6.4 Purification of Hsc70 from bovine brain

Two frozen cow brains (usually 500-600 g) were cleaned of membranes, blood vessels and fat. The brains were crushed with a hammer and homogenized in a blender in 2 l DE53 equilibration buffer (20 mM Tris-HCl pH 7.5, 0.1 mM EDTA and protease inhibitors). The homogenate was centrifuged at 5,000g for 15 min. Supernatant was decanted and centrifuged again at 100,000g for 30 min. The filtrate of the supernatant was loaded on a DE52 column and washed with 1 l of equilibration buffer. Proteins were eluted with 400 ml of Hsc70 elution buffer (150 mM NaCl, 20 mM Tris-HCl pH 7.5, 0.1 mM EDTA and protease inhibitors). Fractions were analysed by SDS-PAGE and Coomassie Blue staining. Samples containing Hsc70 were pooled and adjusted to 3 mM $MgCl_2$ before loading on a 25 ml ATP-agarose column (C8 linkage, Sigma), which was equilibrated with 20 mM NaCl, 20 mM Tris-HCl pH 7.5 and 3 mM $MgCl_2$. The matrix was washed with 50 ml equilibration buffer, followed by 50 ml wash buffer (500 mM NaCl, 20 mM Tris-HCl pH 7.5 and 3 mM $MgCl_2$). Proteins were eluted with 150 ml equilibration buffer, containing 3 mM ATP. The pooled fractions containing Hsc70 were loaded on a Superdex S200 column equilibrated in buffer B. Fractions were again analysed by SDS-PAGE and Coomassie Blue staining. The pooled protein peak was concentrated in Amicon Centriprep concentrators and aliquots were shock frozen in liquid nitrogen before storing them at –80°C.

2.6.5 Determination of protein concentration in solution

Protein concentrations were determined either by using the Bradford assay (Pierce) (Bradford, 1976) and compared to a BSA standard dilution series by measuring the OD_{595}, or by applying the Lambert-Beer equation to the OD_{280} using the theoretical extinction coefficient (Pace et al., 1995; Wetlaeufer, 1962). Extinction coefficients were determined with the ProtParam tool at the Expasy server (www.expasy.ch).

2.6.6 ATPase assay

The rates of ATP hydrolysis were determined as described earlier (Obermann et al. 1998). The ATPase activity was calculated from the amount of α^{32}P-ATP hydrolysed in a certain time period. The 20 µl reactions contained 2 µl 10x ATPase buffer, proteins of interest and 100 µM ATP supplemented with 1 µCi α^{32}P-ATP with a specific activity of 400 Ci/mmole. Samples were preheated to 30°C and the reaction was started by the addition of the radioactive ATP mixture. At each given time 2 µl were transferred to 8 µl 25 mM EDTA stop solution and flash frozen until further use. 1µl of each fraction was analysed by thin layer chromatography (TLC) on polyethyleneimine (PEI)-cellulose plates (Merck) in TLC running buffer. After drying the TLC sheets with a blow-dryer, ATP and ADP spots were quantified by phosphorimaging (Fuij Film FLA-2000) with the Aida software (Raytest).

2.6.7 Covalent coupling of antibodies to Protein G beads

Anitbodies against the c-myc epitope (EQKLISEEDL) were covalently coupled to Protein G sepharose matrix (Pharmacia) as listed below. 1 ml of Protein G beads was washed three times with PBS. Beads were mixed with 2 mg of myc antibody, purified from cell culture supernatant, and incubated for 1 hour at room temperature with gentle shaking. The matrix was washed twice with 10 volumes of 0.2 M Na-borate pH 9.0 followed by centrifugation at 1000g for 5 min. Beads were resuspended in 10 volumes of wash buffer and an aliquot (10 µl) was removed for later analysis of coupling efficiency. Solid dimethylpimelimidate was added to a final concentration of 5.18 mg/ml. At this step the pH of the solution should be above pH 8.3. The sample was incubated at room temperature (RT) for 30 min with gentle shaking. The coupling was stopped by washing the beads with 10 volumes of 0.2 M ethanolamine pH 8.0. Beads were incubated in the same buffer for 2 hours at RT. Finally, the matrix was washed with PBS and stored at 4°C in PBS/0.02% Na-azide. The coupling efficiency was determined by analysing the samples removed before the crosslinking step and taken at the end of the procedure on SDS-PAGE. The heavy chain of the antibody (around 55 kDa) should be visible only in the sample taken before addition of the crosslinker.

2.6.8 Immunoblotting

Western blotting and protein detection were performed as described by Towbin et al. (1979). After proteins were resolved on SDS-PAGE they were transferred to a nitrocellulose membrane (Protran, Schleicher&Schuell) in a tank blot system (Biorad) in 25 mM Tris-HCl pH 8.4, 192 mM glycine and 20% methanol at a constant current of 400 mA for 1 hour at 4°C. The membrane sheets were blocked with PBS, 3% BSA, 0.02% Tween20 for 1 hour room temperature or at 4°C overnight. Blots were washed with PBS, 0.02% Tween20, followed by incubation with the primary antibody for 1 hour in the same buffer at room temperature. Blots were washed 3 times for at least 15 min and the secondary antibody, coupled to horse-reddish peroxidase (Sigma), was applied at a dilution of 1:2000 in the same buffer for 1 hour. Blots were washed as before, followed by a final wash in PBS. Detection was carried out as described in the protocol for the chemiluminescence kit (ECL, Amersham) followed by exposure to X-ray films (Fuij Film).

Polyclonal primary antibodies for the detection of Tpr2 and Hsp90 were provided by Wolfgang Obermann (Bonn, Germany).

2.6.9 Co-precipitation assays with His-tagged proteins

His-tagged proteins (10 µM) were incubated in Reticulocyte lysate (RL, Green Hectares) desalted in buffer B, 30 mM imidazole for 15 min at room temperature. Competitors were added at a 5-fold molar excess. 20 µl Ni-NTA, equilibrated in buffer B, were added and the reaction continued for 15 min with gentle shaking. The samples were transferred to micro spin columns (MoBiTec, Germany) and washed twice with ice cold buffer B, 30 mM imidazole. Control beads from reactions without His-tagged protein were treated equally. Bound proteins were eluted from the resin by boiling the beads in Laemmli buffer containing 100 mM EDTA. Samples were analysed by SDS-PAGE and Coomassie Blue staining or Western blotting.

2.6.10   Substrate release assay

The release of chaperones from substrate was measured as described (Young and Hartl 2000). The purified myc-tagged ligand binding domain (LBD) of the Glucocorticoid receptor served as the substrate in this assay. The isolated LBD is sufficient to be recognized as a substrate and folded by the multichaperone machinery. It was partially denatured during a 10 min incubation in 1% SDS, 50 mM Tris-HCl pH 7.5 at room temperature. The sample was diluted 10 fold into buffer C and incubated for 30 min after the addition of 50 µl) anti-myc antibody resin (1:1 v/v slurry), covalently coupled to Protein G Sepharose. Immuno-precipitates were washed twice in buffer B and added to the refolding reaction, containing 500 µl desalted reticulocyte lysate (Green Hectares), 500 µl buffer B, 10 mM MgAc$_2$, 2 mM ATP supplemented with a TNT reaction containing the radiolabelled chaperone of interest. The TNT T7 system (Promega) is a coupled transcription translation system that allows the *in vitro* production of radiolabelled protein. A standard reaction is set-up as described in Table 5.

Table 5   Standard protocol for TNT translation reaction

TNT reaction
25 µl TNT reticulocyte lysate
2 µl TNT reaction buffer
1 µl amino acid mix, lacking methionine
4 µl ^{35}S-methionine
1 µl RNAguard
1-2 µg DNA (protein of interest downstream of a T7 promotor)
1 µl T7 Polymerase
dd H$_2$O to 50 µl final volume
incubation for 30-60 min at 30°C

Steady state binding of chaperones was attained after 10 min at room temperature. The reaction was stopped by adding 10 units Apyrase (Sigma). The sample was split in 10 reactions by transferring it to micro spin columns (MoBiTec, Germany). Each aliquot was washed twice with ice cold buffer B.

For the release reaction the immunoprecipitants were resuspended in 100 µl buffer B, containing proteins and nucleotides as indicated. After 10 min, when release was finished (Schneider et al. 1996), supernatant and beads were separated. Proteins bound to the beads were eluted by boiling the resin in Laemmli buffer. Supernatants were precipitated with methanol/chloroform. 100 µl methanol and 25 µl chloroform were added. Samples were mixed thoroughly and centrifuged for 5 min in a table top centrifuge at maximum speed. The upper layer was removed while not disturbing the protein pellet at the interphase and 100 µl methanol were added. Again the samples were mixed and centrifuged. Supernatant was removed and residual fluid was evaporated in a heatable vacuum centrifuge (Savant). Pellets were dissolved in Laemmli buffer. Both, pellet fractions and bead eluates were resolved by SDS-PAGE. Gels were dried for 75 min at 80°C on a gel dryer (Savant) prior to incubation on a phosphorimager screen. Quantitative analysis of chaperone release was carried out with the Aida image software. The release from the immunoprecipitants was normalised to the amount of radiolabelled input.

2.6.11 GR gelfiltration assay

The effect of Tpr2 on the hormone binding activity of GR was measured by analysing the elution profile of radiolabelled GR after gelfiltration. 1 µg vector (pRK7-GR), comprising the full length GR sequence, was added to a standard TNT reaction containing ^{35}S methionine. After 1 hour at 30°C, 50 µM hydrocortisone, 10 µM Tpr2 or a combination of both were added and the reaction volumes were adjusted to 100 µl with buffer G. GR folding and hormone binding was allowed to continue for 15 minutes at RT before the reactions were transferred on ice to stabilize receptor/hormone interactions. After 30 minutes the samples were injected on a Superose 6 size exclusion column (Pharmacia Biotech) and 500 µl fractions were collected. 25 µl of each fraction were resolved by SDS-PAGE and analysed by Phosphorimager screening.

2.6.12   Hormone binding of *in vitro* refolded Glucocorticoid receptor

The efficiency of the *in vitro* refolding of recombinant, partially purified human glucocorticoid receptor (GR, Panvera), was monitored by its binding to radiolabelled hormone (Amersham, [1,2,4,5,7-^{3}H]Dexamethasone). 25 µl desalted reticulocyte lysate (buffer B) was supplemented with 2 mM ATP, 5 mM MgAc, 4.7 nM recombinant GR and proteins of interest. The final volume was adjusted to 50 µl with buffer B and the sample was heated to 42°C for 5 min to denature the GR. The reactions were transferred to 30°C and kept for 5 min before adding 10 µM radiolabelled hormone. Refolding and hormone binding was allowed to continue for 10 min. Samples were transferred to 4°C to stabilize the receptor/hormone interaction. Unbound hormone was removed by passing the samples over a pre-chilled Bio-Spin 30 chromatography column (Bio-Rad), equilibrated in buffer B. The high molecular flow through was assayed for radioactivity by liquid scintillation counting (Packard).

2.6.13   Surface Plasmon Resonance (SPR)

All SPR experiments were carried out with the BIAcore2000 Biosensor machine and the biosensore chip B1 at a constant temperature of 25°C.

The cysteine derivatised 12mer peptides, containing the C-terminus of Hsp70 (70C-12, Ac-C-GSGSGPTIEEVD-COOH) or Hsp90 (90C-12, Ac-C-GDDDTSRMEEVD-COOH) were kindly provided by Achim Brinker (Brinker et al. 2002). Immobilization was carried out with HBS buffer at a flowrate of 5 µl/min. To activate the carboxylated dextrane matrix, a mixture of 25 mM NHS (N-hydroxysuccinimide) and 100 mM EDC (N-ethyl-N'-(dimethylaminopropyl) carbodiimide) was injected for 15 min. Amino groups were generated by injection of 1 M pH 6.0 ethylene diamine hydrochloride for 10 min. Maleimido groups were introduced by the heterobifunctional crosslinker Sulfo-GMBS (Pierce, 25 mM, 5 min). Finally, 1 µM 70C-12 or 5 µM 90C-12 were exposed to the modified surface for 5 min and unreacted maleimido groups were inactivated by a 2 min pulse with 0.1 M NaOH. In the control cell the loading with peptides was omitted.

Binding and competition experiments were carried out at a flowrate of 20 μl/min in bufferG. Samples were injected for 2 min and the flow cell was washed for 5 min with buffer. The chip surface was regenerated with two 30 sec injections of 6 M Guanidinium hydrochloride. To avoid carry-over of detergents, washing steps for the flow cell and the injection needle were included into each cycle.

The evaluation of the SPR data was carried out with the BIAevaluation software 3.0. Since binding and release kinetics of Tpr2 and its mutants were too fast to be resolved, the concentration dependent response units during equilibrium binding (R_{eq}) were used to extrapolate the thermodynamic association constant (K_D). The following model, describing the binding equilibrium to surfaces (Langmuirsche adsoption isotherme), was applied to fit the data.

$$R_{eq} = \frac{K_A * C * R_{max}}{1 + K_A * C}$$

R_{eq} response units during equilibrium binding

K_A thermodynamic affinity constant

R_{max} saturated equilibrium response

C   protein concentration in mobile phase

To compare the binding affinities for the Tpr2 mutants, the proteins were injected at a constant concentration of 1 mM in triplicates and the response units (RU) were averaged.

For competition experiments the response units in absence of peptide competitors were set to 100% and response signals from protein/competitor mixtures were normalised against it. The proteins (0.5 μM) were pre-incubated with increasing amounts of peptides for 10 min on ice. Injection and washing cycles were carried out as described above. Response units during equilibrium binding were plotted against the competitor concentration. A 4-parameter curve fit was performed with the BIAevaluation software to determine the IC_{50} value.

2.6.14   Luciferase refolding

1 µM recombinant his-tagged luciferase was chemically denatured in 6 M guanidinium hydrochloride for 15 min before diluting it 1:100 into refolding buffer (10 mM MOPS pH 7.5, 100 mM KCl, 5 mM Mg acetate), substituted with 3% desalted reticulocyte lysate, 2 mM ATP, 5 mM MgAc and proteins of interest. Refolding was followed at 30°C over time by mixing 1 µl of the refolding reaction with 50 µl of luciferase reagent (Promega) and assaying the luciferase activity in a luminometer (EG&G Berthold). The results were standardised to the same dilution of native luciferase.

2.7 Mammalian cell culture

Cell culture media were obtained from Biochrom AG, supplements from GibcoBRL.
If not mentioned otherwise, cell culture media were supplemented with 10% fetal bovine serum (FBS), 1x Penicillin/Streptomycin and 1x L-glutamine. Cells were grown at 37°C in 5% CO_2. For maintenance, cell lines were split 1:10 twice a week, using Trypsin/EDTA (1x, GibcoBRL) to detach them from the tissue culture plate surface.

2.7.1 Purification of anti-myc antibody

The myc-antibody was purified from the cell culture supernatant of the monoclonal 9E10 hybridoma cell line. Cells were incubated for 4 days (RPMI 1640, 5% FBS) until the growth medium turned orange to achieve a high antibody titer. The supernatant was cleared from cells by a 5 min centrifugation at 1,000g. Protein G-sepharose slurry (50:50 v/v) was added in a 1:50 ratio and incubated overnight at 4°C with gentle shaking. The matrix was recovered and washed with 10 column volumes of PBS before eluting the antibody with 100 mM glycine pH 3.0. The pH of the eluate was immediately neutralized by adding 1/10 volume of Tris pH 8.0.

2.7.2 Immunofluorescence staining

Cells were grown on glass cover-slips to about 50% confluency. Cells were washed 3 times with pre-warmed PBS before fixation in 3% paraformaldehyde (PFA dissolved in PBS) at 37°C for 40 min. After removing of the PFA, the fixation reaction was quenched with 50 mM NH_4Cl for 10 min. Cells were washed again (3x, PBS) and membranes were permeabilised with 0.5% Saponin in PBS for 5 min. From this step onwards, all buffers contained 0.5% Saponin to keep the cells in a permeabilized state. The primary antibody was applied for 1 hour, then cells were washed 3 times for 10 min each before applying the secondary, fluorescence labelled antibody. Finally cells were washed 3 times in PBS/Saponin for 10 min each and one time in dd H_2O to remove salts from the cover-slip surface, before fixing them on a microscope glass-plate with Moviol (Hoechst).

2.7.3 Pulse-chase technique for determination of protein half life in mammalian cells

Cells were split the day before labelling to achieve about 90% confluency the next day. After washing the cells once with PBS they were incubated in starvation-medium, lacking methionine and cysteine, removed from the fetal bovine serum (FBS) by dialysation, supplemented with 20 mM HEPES pH 7.5. For radiolabelling, Pro-Mix (Amersham, 100 µCi / 3 cm dish) was added. After 1 hour cells were washed once with PBS and transferred to normal growth media, containing 500 µM methionine and 500 µM cysteine. The labelling was followed over time. Samples were lysed in 500 µl (20 mM Tris-HCl pH 7.7, 150 mM NaCl, 0.5% TritonX100, protease inhibitors) for 10 min on ice, followed by centrifugation at 20,000g for 10 min at 4°C, to remove crude cell debris. The supernatant was centrifuged again at 60,000g for 20 min to clear all insoluble remnants. To avoid unspecific immune-interactions, the supernatant was incubated with 1 µl of pre-immuneserum and 50 µl Protein A sepharose for 1 hour. After discarding the matrix, 5 µl polyclonal antiserum were added and incubation continued overnight at 4°C with gentle shaking. To recover the immunocomplexes, 50 µl protein A Sepharose were added and incubated for 1 hour at 4 °C. The matrix was washed with 500 µl of Neufeld buffer, IMM, IMM/2 M KCl and 3 times 500 µl 0.1x PBS. The Sepharose beads were transferred to a new tube and washed once more with 0.1x PBS before elution with Laemmli buffer. The samples were resolved on SDS-PAGE, the

gels were fixed (20 min, 30% methanol, 10% acetic acid), incubated in Amplify for 15 min (Amersham), dried and exposed on a Phosphorimager screen.

2.7.4 Transfection

Cell lines were transfected with the LipofectAMINE PLUS reagent (Invitrogen), following the manufacturer's manual. DNA sequences encoding human Hop, Tpr2 or the respective mutants were inserted into pcDNA3.1 (Invitrogen) in frame with the C-terminal myc-his tag. A vector expressing ß-galactosidase from a constitutively active promotor (pSV-ß-Gal, Promega) was used to normalize for transfection efficiency. pGRE-luc (Clontech) provided GR-dependent luciferase expression.

The day prior to transfection cells were splitted and 10^6 N2a cells or $0.7*10^6$ HeLa cells were plated per 3 cm dish. A mixture containing 0.5 µg pGRE-luc, 0.5 µg pSV-ß-Gal and 1 µg pcDNA-Tpr2 (wild type or mutant), pcDNA-Hop, pGRΔLBD, empty vector or a combination was incubated for 15 minutes at room temperature with 8 µl PLUS reagent (Promega), diluted in 100 µl OPTIMEM1 (Invitrogen). A premix of 100 µl OPTIMEM1 and 6 µl LipofectAMINE reagent (Invitrogen) was added to each transfection reaction and the samples were incubated for additional 15 min. Finally 800 µl OPTIMEM1 was added and the transfection mixture was applied on the cells which have been washed twice with pre-warmed OPTIMEM1. After 5 hours, 2 ml normal growth media was added. The next day cell culture media was exchanged with medium containing 1 µM dexamethasone or the respective volume of the ethanol solvent control. After 24 hours the cells were washed three times with PBS and harvested with a cell-scraper. Cells were pelleted by centrifugation and lysed in 150 µl reporter lysis buffer (RLB, Promega).

For siRNA experiments, the double-strand RNA oligomers were packed in a separate reaction with LipofectAMINE PLUS using the same conditions as for the plasmids and applied together with the reporter vector transfection. All siRNAs were ordered from Dharmacon as annealed double strands with a concentration of 20 µM. 7.5 µl of each double strand was used to transfect a 3 cm dish. The siRNA oligomers were directed against the sequence 5'-TGCCCAGGCACAGCAGGAGTT of human Tpr2, 5'-TGCTCAGGCACAACAAGAGTT of mouse Tpr2 or comprised a scrambled sequence 5'-

ACTCTATCGCCAGCGT (Non-specific Control VII, Dharmacon) for control purpose. The transfection procedure and hormone stimulation was carried out as described for the plasmid transfections.

2.7.5 β-Galactosidase enzyme assay

Cell culture supernatant from transfection experiments were diluted in RLB to a final volume of 100 µl and preheated for 5 min at 37°C. The two-fold assay buffer (Promega) was also adjusted to 37 °C before use and 100 µl were added to each reaction. The color assay was allowed to continue until all samples showed a weak yellow coloring. 500 µl of 1 M sodium carbonate were added to each sample and the absorbance was measured at 420 nm. The results were corrected for the dilution factor.

2.7.6 Luciferase assay

Luciferase activity in transfected cells was tested by diluting 5 µl of the cell culture supernatants into 100 µl luciferase reagent (Promega). The samples were immediately transferred to a luminometer (EG&G Berthold) and measured for two seconds. Each measurement was repeated twice and the results were averaged.

3 Results

3.1 In silico analysis of Tpr2

Tpr2 was first described by Murthy et al. and named so because it was the second TPR-containing protein listed in their publication (Murthy et al. 1996). Initial work by Wolfgang Obermann led to the preliminary identification of Tpr2 as a novel binding partner of Hsp90. A yeast two-hybrid screen was carried out using the Hsp90 C-terminus as bait (Brychzy et al. 2003), returning Tpr2 as a positive interaction partner. The re-screening of the library with Tpr2 as the bait yielded 4 positive isolates. One encoded for Hsp90 and three for Hsp70. In each case the clones contained the complete C-terminus of the respective chaperone.

The structural features of Tpr2, such as the TPR-motifs and a J-domain, were already reported in the original publication (Murthy et al. 1996). Because the knowledge about TPR interactions has grown since then and more putative domains can be predicted, the protein sequence was analysed again using updated databases. The next paragraph will summarise the relevant information about the Tpr2 protein sequence gained by computer analysis.

3.1.1 Tpr2 sequence analysis

The protein sequence of human Tpr2 (NP_003306) was analysed with the SMART program at the EMBL-Heidelberg (http://smart.embl-heidelberg.de) to obtain an overview of predicted structural motifs.
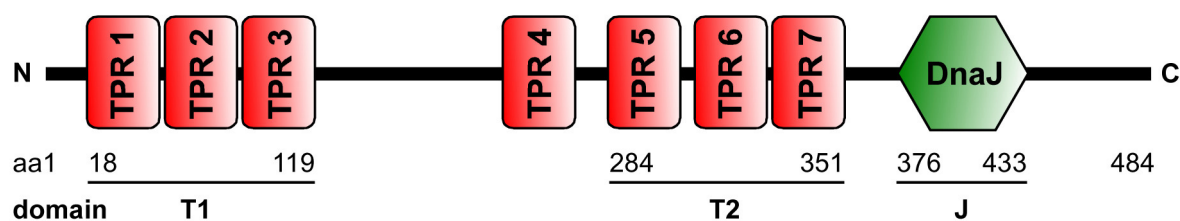
Figure 10   Tpr2 domain prediction.

The Tpr2 protein sequence (NP_003306) was analysed with the SMART program, available at http://smart.embl-heidelberg.de. The domain prediction revealed 7 TPR-motifs (TPR1-7) and a DnaJ like domain (DnaJ). The first (aa 18-119) and the last (aa 284-351) triplet of TPR-motifs were predicted to form a TPR-clamp domain each (T1 and T2). For simplification, the DnaJ domain (aa 376-433) is abbreviated as J. All domain boundaries are indicated by their amino acid residues (aa). The full-length protein consists of 484 amino acids in total.

The human Tpr2 protein has an overall size of 484 amino acids. The SMART-software identified 7 putative TPR-motifs and a DnaJ-domain, as depicted in Figure 10. The first three (aa 18-119) and the last four (aa 200-351) TPR-motifs clustered in two separate regions, divided by an intervening sequence of unknown structure. The DnaJ-domain is located in the C-terminal fourth of the protein and spans from aa 376 to 433. No additional structurally relevant domains, modification sites or signal sequences were predicted for Tpr2. The protein has a calculated molecular mass of 55.5 kDa and a theoretical pI of 7.08.

All four clones, which were identified in the second yeast two-hybrid screen as binding partners of Tpr2, contained at least the C-terminal part of either Hsp70 or Hsp90. This pointed towards the possibility that the TPR-motifs in one or both TPR-clusters may act as TPR-clamp binding sites. To identify if and which TPR-motifs can possibly participate in the formation of a two-carboxylate clamp-anchor, the TPR regions of Tpr2 were aligned with the chaperone binding segments of Hop (TPR1 and TPR2A).

```
Hop TPR1       4  VNELKEKGNKALSVGNIDDALQCYSEAIKLDP----HNHV
Hop TPR2A    225  ALKEKELGNDAYKKKDFDTALKHYDKAKELDP----TNMT
Tpr2 T1       18  AETFKEQGNAYYAKKDYNEAYNYYTKAIDMCP----KNAS
Tpr2 T2      246  LKAKKEDGNKAFKEGNYKLAYELYTEALGIDPNNIKTNAK


Hop TPR1      40  LYSNRSAAYAKKGDYQKAYEDGCKTVDLKPD-------WG
Hop TPR2A    261  YITNQAAVYFEKGDYNKCRELCEKAIEVGRENREDYRQIA
Tpr2 T1       54  YYGNRAATLMMLGRFREALGDAQQSVRLDDS-------FV
Tpr2 T2      286  LYCNRGTVNSKLRKLDDAIEDCTNAVKLDDT-------YI


Hop TPR1      73  KGYSRKAAALEFLNRFEEAKRTYEEGLKHEANN
Hop TPR2A    301  KAYARIGNSYFKEEKYKDAIHFYNKSLAEHRTP
Tpr2 T1       87  RGHLREGKCHLSLGNAMAACRSFQRALELDHKN
Tpr2 T2      319  KAYLRRAQCYMDTEQYEEAVRDYEKVYQTEKTK
                        *
```

Figure 11   **Alignment of TPR-clamps from Hop and Tpr2.**

The sequences of the predicted TPR-clamp domains (T1 and T2) in Tpr2 were aligned against the Hsp70 (TPR1) and Hsp90 (TPR2A) binding two-carboxylate clamp domains of Hop. The conserved residues, which participate in the formation of the two-carboxylate clamp anchor are highlighted in red. Residues in bold contribute to the specificity of chaperone binding. The arginine residues, which are mutated to an alanine in the clamp mutants (dT1 and dT2, see also Figure 20), are marked with an asterisk. The numbers in front of each line refer to the respective amino acid residue of each protein.

The conserved residues, which are essential for the formation of the two-carboxylate clamp anchor are highlighted in red (Scheufler et al. 2000). They were used as the main criteria to predict putative TPR-clamps. Only the first three (TPR1-3) and the last three (TPR5-7) TPR-motifs in Tpr2 fulfil this criterion. These predicted TPR-clamp domains were therefore termed T1 and T2 respectively (Figure 10). The fourth clamp-residue of T1 is an arginine instead of the expected lysine. As predicted from the crystal structure, this exchange should not abrogate TRP-clamp function (Moarefi, personal communication). The TPR4 motif could not be combined with adjacent TPR motifs in a manner such that it would contribute important residues for a two-carboxylate clamp. This makes it unlikely that TPR4 can act as a part of a TPR-clamp, in which an intermediate TPR-motif is structurally looped out to combine otherwise separated regions into one domain. The database entry for Tpr2 lists additional TPR-motifs upstream of TPR4 in the area between aa 132-165 and 167-199. However, the homology of these motifs to a standard TPR-motif is too weak to be recognized by the SMART algorithm as a significant folded unit. Moreover, the whole middle region (aa 132-233) does not fit with the alignment of the classical Hop TPR-clamps and is therefore unlikely to interact with the C-termini of the chaperones. Together, the data suggests, that it is

unlikely that TPR4 is part of either T1 or T2. Since the TPR-motif sequence is highly degenerate it cannot be completely excluded that a third TPR-region is present between T1 and T2, which might contribute to protein-protein interactions other than TPR-clamp formation.

Residues in Hop, which were critical to determine the specificity for binding to one or the other chaperone class (Figure 11, bold letters) were not conserved in either the T1 or the T2 domains of Tpr2. Therefore, it was not possible to predict if Hsp90 or Hsp70 would bind in a domain specific manner, or which TPR-clamp would be preferred by which chaperone. Recent findings show that the specificity of TPR-clamp interactions cannot easily be assigned to certain residues (Odunuga et al. 2003). This means that biochemical data have to complement the *in silico* findings. For this, point-mutants of Tpr2 were constructed in which the last of the five conserved residues in each TPR-clamp was mutated to obtain a disruption of the TPR-clamp function (termed dT1 and dT2 respectively). Details on these mutants are given in chapter 3.3.1 and the mutated residue is marked with an asterisk in Figure 11.

To validate the predicted DnaJ-domain in Tpr2 (also referred to as J-domain for simplicity), the sequence was aligned with the relevant domains of the two major human J-domain cofactors Hsp40 and Hdj2. The alignment is shown in Figure 12.

```
Hsp40 J     3 -DYYQTLGLARGASDEEIKRAYRRQALRYHPDKNK------
Hdj2 J      5 TTYYDVLGVKPNATQEELKKAYRKLALKYHPDKN-------
Tpr2 J    370 KDYYKILGVDKNASEDEIKKAYRKRALMHHPDRHSGASAEV
                                             *


Hsp40 J    37 EPGAEEKFKEIAEAYDVLSDPRK
Hdj2 J     39 -PNEGEKFKQISQAYEVLSDAKK
Tpr2 J    411 QKEEEKKFKEVGEAFTILSDPKK
```

Figure 12   J-domain sequence alignment.

The predicted J-domain sequence of Tpr2 (J) was aligned against the J domain sequence of the human DnaJ homologs Hsp40 and Hdj2. The functional HPD motif, a prerequisite for triggering the Hsp70 ATPase activity, is highlighted in green. Residues in bold mark sequence identities between Tpr2 and Hsp40 and/or Hdj2. The histidine residue, which was mutated to an alanine in the J domain mutant of Tpr2 (dJ, see also Figure 20), is marked with an asterisk.

The sequence comparison revealed a high identity of 45 to 48% between the J-domains (Figure 12, bold letters). The functional indispensable HPD motif (Figure 12, letters

highlighted in green) was absolutely conserved in all sequences. The J-domain of Tpr2 contained 6-8 amino acids adjacent to this motif, which could not be aligned with Hsp40 or Hdj2. Since the HPD motif is localized at a loop between two helixes, the additional amino acids could either extend this loop or be part of the second helix (Huang et al. 1999). For a biochemical verification of the predicted J-domain function, a point mutant of Tpr2 was constructed which exhibited a disruption in its DnaJ function (dJ, see chapter 3.3.1). The mutated residue is marked with an asterisk in Figure 12

The evaluated sequence information on Tpr2, together with the initial data obtained from the yeast two-hybrid screen, strongly suggests that Tpr2 can interact with both Hsp90/Hsp70 via one or more TPR-clamp sites. Tpr2 should also be capable to stimulate the activity of the Hsp70 ATPase via its J-domain.

3.1.2 Taxonomic inspection of Tpr2

The result that Tpr2 is an effector in a chaperone-mediated response on huntingtin aggregation in a fly model (Kazemi-Esfarjani and Benzer 2002) indicated that Tpr2 might be present in more taxonomic classes. A Blast search returned 169 hits, which ranged from Eukarya to Bacteria to *Thermoplasma volcanium*. The closest homologs of Tpr2 are found in the class of the Eukarya and some are listed in Table 6. The protein sequence is best conserved between higher Eukaryotes and the percent identity declines to 27 % in the case of the Tpr2 homolog in plants (e.g. *Arabidopsis thaliana*).

Table 6   **Homologs of Tpr2 in different taxonomic classes.**

organism	identity	Accession number
M. musculus	95 %	NP_062769
D. melanogaster	45 %	NP_523584
S. pombe	38 %	NP_596790
A. thaliana	27 %	NP_850351

The Tpr2 sequence was used in a Blast search (http://www.ncbi.nlm.nih.gov/BLAST) to identify homologs of the protein. A selection of known proteins is summarised with their respective organism, accession number and percent identity. Putative sequences were not considered.

Despite the overall decrease in protein identity towards more unrelated taxonomic classes, the functional conserved TPR-clamp domains and the J-domain retain a significantly high conservation amongst species (Figure 13). Only one of the five conserved two-carboxylate clamp residues (Figure 13, asterisks) in the Tpr2 homologs of *Arabidopsis thaliana*, *Homo sapiens* and *Mus musculus* shows a conservative exchange from lysin to arginine, when compared with the classical TPR-domains of Hop. Interestingly this amino-acid exchange affects the same position in *M. musculus* and *H. sapiens*, which are the closest relatives in this list.

T1-domain alignment

```
H. sapiens        18   AETFKEQGNAYYAKKDYNEAYNYYTKAIDMCPKN--ASY--------
M. musculus       28   AESFKEQGNAYYAKKDYNEAYNYYTKAIDMCPNN--ASY--------
D. melanogaster   49   AEEKKKLGNDQYKAQNYQNALKLYTDAISLCPDS--AAY--------
S. pombe          23   AEKQKAIGNAFYKEKKYAEAIKAYTEAIDLGSDSALAIY--------
A. thaliana      553   CEVWRLRGNQAYKNGYMSKAEECYTHGINSSPSKDNSEYSVKPLALC
                          *       *

H. sapiens        55   YGNRAATLMMLGRFREALGDAQQSVRLDDSFVRGHLREGK-
M. musculus       65   YGNRAATLMMLGRFREALGDAQQSVRLDDSFVRGHLREGK-
D. melanogaster   86   YGNRAACYMMLLNYNSALTDARHAIRIDPGFEKAYVRVAK-
S. pombe          62   YSNRAATYMQIGEFELALCDAKQSDRIKPDVPKTQSRIRQ-
A. thaliana      600   YGNRAAARISLGRLREAISDCEMAASLDPSYIKAYMRAANC
                          *                        *   *
```

T2-domain alignment

```
H. sapiens       244   KALKAKKEDGNKAFKEGNYKLAYELYTEALGIDPNNIKTNAKLYCNR
M. musculus      254   KALKAKKEDGNKAFKEGNYKLAYELYTEALGIDPNNIKTNAKLYCNR
D. melanogaster  275   KQLKEMKENGNMLFKSGRYREAHVIYTDALKIDEHNKDINSKLLYNR
S. pombe         221   RKLENTKNQGNDLFRQGNYQDAYEKYSEALQIDPDNKETVAKLYMNR
A. thaliana      830   SELLRYKNAGNEAVRDRKYMEAVEQYTAALSRNVDSRPFAAICFCNR
                          *      *                               *

H. sapiens       291   GTVNSKLRKLDDAIEDCTNAVKLDDTYIKAYLRRAQCYM-
M. musculus      301   GTVNSKLRQLEDAIEDCTNAVKLDDTYIKAYLRRAQCYM-
D. melanogaster  322   ALVNTRIGNLREAVADCNRVLELNSQYLKALLLRARCYN-
S. pombe         268   ATVLLRLKRPEEALSDSDNALAIDSSYLKGLKVRAKAHE-
A. thaliana      877   AAANQALVQIADAIADCSLAMALDENYTKAVSRRATLHEM
                                              *   *
```

J-domain alignment

```
H. sapiens        370  KDYYKILGVDKNASEDEIKKAYRKRALMHHPDRHSGASA-
M. musculus       380  -DYYKILGVDKNASEDEIKKAYRKRALMHHPDRHSGASA-
D. melanogaster   401  KDYYKILGIGRNASDDEIKKAYRKKALHHPDRHANSSA-
S. pombe          348  KDHYKILGVSKEATDIEIKKAYRKLALVYHPDKNAGN---
A. thaliana       977  LDFFLIMGVKTSDSAADIKKAYRKAALRHHPDKAAQILVR
                                                     +++    :::::

H. sapiens        408  -------------EVQKEEEKKFKEVGEAFTILSDPKK-
M. musculus       417  -------------EVQKEEEKKFKEVGEAFTILSDPKK-
D. melanogaster   439  -------------EERKEEELKFKEVGEAYAILSDAHKK
S. pombe          384  ----------------LEAEARFKEVGEAYTILSDPES-
A. thaliana       1016 SESEGPWLKEILEEVHKGADRLFKMIGEAYSVLSDPTK-
                            ::::::::::::::::
```

Figure 13   Domain-wise alignment of Tpr2 homologs.

The homologs of Tpr2 from different species show a high degree of identity in the regions, which are important for chaperone interaction. The alignment covers the first (T1-domain) and second (T2-domain) TPR-clamp and the DnaJ-domain (J-domain). Identical residues are marked in black and similar amino-acids are highlighted in grey. The conserved TPR-clamp residues, as predicted from the Hop TPR-clamp domain (Scheufler et al. 2000) are indicated with an asterisk. The J-domain specific HPD tripeptide motive is marked with plus signs. The amino-acid stretch between helix 2 and 3 of the J-domain, which is absent in Hsp40, is indicated with colons.

Compared with the highly degenerated TPR-regions, the J-domain in all Tpr2 homologs is conserved to a much higher degree. The functional relevant HPD-motive is present in every sequence (Figure 13, plus signs). Interestingly, when compared with Hsp40, all Tpr2 homologs have additional amino-acids in the region between helix 2 and 3 of the J-domain (Figure 13, colon). This stretch is longest in *Arabidopsis thaliana*, which has the least homology to the human form of Tpr2. This protein also contains a long N-terminal stretch of 553 amino-acids which does not contain predictable domains. Unfortunately no homolog of Tpr2 can be found in *Saccharomyces cerevisiae*.

The E (expect) value for the search-hits in the group of Bacteria and *Thermoplasma* was quite high (up to 1e-12), indicating that only parts of the protein matched with the Tpr2 sequence. This disqualifies them as putative functional homologs. To further evaluate this point, a SMART search was performed, seeking for proteins, which consist of any combination of TPR- and DnaJ-domain. A corresponding arrangement was only found in the superkingdom of Eukarya. This makes it likely that Tpr2 has a specialised function in Eukarya, and has co-evolved with the eukaryotic Hsp70/Hsp90 systems.

3.2 In vivo analysis of Tpr2

The cumulative *in silico* data strongly indicated that Tpr2 is an interaction partner of the main players of the multichaperone machinery. In addition, it contains at least one predicted regulatory domain for Hsp70. This suggests that Tpr2 could affect chaperone interactions and substrate folding. To test this hypothesis, an approach was used which analysed the folding of a stringently Hsp70/Hsp90 dependent substrate. This has been established for the class of steroid hormone receptors in *in vivo* studies. The ability of the receptors to bind hormone and trigger the transcription of genes located downstream of receptor-specific DNA response elements is strictly connected to chaperone function. If the Hsp70/Hsp90 dependent activation cycle is disturbed, the hormone-binding domain of the receptor will remain incapable of binding to its ligand. Although the complex pathways in the cellular environment are less controllable than the conditions in an *in vitro* experiment, the setup is suitable to detect a biologically significant effect of Tpr2 on receptor folding.

3.2.1 Influence of Tpr2 overexpression on GR folding *in vivo*

The activation of the glucocorticoid receptor through the Hsp70/Hsp90 system has been extensively demonstrated. This steroid hormone receptor is endogenously present in most standard cell-culture lines and an activity assay was already established in mouse N2a cells. They could be easily transfected with multiple vectors following a standard protocol for LipofectAMINE (see methods section) and gave a high transfection efficiency of up to 70% for a single vector. Treating the cells with dexamethasone-supplemented medium activated the endogenous GR. To measure the degree of activation, the cells were cotransfected with a plasmid that contained a GR response element (GRE) upstream of a luciferase reporter gene (luc). Hormone-activated receptor bound to the GRE sequence and triggered the expression of the downstream located luciferase gene. After cell lysis the luciferase activity was measured according to a standard assay (Promega) in a luminometer based detection system. A plasmid expressing β-galactosidase under the regulation of a constitutively active promoter was cotransfected to provide a means for normalising the luciferase levels to the efficiency of transfection.

The first approach to look for an effect of Tpr2 on GR folding was to overproduce the protein during a transient transfection. The Tpr2 plasmid (pcDNA-Tpr2) added a C-terminal myc-his tag to the protein, which caused a slower migration behavior on SDS-PAGE and made it distinguishable from the endogenous protein (Figure 14, panel A).
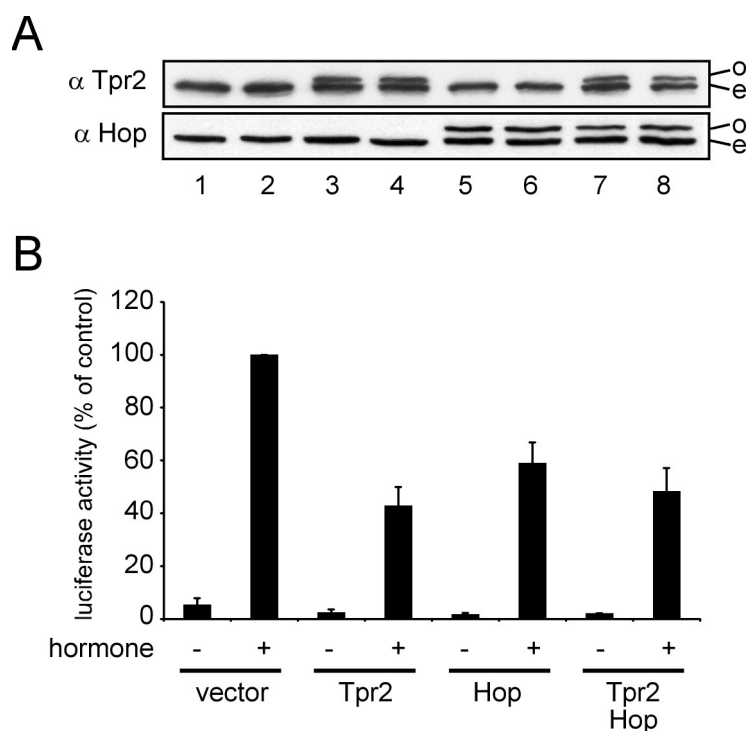

Figure 14   Tpr2 overexpression in N2a cells

Overexpression of Tpr2 reduced the glucocorticoid receptor (GR) dependent activation of a response element (GRE) dependent luciferase construct. The same effect was seen for Hop overproduction or in combination of both. An empty vector (lanes 1 and 2) or vectors containing a myc-tagged Tpr2 (lanes 3 and 4), a myc-tagged Hop (lanes 5 and 6), or a combination of Tpr2 and Hop (lanes 7 and 8), were cotransfected together with the reporter plasmid (pGRE-luc, Clontech) and the control plasmid (pSV-β-Gal, Promega) into N2a cells. After 24 hours cells were treated with medium containing dexamethasone where indicated and harvested after another 24hour incubation. (A) Immunoblot with antibodies against either Tpr2 (α Tpr2) or Hop (α Hop). The endogenous proteins are marked with (e). Overexpressed myc-tagged proteins are labelled with (o). (B) The bars represent GR activated, normalised luciferase levels under the indicated conditions. The error bars show standard deviation from at least three independent experiments. The columns in (B) correspond to the lanes of the immunoblot (A).

The normalised luciferase level in the control cells, cotransfected with an empty vector, was efficiently increased in the presence of hormone (Figure 14B, lane 2) as compared to untreated cells (Figure 14B, lane 1). This induction level was set to 100% and other experiments were normalised accordingly for better comparison. The amount of endogenous Tpr2 was not influenced by the application of steroid (Figure 14A, lanes 1 and 2). Co-

transfection with pcDNA-Tpr2 resulted in production of exogenous Tpr2, as detected by western blot (Figure 14A, lane 3 and 4). The steady state protein level of endogenous Tpr2 was not changed by the overproduction. The myc-tagged Tpr2 did not affect the basal luciferase level in the absence of hormone (Figure 14B, lane 3), but significantly lowered the transcription level after hormone stimulation (Figure 14B, lane 4) to about 40 % of control. This supports the view that Tpr2 does influence the Hsp70/Hsp90 machinery in the activation process of GR. Interestingly, increased amounts of Tpr2 do not improve receptor folding, but inhibit it.

By *in vitro* reconstitution of GR folding with purified proteins it was shown that two ATP consuming steps occur during the transition and folding of the receptor. The first one is during substrate binding to Hsp70 and normally stimulated in the presence of the DnaJ-domain containing protein Hsp40. The second nucleotide hydrolysis occurs after Hsp90 binding (Morishima et al. 2000; Kanelakis et al. 2002). The presence of Hop manipulates Hsp90 by inhibiting its ATPase activity and keeping it in an ADP-bound, high-substrate-affinity state (Prodromou et al. 1999). It was suggested that the modulation of the multichaperone machinery by Hop stimulates the substrate transfer from Hsp70 to Hsp90 and one might speculate that this yields better folding rates. Accordingly, this could be used to rescue the negative effect of Tpr2 on GR folding *in vivo*. To test this possibility, an overexpression vector for Hop was used, which also contained a myc-his tag to make the protein distinguishable from its endogenous form (Figure 14 A, lane 5 and 6). The overexpression did not change the endogenous Hop levels. In the presence of elevated cellular Hop concentrations the luciferase activity after hormone stimulation was reduced to about 60 % compared to the control (Figure 14 B, Hop). This means that the overall effectiveness of chaperone dependent GR folding is already maximised and excess Hop disturbs the system much like Tpr2 does. Since biological systems are usually optimised in their function it might be unlikely to find proteins that actually achieve an improvement of these processes after overexpression *in vivo*. Interestingly, when both cofactors were overexpressed at the same time, the negative effects were not additive (Figure 14 A, lane 7 and 8; B). This indicates that the folding of GR cannot be completely abrogated below a certain background level, solely by the overexpression of the two cofactors.

3.2.2 Influence of Tpr2 knock-down on GR folding

If increased Tpr2 levels influence the efficiency of the multichaperone machinery, its absence could also result in a change in the GR activity rates. Reducing endogenous protein levels with conventional methods involves time-consuming experiments, including the construction of stable cell lines. Only recently an easily applicable method to down-regulate endogenous protein levels became available for cell culture cells. siRNAs (small interfering RNA) are transfected by conventional methods like Oligofectamine or other lipofectants and cause a transient knock-down of the target protein (Elbashir et al. 2001). Although the mechanism behind this process is not completely understood at the moment, the working model is summarised here. A 21mer RNA duplex, complementary to the target RNA sequence, is transfected into cells where it recruits additional cofactors. In this process the double strand is partially opened and this allows it to hybridize with the complementary endogenous target RNA. This in turn is initially modified or cleaved, which finally leads to its complete degradation. The siRNA oligomer stays bound to its cofactors and can target the next RNA. Finally this process leads to a so-called knock-down effect, that is a transient reduction of the target protein levels.

In order for the siRNA treatment to obtain a measurable result, it is important that the target protein half-life is lower than the time span of the experiment. Proteins with longer half-life times must be knocked-down by successive siRNA treatments. To determine the half-life of Tpr2, a pulse-chase experiment was carried out, in which the endogenous proteins were labeled with radioactive methionine and cysteine followed by a chase with unlabelled amino acids. At different time-points cells were lysed and Tpr2 was immunoisolated from the supernatant by antibody precipitation. The samples were resolved on SDS-PAGE and evaluated with the Phosphorimager (Figure 15).
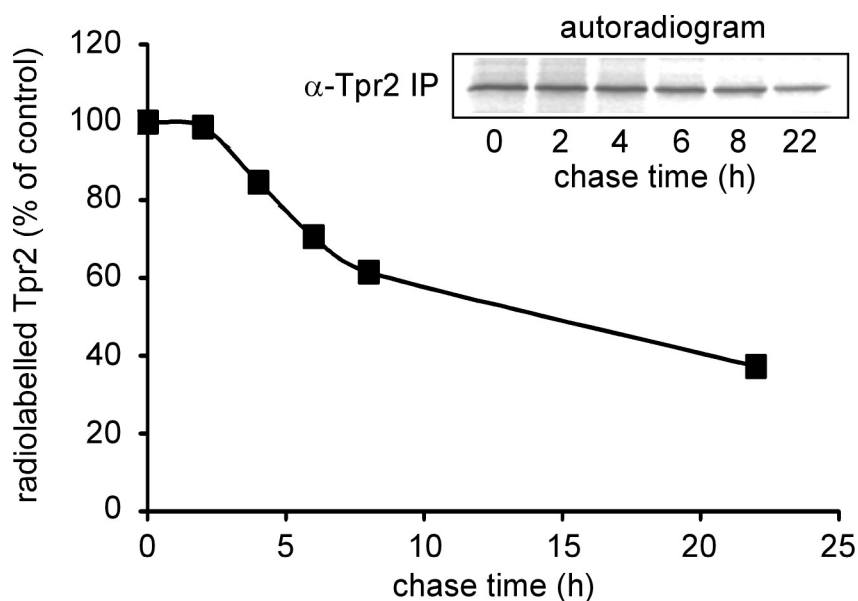
Figure 15   Estimation of Tpr2 half-life.

The Tpr2 half-life was calculated by immunoprecipitation from radio-labelled N2a cells. Cells were incubated in starvation medium containing radioactive mehionine and cystein (Promix, Amersham) for 1 hour. After washing, cells were incubated in normal growth media containing excess cold methionine and cystein (500 µM each). At the indicated time points the cells were harvested and Tpr2 was immunoprecipitated. The immunopellets were resolved on SDS-PAGE and quantified with a Phophorimager system. The percentage of radiolabelled Tpr2 was plotted against the time of the chase-period. The inset shows the original autoradiogramm.

The calculated half-life for Tpr2 is about 14 hours. If the siRNA technique works, it should theoretically be possible to achieve a knock-down effect during the normal experimental time frame used for the GR activity assay, which is designed to be 2 days. To test this assumption, mouse Tpr2-siRNA was applied to N2a cells and samples were taken 24 and 48 hours after transfection. Unfortunately it was not possible to obtain a significant knock-down efficiency when siRNA was used in this cell line, as detected by immunoblotting. Experimentally, the choice was either to order one or more siRNAs directed against other sequences in mouseTPR2 or to switch to a human cell line instead. Since the Tpr2 detected in the yeast two-hybrid screen was from a human cDNA library, it seemed reasonable to switch to a human cell culture line. The target region was kept the same, but it contained differences in three nucleotides between the species (Table 7, letters in bold red). Therefore, an adequate siRNA oligomer was used for the human cell line.

```
mouse         TGCCCAGGCACAGCAGGAGTT

human         TGCTCAGGCACAACAAGAGTT

scrambled     ACTCTATCGCCAGCGTGACTT
```

Table 7   siRNA target sequences for Tpr2 knock-down.

The human and mouse target sequences for siRNA differ at three positions. The forward nucleotide sequences of the siRNA double-strand oligomers, used for Tpr2 knock-down, are aligned against the scrambled control sequence. Differences between the human and mouse homolog of Tpr2 are highlighted in red.

In the search for a good host system, HeLa cells appeared to be the best candidates for siRNA treatment. They survived transfection conditions without visible defects and displayed a Tpr2 knock-down after 48 hours, as detected by immunoblotting (Figure 17 A, lane 3 and 4). To make sure that the new cellular background gave a comparable result to the established N2a assay, the overexpression of Tpr2 in HeLa cells was repeated first. Overproduction resulted in 60% reduction of GR activity after hormone treatment, as compared to mock transfected cells (data not shown). Although the effect is less pronounced than in N2a cells, increased Tpr2 levels reproducibly showed a negative influence on GR activity in both cell lines.

Immunofluorescence (IF) pictures of HeLa cells were taken to monitor the efficiency of the Tpr2 siRNA treatment (Figure 16 g-i). To detect unspecific effects, control cells were either mock transfected (Figure 16 a-c) or treated with a commercially available scrambled RNA control duplex (Table 7, scrambled). The sequence chosen has approximately the same GC content as the Tpr2-siRNA oligomer, but does not target any known RNA sequence (scRNA, Figure 16 d-f).
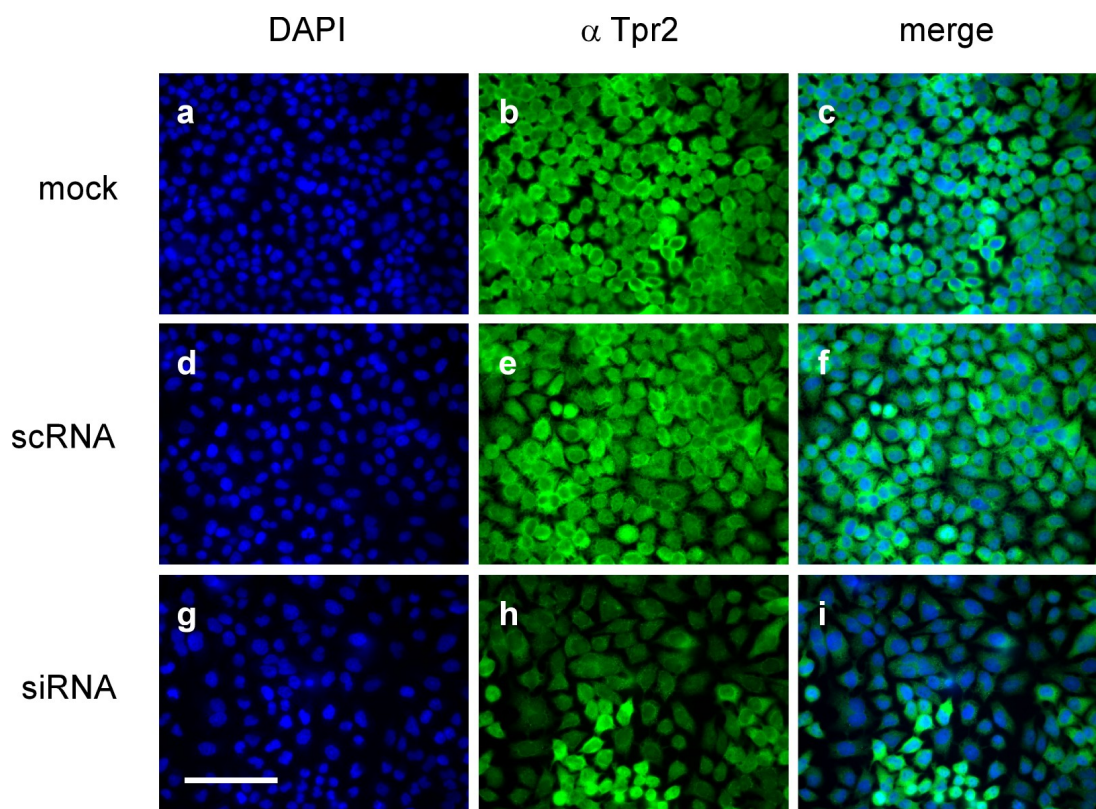
Figure 16   Immunofluorescence of Tpr2 siRNA knock-down.

Immunofluorescence of HeLa cells after paraformaldehyde (PFA) fixation and Saponin treatment. Nuclei were stained with DAPI (a, d, g) and Tpr2 was detected with an affinity purified Tpr2 antibody (α Tpr2) and visualized with a FITC conjugated secondary antibody (b, e, h). The last column (c, f, i) contains a merged image of the preceding pictures in the row. The cells were either mock treated with transfection reagent alone (a-c), or transfected with 7.5 µl (20nM) of a commercially available scrambled RNA (scRNA, control oligo V, Dharmacon) control oligomer (d-f), or the same concentration of a specific Tpr2-siRNA double-strand oligomer (g-i). The pictures were taken at a 40-fold magnification. The scale bar (g, white bar) represents 100 µm.

An affinity purified polyclonal Tpr2 antibody was applied to detect the endogenous protein. A secondary FITC-labeled antibody was used to visualise the localisation of the primary Tpr2 antibody during fluorescence microscopy (Figure 16 b, e, h). The nuclei were stained with DAPI (Figure 16 a, d, g) and both pictures were merged for ease of comparison (Figure 16 c, f, i). Endogenous Tpr2 shows a uniformly cytoplasmic distribution (Figure 16 b). A partial nuclear localisation cannot be completely excluded with this microscope technique, but the abundance of Tpr2 in the nucleus is comparatively low. siRNA treatment showed a clear reduction of Tpr2 expression in transfected cells (Figure 16 i), which did not occur in both control experiments (Figure 16 c, f). Residual amounts of Tpr2 remained in the siRNA treated cells. It is likely that transfected cells diverge in the level of Tpr2 reduction due to unequal uptake of the siRNA oligomer. Since the transfection efficiency was

incomplete, a number of untransfected cells retained normal Tpr2 levels (Figure 16 i). Together the IF-data demonstrate that siRNA can be used as a tool to transiently knock-down endogenous Tpr2 levels in HeLa cells. This was also confirmed by western blot (Figure 17 A, lane 3 and 4).
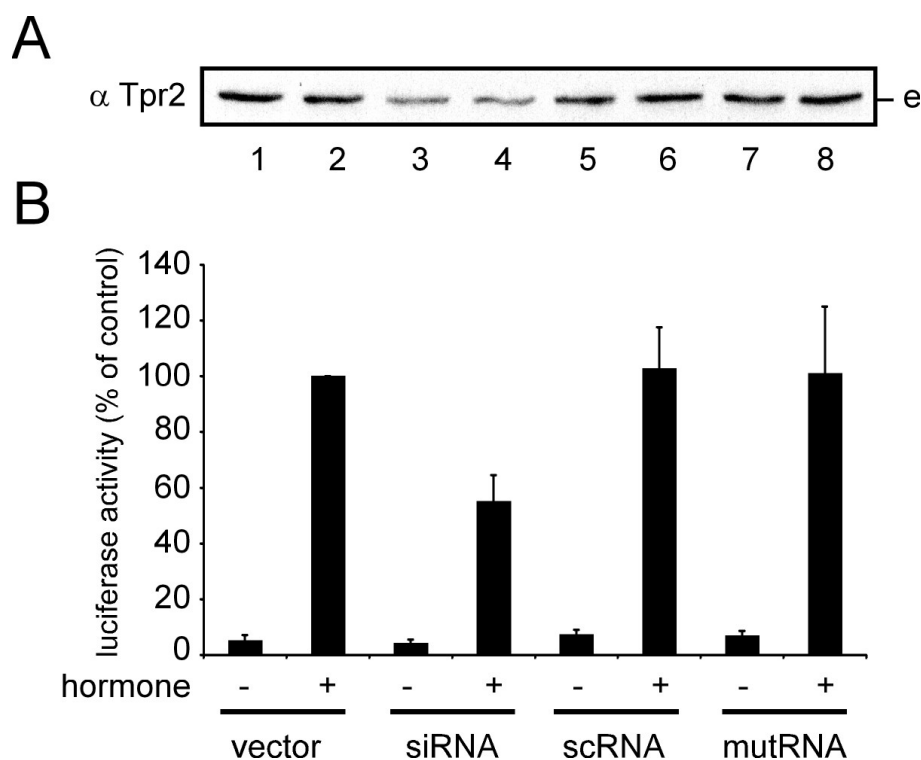

Figure 17   Tpr2 knock-down in HeLa cells.

Treatment of HeLa cells with siRNA against Tpr2 results in a detectable knock-down of the protein level and a decrease in the efficiency of GR mediated luciferase transcription. HeLa cells were seeded in 3cm dishes and transfected with the reporter vector (pGRE-luc, Clontech) and the control vector (pSV-β-Gal, Promega) (Figure 17, lanes 1-8). Where indicated, 7.5 µl (20 nM) RNA double-strand oligomers were cotransfected as a separately packed transfection reaction. These transfections contained siRNA directed against Tpr2 (lanes 3 and 4), a scrambled sequence control oligomer (scRNA, lanes 5 and 6), or a mutated RNA double strand oligomer, which contained three nucleotide exchanges (mutRNA, lanes 7 and 8). One day after transfection cells where treated for 24 h with 1 µM dexamethasone where indicated and harvested. (A) Immunoblot with antibodies against Tpr2 (α Tpr2). The endogenous protein is marked with (e). (B) The cell lysate was tested for luciferase activity. The columns represent GR-activated normalised luciferase levels under the indicated conditions. The error bars show standard deviation from at least three independent experiments. The columns in (B) correspond to the above immunoblot (A).

To determine the influence of lower Tpr2 levels on the efficiency of GR folding the siRNA duplex had to be cotransfected together with the reporter vectors. It turned out that when vector and siRNA oligmomer were combined in the packing step of the transfection, the

uptake of at least the plasmids was drastically reduced. This was determined by measuring the levels of the constitutively expressed β-galactosidase. The reason for this remained unknown. To overcome this problem the siRNA and the plasmids were packed in two separate preparations and then applied simultaneously. This increased the possibility that transfected cells took up only one component or took up different ratios of plasmid and RNA-duplexes. In addition to that, the transfection efficiency was never complete. Together these factors contribute to an underestimation of the effect of the Tpr2 knock-down. In a control experiment the scrambled RNA control-oligomer (scRNA) was used to trace unspecific effects. A difference of three nucleotide exchanges in the 21-mer target sequence was reported to be sufficient to abolish the knock-down effect on the target protein (Elbashir et al. 2001). Therefore, the mouse Tpr2-siRNA duplex was used as a mutated siRNA control (mutRNA). Vector transfected (Figure 17 A, lane 1 and 2) or control transfected cells (Figure 17 A, 5-8) had equal amounts of endogenous Tpr2 and this was not affected by hormone treatment. When the Tpr2-siRNA was co-applied, the Tpr2 expression levels were diminished significantly (Figure 17 A, lane 3 and 4) 48 hours after the transfection, independent of the hormone state. Treatment of control cells with dexamethasone caused a strong activation of endogenous GR relative to untreated cells, which was again measured by the luciferase activity, normalised for the β-galactosidase levels (Figure 17 B, vector). The basal level of luciferase transcription activity was not changed after the addition of the control RNAs, when compared to the vector control (Figure 17 B, compare lane 1, 3 and 5). After hormone application only the siRNA treated HeLa cells displayed a significant reduction in the luciferase activity (Figure 17 B, compare lane 2, 4, 6 and 8), which was equal to the reduction seen after overexpression of Tpr2 in HeLa cells. This demonstrates that the lower abundance of Tpr2 is accompanied by a reduced efficiency of Hsp70/Hsp90 mediated GR activation.

3.2.3 Effects of Tpr2 on receptor transactivation events

To show that the reported effects were based exclusively on the efficiency of chaperone mediated GR folding, the endogenous levels of GR were measured under the applied transfection conditions (Figure 18).
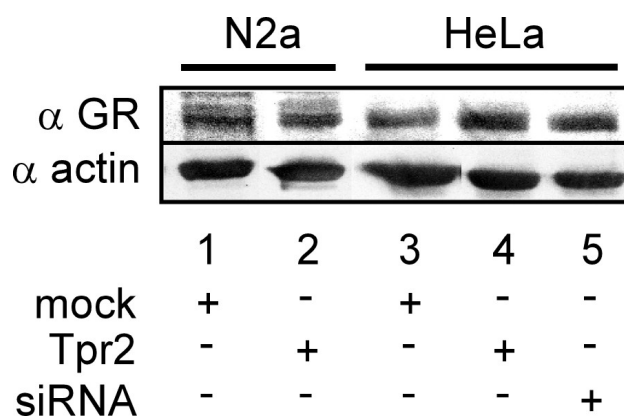
Figure 18   GR levels under transfection conditions.

The endogenous GR levels are not changed by Tpr2 overexpression or knock-down. N2a or HeLa cells were seeded in 3cm dishes and transfected with an empty vector control (lanes 1 and 3), with a Tpr2 overexpression plasmid (lanes 2 and 4), or with siRNA oligomer directed against Tpr2 (lane 5). One day after transfection the medium was exchanged and cells were harvested and lysed in reporter lysis buffer (RLB, Promega) 24 h later. Equal amounts of total cell lysates were resolved on SDS-PAGE and analysed by immunoblotting. Actin served as a loading control (N350, Amersham) and GR was detected with a commercially available polyclonal antibody (H-300, Santa Cruz).

GR and actin were detected by western blot and actin served as a loading control. The endogenous levels of GR in N2a cells (Figure 18, lane 1 and 2) were much lower compared to HeLa cells (Figure 18, lane 3-6). For a better comparison between the two cell lines, the darkness of the blot was adjusted in Figure 18. Importantly, the amounts of endogenous GR did not change under all experimental conditions. This applied to both cell lines. The result strengthens the view that the influence of Tpr2 on the activation of GR happens at the level of folding rather than by changes in the expression pattern.

Although the previous data indicated that Tpr2 acts at the folding step, it cannot be completely excluded that downstream events in the receptor cascade are influenced as well. For example, it has been reported recently that the Hsp90 cofactor p23 alone or in combination with the chaperone can act in the disassembly of transcriptional regulatory complexes (Freeman and Yamamoto 2002). Since Tpr2 is a putative Hsp90 binding protein such an effect needed to be taken into account. To answer this question, a constitutively active form of GR was overproduced in N2a cells. This mutant lacked the LBD-domain, which is normally stabilised by Hsp90 in a hormone-receptible state (Hollenberg et al. 1987). It therefore becomes independent of hormone and chaperone activity regarding its activation.
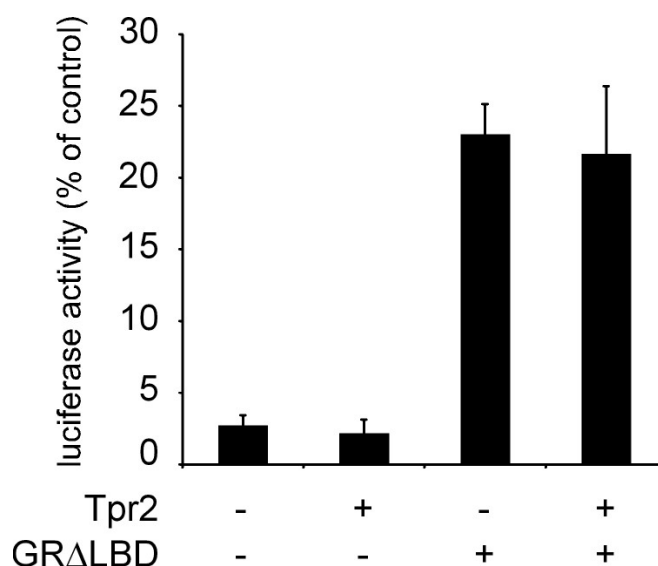
Figure 19   **Transient expression of a constitutively active GR (GRΔLBD)**

The GR dependent activation of luciferase by a constitutively active receptor (GRΔLBD) is not changed by Tpr2 co-overexpression. N2a cells were transfected with the luciferase response plasmid (pGRE-luc, Clontech), the β-Gal control plasmid (pSV-β-Gal, Promega) and the indicated overexpression vectors. One day after transfection, medium was exchanged and cells were lysed 24 h later. Normalised GR-activated luciferase levels are plotted. The error bars show standard deviations of at least three independent experiments. The constitutively active GR (GRΔLBD, (Hollenberg et al. 1987)) lacks the LBD domain and is independent of hormone and Hsp90 function.

As the activity of the mutant GR (GRΔLBD) is independent of hormone, the bars in Figure 19 represent experiments in the absence of dexamethasone. Overexpression of GRΔLBD increased the luciferase expression to about 10-fold over the basal level. The overexpression of Tpr2 did not influence the activation of the GRE-luc construct, neither in the absence, nor in the presence of the constitutively active GR. This result is in agreement with an influence of the Tpr2 only on the Hsp90 dependent activation step of the receptor and not on downstream signaling events.

The cumulative *in vivo* data show that whenever the cellular level of Tpr2 is changed, no matter if it is increased or decreased, the multichaperone machinery works less efficiently in the folding of its stringent substrate, the glucocorticoid receptor. Since Tpr2 has not been reported as a major component of the Hsp70/Hsp90 system, it is likely that it only interacts on a transient basis and is underrepresented in isolated complexes. In agreement with this observation, its abundance is about ten-fold lower than that of Hop (Wolfgang Obermann, personal communication), which would be consistent with a more regulatory role. In

summary the *in vivo* data provide evidence that the cellular levels of Tpr2 are finely tuned for maximum efficiency of the chaperone machinery and Tpr2 influences the folding of Hsp70/Hsp90 dependent substrates.

3.3 In vitro dissection of Tpr2 effects

To address the question of how Tpr2 participates in the regulation of the multichaperone machinery, a set of *in vitro* experiments were carried out, which allowed to look at isolated aspects of the folding process.

3.3.1 Construction of Tpr2 mutants

The appropriate approach, designed to attribute certain effects of Tpr2 to its structural elements, was to construct mutants, which retained only some functional domains. It turned out that a number of deletion mutants had a strong tendency to become insoluble and to aggregate during purification. To avoid this, point mutants of Tpr2 were constructed by site-directed mutagenesis and all of them remained soluble after purification. This approach had the positive effect that experimental observations could be closely linked to specific changes in the protein, excluding false results arising from folding problems of differently sized deletion mutants.
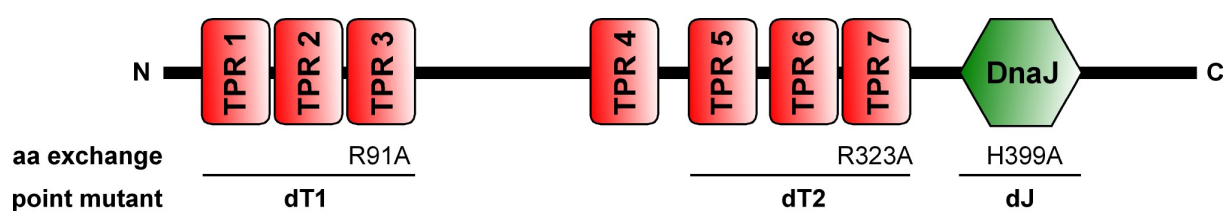

Figure 20   Overview of Tpr2 point mutants.

Point mutations were introduced into Tpr2 to disrupt functional chaperone interactions. The mutations are marked with the respective amino-acid number, preceded by the original amino-acid and followed by the altered one. The mutated proteins were marked with a "d" to indicate that the respective part is defective in it function. For the TPR mutants, the last of the five conserved dicarboxylate clamp residues was mutated (dT1 and dT2). The double clamp mutant was termed dT12 respectively. In the case of the J-domain mutant, the histidine of the conserved HPD motif was mutated to an arginine and the mutant was called dJ. The triple mutant carries the name dT12J.

Based on the available information from the Hop-TPR interaction studies (Scheufler et al. 2000; Brinker et al. 2002) it was decided to mutate the fifth of the conserved residues, which mediate the two-carboxylate clamp function, to an arginine. This should result in a more than 90% reduced binding capacity between the chaperone C-termini and the TPR-clamp domain. The respective amino acids are marked with an asterisk in Figure 11. Because the resulting mutants were expected to be disrupted in their TPR-clamp function, they were labeled with the affix "d" (Figure 20). Single clamp mutants (dT1: R91A, dT2: R232A) and a double clamp mutant (dT12: R91A R323A) were constructed, using the pProEX-HTa-Tpr2 plasmid as a source vector (Brychzy et al. 2003). Thus, the proteins contained an N-terminal his-tag, followed by a TEV cleavage sequence. This offered the advantage that the proteins were easy to purify via a Ni-NTA preparation protocol and the tag could be removed by a TEV digestion if desired. To disrupt the function of the J-domain it was necessary and sufficient to mutate the histidine in the functional HPD motif (Tsai and Douglas 1996) to an arginine. The respective amino acid is marked with an asterisk in Figure 12. Two mutants were constructed, one that carried only the J-domain mutation (dJ: H399A) and another which combined it with the double clamp mutant (dT12J: R91A R323A H399A). Combined mutations were introduced in successive steps and the accuracy of each mutation was verified by DNA sequencing. The proteins were expressed in *E. coli* BL21 pLysS cells after IPTG induction for 5 hours at 21°C. Purification was carried out as described in Materials and Methods. All proteins expressed equally well and had the same size as judged by SDS-PAGE.

When the purified recombinant Tpr2 protein was subjected to size exclusion chromatography, it eluted at about the size of the monomer (Figure 21 A, blue gel). The resolution of the column was not sufficient to exclude a possible dimerisation of the protein, but more important, there was no evidence for multimer formation or aggregated material.
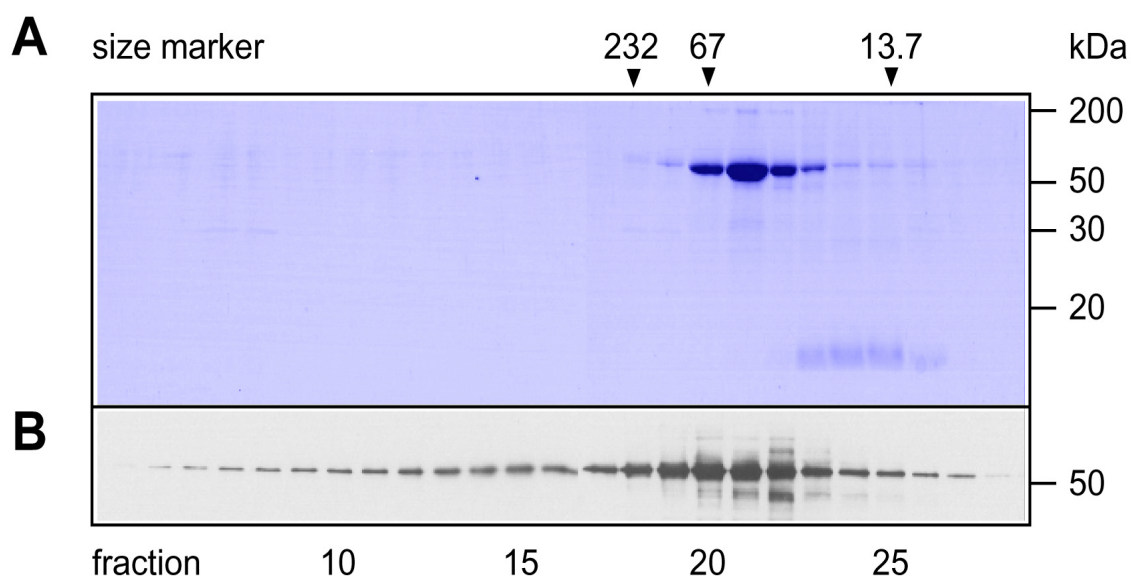
Figure 21   Tpr2 gel filtration on S200 column

Tpr2 elutes from gel filtration as a single peak in the monomeric size range. Recombinant Tpr2 was Ni-NTA purified from BL21pLysS cells as a myc-his tagged fusion protein with a TEV cleavage site. After removing the tag, the protein was subjected to gel filtration on an S200 column. (A) Gelfiltration profile of purified Tpr2. The protein elutes as a symmetric peak around the size predicted for a monomer. (B) Immunoblot of Tpr2, which was preincubated in RL before gelfiltration. The protein was detected with a polyclonal αTpr2 antibody. The main protein peak matches the elution profile of the purified protein in buffer.

When Tpr2 was incubated at a final concentration of 15 µM in desalted rabbit reticulocyte lysate (RL) before gel filtration (Figure 21 B, western blot), the majority eluted at the same position as the purified protein. A smear towards the high molecular weight fractions was observed which might indicate interactions between Tpr2 and higher order complexes. The fact that no clearly defined secondary peak was found means that interactions were only transiently stable under these conditions or Tpr2 can participate in a number of differently assembled complexes. In summary, the information obtained from the gel filtration experiment only indirectly contributes to the hypothesis that Tpr2 is a transient factor of the multichaperone machinery. To clarify this point, co-precipitation experiments from reticulocyte lysate were carried out.

3.3.2 Tpr2 co-precipitation experiments from RL

The set of his-tagged Tpr2 mutants was tested in co-precipitation experiments to screen for the predicted chaperone interactions. To obtain amounts of binding partners visible on Coomassie Blue stained gels, the mutants had to be added in excess, at a final concentration of 10μM. The binding reaction was carried out at 4°C, which stabilised protein-protein interactions. The recovered beads were washed and eluted with a high salt incubation (Figure 22 A, top panel). High salt is known to be sufficient to disrupt TPR-clamp binding (Young et al. 1998; Brinker et al. 2002). His-tagged Tpr2 proteins were subsequently eluted from the Ni-NTA beads with Laemmli buffer containing 25 mM EDTA (Figure 22 A, lower panel, blue-gel).

When compared to the control experiment without Tpr2 (Figure 22 A, lane 7), the high salt elution after the incubation with Tpr2 wild-type protein yielded two major protein bands at the size of about 70 and 90 kDa (Figure 22 A, lane 1). The proteins were later identified by immunoblotting as Hsp70 and Hsp90 respectively (Figure 22 B, lane 2). The dT1 mutation had no obvious visible effect on chaperone binding, whereas the dT2 mutant demonstrated a clearly reduced binding to Hsp90 as compared to wild-type (Figure 22 A, lane 1-3). The double clamp mutant (dT12) bound both chaperones very poorly (Figure 22 A, lane 4). This result provides evidence that both TPR regions contribute to chaperone binding. In addition, it suggests that the clamp binding has a certain degree of cooperativity and selectivity between T1 and T2. The mutated J-domain (dJ) had no obvious negative influence on Hsp70/Hsp90 interaction (Figure 22 A, lane 5). Again the triple mutant (dT12J) retained the lowest binding capacity, comparable to the Ni-NTA control without additional protein (Figure 22 A, lane 6 and 7). In summary, Hsp70 and Hsp90 appear to be the main interaction partners of Tpr2 in RL under these conditions. The binding is sensitive to high salt and to a mutation in one of the conserved clamp residues. Therefore, a TPR-clamp protein interaction, similar to that seen with Hop, is likely. In contrast to the specific selectivity of the Hop TPRs, the TPR-clamps in Tpr2 do not seem to discriminate between the two chaperone classes. To emphasize this point, competition experiments were carried out.
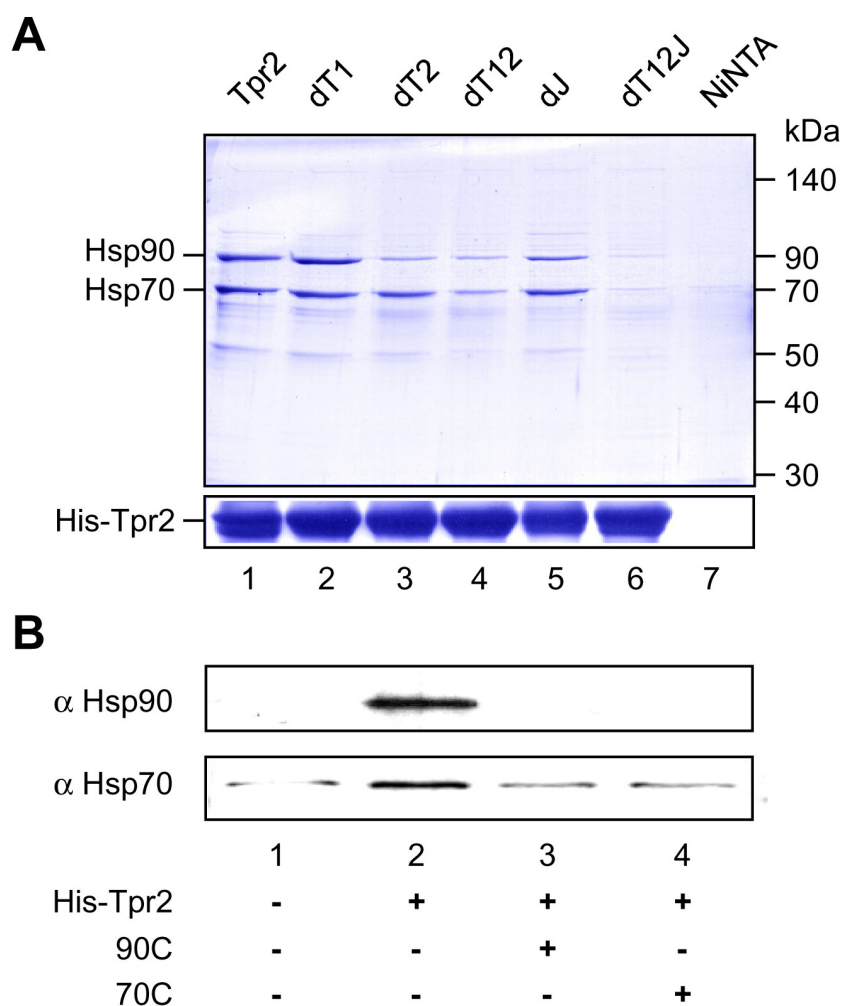
Figure 22 **Tpr2 co-precipitations from RL and chaperone binding competition.**

Both TPR clamps in Tpr2 serve as binding sites for Hsp70 and Hsp90 without discriminating between the chaperones. The recombinantly expressed his-tagged Tpr2 proteins were incubated in RL, desalted in buffer B and substituted with 30 mM imidazole at 4°C. After 30 min Ni-NTA beads were added and the samples were incubated for additional 30 min with gentle shaking. After recovering the beads, TPR interactions were disrupted by a high salt elution (20 mM Tris-HCL, pH 7.5, 500 mM NaCl). The remaining protein was eluted by boiling in Laemmli buffer, substituted with 25 mM EDTA. The samples were then resolved on SDS-PAGE. (A) Coomassie Blue stained gel of Tpr2 co-precipitation after high salt elution (top) and Laemmli elution (bottom). 10 μM of wild type protein (Tpr2), the single clamp mutants (dT1 and dT2), the double clamp mutant (dT12), the J domain mutant (dJ) or the triple mutant (dT12J) were used. The two major protein bands in the high salt elution step were identified as Hsp70 and Hsp90 by immunoblotting (see also (B)). Ni-NTA without additional protein was used as a background control (Ni-NTA). The bottom panel shows the subsequently eluted Tpr2 proteins. (B) Immunoblot of a Tpr2 co-precipitation high salt elution. The proteins were identified with antibodies against Hsp70 (SPA820, Stressgen) and Hsp90 (polyclonal peptide antibody). Tpr2 was used at a concentration of 10 μM and where indicated C-terminal fragments of Hsp70 (70C) and Hsp90 (90C) were present at five-fold molar excess over Tpr2 during the incubation.

To compete with the binding of chaperones to Tpr2, a 5-fold excess of the respective chaperone C-terminal fragments (70C, 90C) over Tpr2 was added during the co-precipitation experiment (Figure 22 B, lane 3 and 4). The control co-precipitation showed minimal background binding of Hsp70 and Hsp90, as detected by immunoblotting (Figure 22 B, lane 1). The addition of Tpr2 alone resulted in a maximal co-precipitation efficiency for both chaperones (Figure 22 B, lane 2). In the presence of either 70C or 90C, the binding of both chaperone classes was equally reduced to background levels (Figure 22 B, lane 3 and 4). Thus, the competition of Hsp70 and Hsp90 for binding to the same TPR-clamp sites in Tpr2 can best be compared to CHIP, where one clamp interacts with both Hsp70 or Hsp90. Although the co-precipitation experiments clearly demonstrate that the chaperone binding is mediated by TPR-clamps, they only allow a rough estimation of the interaction affinity. To obtain a quantitative data set, surface plasmon resonance (SPR) experiments were carried out with a BIAcore setup.

3.3.3 Quantitative analysis of Tpr2-TPR interactions

The SPR analysis of biomolecular interactions has already been established to monitor TPR-clamp protein contacts between Hop and Hsp70 or Hsp90 (Brinker et al. 2002). Its advantages are real-time measurements and relatively low sample consumption compared to stoped-flow measurements. Plasmon resonance is a phenomenon which is induced by a total internal reflection event of incoming light at the boundary between two media with different refraction indexes. The sensor chip in the BIAcore machine forms such a boundary by placing a gold-film next to a liquid phase. Monophasic light is focused on the gold side and a two-dimensional array detects the reflected contingent. A software program back-converts this information into the respective maximum plasmon resonance angle. Changes in this angle correspond to changes in the concentration of biomolecules at the surface of the sensor chip. This provides the means to directly detect protein-protein interactions when one of the partners is immobilised to the chip. For the following experiments a peptide, composed of the last 12 C-terminal amino acids of either Hsp70 (70C-12) or Hsp90 (90C-12), was immobilised to the surface of a B1 sensor chip. Data obtained with Hop-TPR interactions demonstrated that these peptides are sufficient to form a stable TPR-clamp contact and have binding kinetics equal to the full-length proteins (Scheufler et al. 2000; Brinker et al. 2002). Additionally, this approach avoids side effects arising from interactions with other parts of the

chaperones. Also, it was not possible to immobilise native full-length proteins since the washing conditions for removing bound Tpr2 after each experiment included harsh, denaturing conditions, which cause irreversible denaturation to native proteins. Therefore, this experimental setup is designed to focus on TPR interactions and disregards additional protein-protein contacts. The binding kinetics of Tpr2 to either 70C-12 (Figure 23 B) or 90C-12 (Figure 23 A) showed very fast on and off kinetics. They looked very similar to Hop-chaperone interactions and cannot be resolved on the time scale of the experiment. Thus, association and dissociation constants could not be directly calculated. To obtain the binding affinities (K_D), a dilution series of Tpr2 was injected and the relative response units during equilibrium binding (R_{eq}) were plotted against the protein concentration (Figure 23 A). Ideally, the graph should reach saturation, but due to limitations of the maximal concentration of Tpr2 in solution, it was not possible to achieve more than 30 μM.
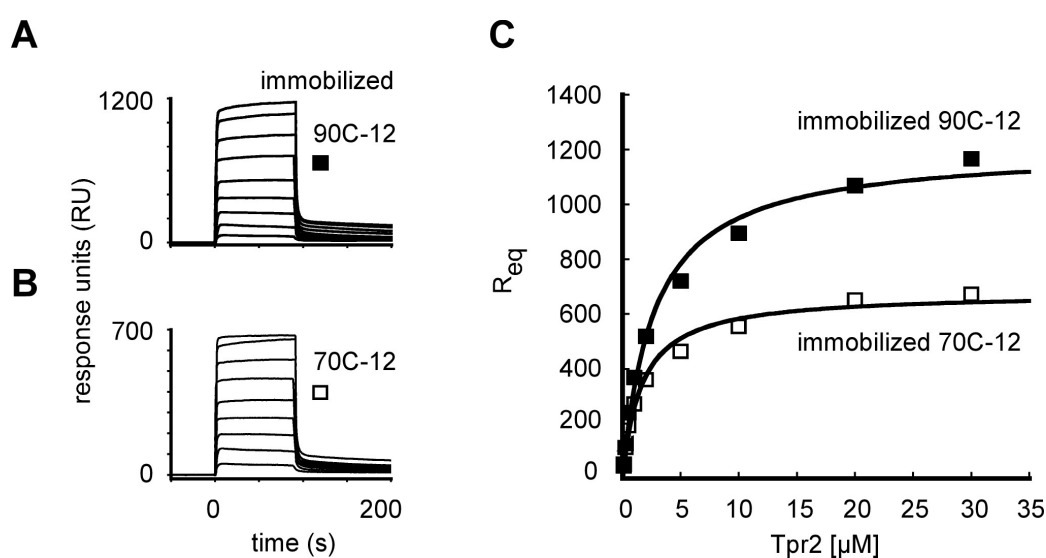

Figure 23   SPR measurement of Tpr2 interactions with immobilised C-terminal chaperone peptides.

12mer peptides containing the C-terminus of either Hsp70 (70C-12) or Hsp90 (90C-12) were covalently coupled to a B1 BIAcore chip. Increasing concentrations of Tpr2 were injected for 1 min, followed by a 5 min dissociation period and regeneration of the chip surface before the next injection. (A) The Hsp90 peptide (90C-12) was immobilised on the chip. Binding kinetics of a dilution series of Tpr2 (0.1, 0.25, 0.5, 1, 2, 5, 10, 20, 30 μM) were followed with the BIAcore device. The consecutive runs are merged in one graph. Response units (RU) are in arbitrary units. (B) The Hsp70 peptide (70C-12) was immobilised on the chip. The experiment and the graphic analysis was carried out as described for A. (C) The response units during equilibrium binding (R_{eq}) of the previous experiments are plotted against the Tpr2 concentration. The data were processed assuming a simple steady-state binding model, using the BIAcore software and the curve fit is plotted. Black squares are response units measured with immobilised 90C-12, open squares are equilibrium response units measured with immobilised 70C-12.

The binding affinities summarised in Table 8 were calculated with a standard BIAcore program that carries out a curve fit based on the equilibrium response units dependent on the corresponding protein concentration in the liquid phase. As mentioned before, the limitations in the achievable concentration of the protein in solution decreases the accuracy of the curve fit for weaker interactions (dT1 and dT2) and leads to an underestimation of the respective K_D value.

Table 8   **Thermodynamic binding constants (K_D) of Tpr2 chaperone interactions.**

	K_D (µM)		
	Tpr2	dT1	dT2
70C-12	1.6 ± 0.2	9 ± 0.6	12.9 ± 0.3
90C-12	2.7 ± 0.4	9.3 ± 1.1	21.3 ± 3.5

The data acquisition for the clamp mutants (dT1 and dT2) was carried out as described for the wild type protein in Figure 23. A steady-state binding model, available with the BIAcore software was used to calculate the K_D values from the titration curves.

The binding constants for Tpr2 wild type are in the range of the equivalent Hop interactions and therefore in a biological relevant range, varying from 1.6 µM for 70C-12 to 2.7 µM for 90C-12 (Table 8). Consistent with the RL co-precipitation experiments the dT2 mutant had a stronger reduction in binding as compared with the dT1 mutant (Table 8, compare dT1 and dT2). Both single clamp mutations reduced the affinity to the C-terminal peptide, strengthening the conclusion that the system relies on a TPR-clamp interaction, as there are no additional interaction sites available in this experimental set-up. Since the binding of the double clamp mutant dT12 yielded a very weak signal, it was not feasible to obtain analysable binding affinities with this technique. To be able to compare the different mutants, they were injected at a constant concentration of 1 µM and the relative response units during equilibrium binding are summarised in Figure 24.
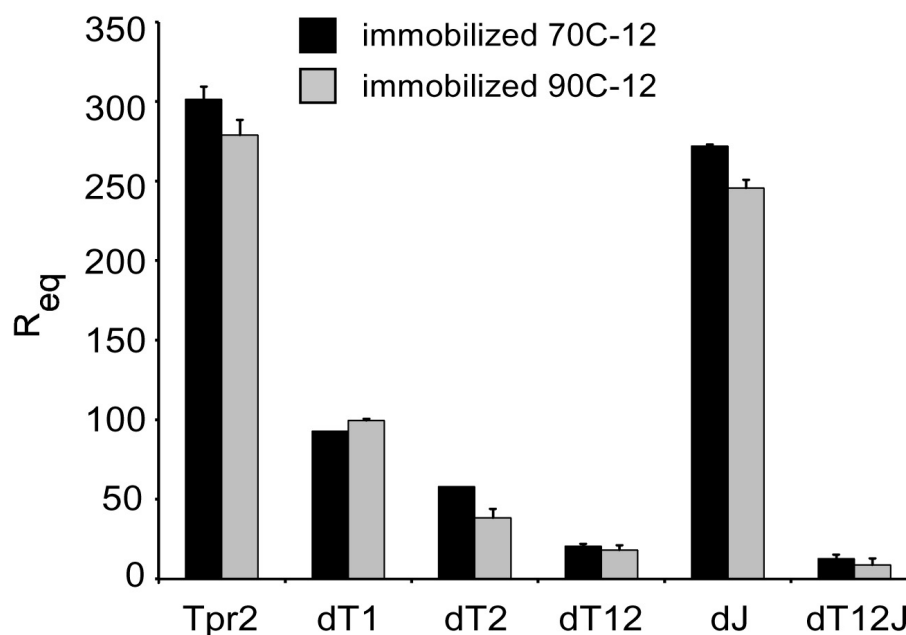
Figure 24 **Binding efficiency of Tpr2 and its mutants to Hsp70/Hsp90 C-terminal peptide.**

Tpr2 or its mutants were injected at a constant concentration of 1 μM on a BIAcore chip, loaded with covalently coupled 70C-12 (black columns) or 90C-12 (grey columns) peptides. The columns represent the relative response units during equilibrium binding after correction for background effects. The error bars are standard deviations from at least three independent experiments.

As already demonstrated, the binding affinity of the dT2 mutant to either 70C-12 or 90C-12 was lower than that of dT1 in both cases. The double-clamp mutant (dT12) exhibited a further reduced binding as low as 7% compared to wild type (Figure 24). The single mutation in the J-domain had a negligible effect for the clamp binding and the triple-mutant (dT12J) was equally low as the dT12 mutant. Although the changes in the binding affinity to 70C-12 and 90C-12 were different between the Tpr2 mutants, each mutant had a similar effect on both binding partners. This means that although T2 might be the preferred TPR-binding site, both clamps interact equally well with Hsp70 and Hsp90. Compared to the co-precipitation experiments, this quantitative setup shows a much clearer phenotype for the dT1 mutant (Figure 22 A, lane 2) and reliably reproduces the previous data. The initial prediction of a TPR-clamp interaction was faithfully demonstrated by the fact that only the very C-terminal part of the chaperones, containing the EEVD motif, was sufficient to serve as a binding partner for Tpr2.

The following competition experiments were carried out in analogy to the RL binding studies. Instead of using the complete C-terminal domain of Hsp70/Hsp90, only the respective 12mer peptides were used as competitors. Either the 12mer C-terminal peptide of Hsp70 (Figure 25) or Hsp90 (Figure 26) was immobilised on the sensor chip. A 0.5 µM solution of Tpr2 was pre-incubated with increasing amounts of free peptide before being subjected to SPR analysis. The competitors were the same peptides that were immobilised on the chip or an extended SKL sequence, which served as a control. The SKL peptide is recognized by the TPR-domain in the peroxisomal protein receptor Pex5, but not by the TPR-clamp mechanism of Hop (Brinker et al. 2002). This is an example of another kind of TPR-protein interaction, which does not possess or require the two-carboxylate clamp mediated EEVD specificity of Hop, CHIP or Tpr2. The relative binding affinities were normalised against a sample without competitor and plotted against the peptide concentration (Figure 25 A, Figure 26 A).

Figure 25 summarises the data collected with the immobilised 70C-12 peptide. The original SPR graphs are shown in the right panel (Figure 25 A-C) and the normalised data set is presented in the left panel (Figure 25 D). The SKL peptide was not capable to compete for Tpr2 binding to 70C-12 (Figure 25 C, D) up to a 200-fold molar excess over the protein. In contrast, both chaperone peptides inhibited the binding in a dose-dependent manner (Figure 25 A and B). The 70C-12 peptide was slightly more effective and reduced binding to background levels (Figure 25 A, B). A half maximal inhibition (IC_{50}) was obtained in the range of about a 20-40 fold molar excess of free peptide over Tpr2 for both chaperone competitors (Figure 25 A).
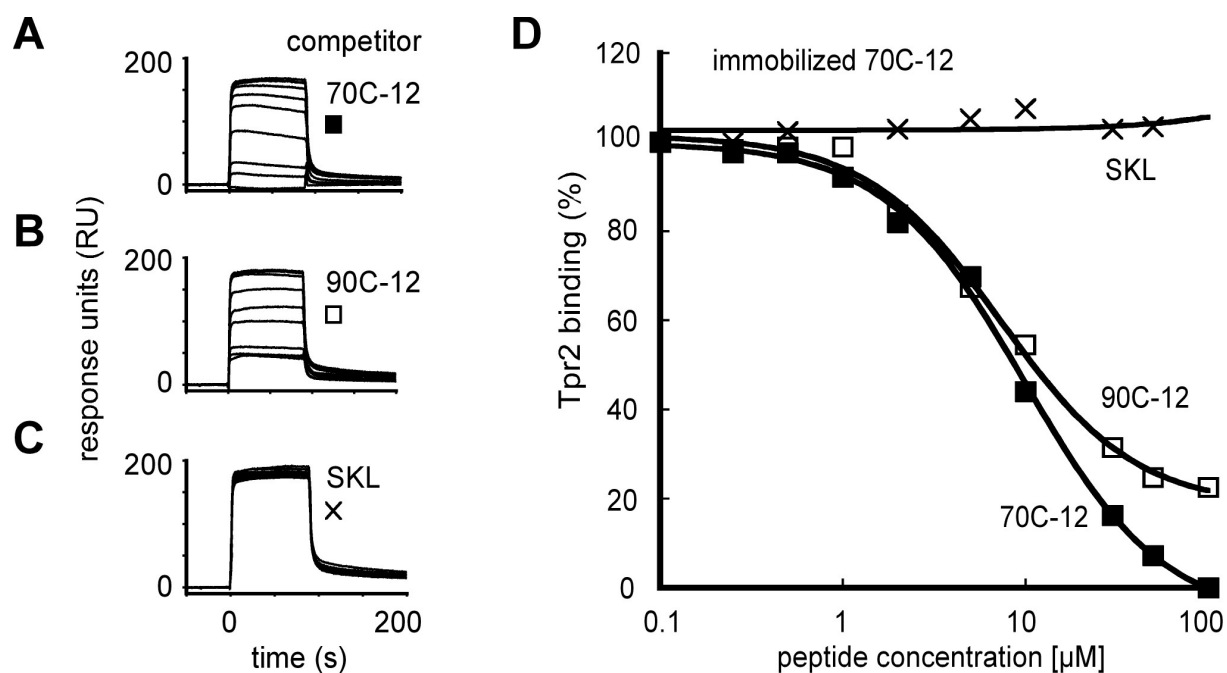
Figure 25   Competition of Tpr2 binding to immobilised 70C-12

The 12mer peptide, containing the C-terminal part of Hsp70 (70C-12) was covalently coupled to a sensor chip. Tpr2 (0.5 μM) was pre-incubated for 5 min on ice with increasing amounts of soluble peptide competitors (0.1, 0.25, 0.5, 1, 2, 5, 10, 30, 50, 100 μM) before injection. The binding kinetics were monitored for 1 min, followed by a 5 min dissociation period and regeneration of the chip. The primary data are presented in the panels to the left. Sequential injections are superimposed in one graph each. (A) The 70C-12 peptide was used as a competitor. (B) Increasing amounts of C90-12 peptide were used for competition. (C) A control peptide terminating in SKL, which is recognized by the TPR-domains of Pex5p, but not by the TPR-clamps of Hop, was used as a negative control. (D) The response units during equilibrium binding (R_{eq}) of the previous experiments were plotted against the competitor concentration. The curve fit was calculated with the BIAcore software. The competitors were: 70C-12 (black squares), 90C-12 (open squares) and the SKL control-peptide (cross).

Similar results were obtained when 90C-12 was immobilised to the sensor chip (Figure 26). In contrast to the dose dependent competition seen with 70C-12 (Figure 26 A, D) and 90C-12 (Figure 26 B, D), the SKL peptide showed no specific inhibition (Figure 26 C, D). Again the competition effect of 70C-12 was slightly better than 90C/12 and the IC_{50} value for both chaperone peptides was in the range of a 20-fold molar excess (Figure 26 A).
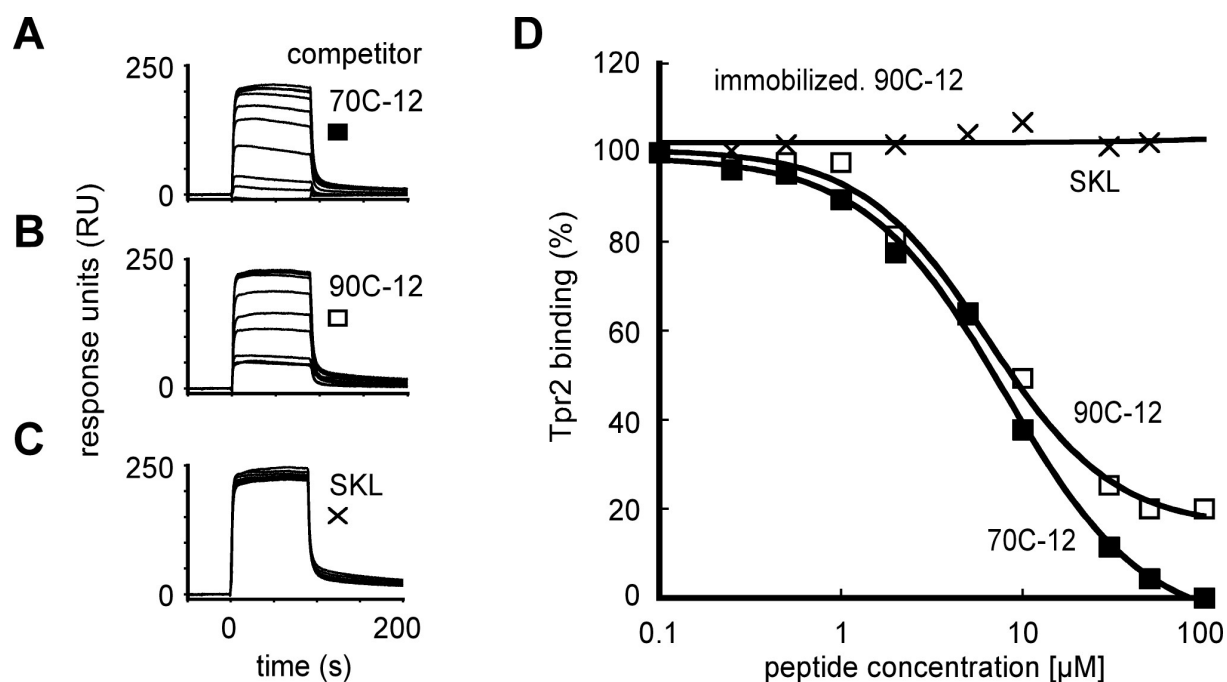
Figure 26   Competition of Tpr2 binding to immobilised 90C-12

The C-terminal peptide of Hsp90 (90C-12) was covalently coupled to the sensor chip. Tpr2 (0.5 µM) was pre-incubated for 5 min on ice with increasing amounts of soluble peptide competitors (0.1-100 µM) before injection. The binding kinetics were monitored and the primary data are presented in the panels to the left. Sequential injections are superimposed in one graph each. (A) The 70C-12 peptide was used as a competitor. (B) C90-12 peptide was used for competition. (C) A negative-control SKL-peptide was used to compete binding. (D) The response units during equilibrium binding (R_{eq}) of the previous experiments were plotted against the competitor concentration. The curve fit was calculated with the BIAcore software. The competitors were: 70C-12 (black squares), 90C-12 (open squares) and the SKL control-peptide (cross).

The competition experiments with the SKL peptide demonstrate that the TPR interaction can be assigned to a clamp mechanism, which is specific for the chaperone C-termini. The SPR technique reproduces the data obtained from RL competition experiments (Figure 22 B) and shows that the TPR-clamps in Tpr2 contribute independently to the binding of both Hsp70 and Hsp90. The IC_{50} calculated from the competition experiments is lower than that of Hop (Brinker et al. 2002). This would allow Tpr2 to contact the multichaperone machinery in a competitive manner. Since it is about 10 times less abundant in the cell than Hop, only a subpopulation of the multichaperone machinery will be connected to Tpr2.

The experiments described up to this point have established the physical role of the Tpr2 TPR-clamp interactions. They omitted ATP, which is normally involved in a transient Hsp70 J-domain interaction. To address the question of the contributions of the Tpr2 J-domain, the experimental conditions were adjusted with respect to nucleotide

3.3.4 Functional analysis of the Tpr2 J-domain

J-domain cofactors of Hsp70 stimulate its ATPase activity and thereby induce conformational changes which lead to tight binding of the chaperone to polypeptide substrates (Bukau and Horwich 1998). The cycle is completed by nucleotide exchange and substrate release. Iterative rounds of this process help the folding of Hsp70 dependent substrates. All basic aspects of this process can be tested *in vitro* with different experimental approaches. A protein that contains a functionally active J-domain should be able to stimulate Hsp70 ATPase activity, induce substrate binding and accelerate Hsp70 mediated substrate refolding. Since the sequence comparison (Figure 10) identified a J-domain in Tpr2 with very high homology to the abundant Hsp70 co-chaperone Hsp40 (Figure 12) it was a logical decision to test its functionality.

Hsc70 from a bovine brain tissue preparation was used for the following assays. The samples containing 1 μM chaperone were supplemented with 2 μM of the indicated proteins. After pre-heating to 30°C the experiment was started by the addition of an excess of ATP (0.1 mM), which contained 1 μCi α^{32}P-ATP. Samples were taken at different time points and the hydrolysis reaction was rapidly stopped by mixing with 25 mM EDTA and shock frozen in liquid nitrogen. ATP and ADP were separated by thin layer chromatography (TLC) and the percentage of the hydrolysed material was counted as a proportion of the applied radioactivity. The numbers from the linear range of the experiment were converted to the steady-state hydrolysis rates, which stand for mole ADP formation per mole ATPase active protein per minute. A summary of the tested protein combinations is given in Figure 27.
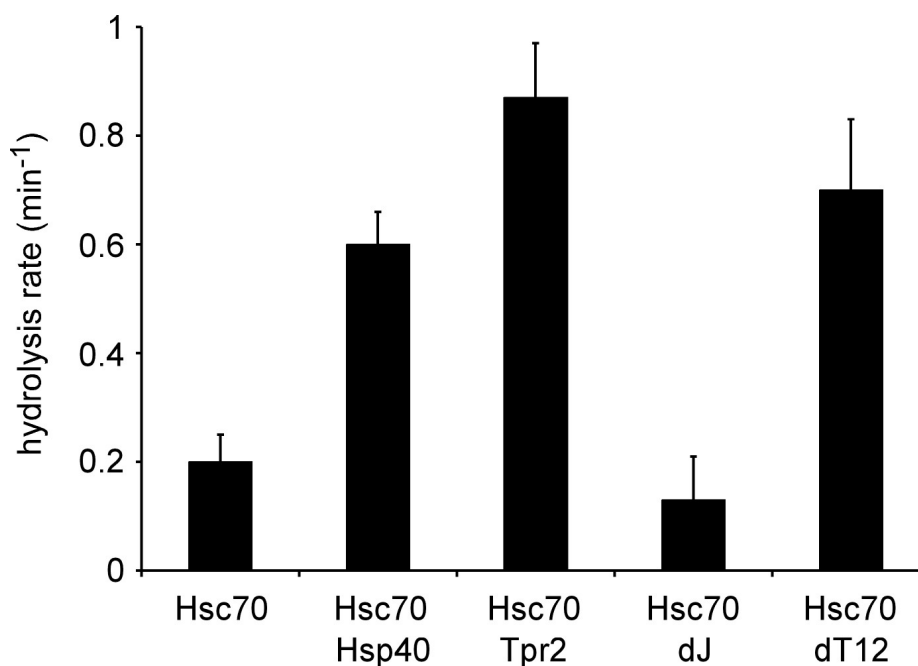
Figure 27   Cofactor-dependent stimulation of the Hsc70 ATPase rate.

The J domain of Tpr2 is responsible for regulating the ATPase rate of Hsc70. 1 μM Hsc70, purified from bovine brain, was incubated at 30°C alone, with additional 2 μM Hsp40, Tpr2 wild-type, the double clamp-mutant (dT12), or the J domain mutant (dJ). The reactions contained 0.1 mM ATP, substituted with 1 μC [α–^{32}P]ATP. Aliquots of the reactions were stopped at different time points by transferring them to 25 mM EDTA and freezing in liquid nitrogen. The ATP hydrolysis products were resolved by thin layer chromatography and evaluated by Phosphorimager screening. The steady-state ATP hydrolysis rates were calculated from the linear range of the reactions.

The background ATPase activities of the isolated protein preparations were measured and subtracted from the bars in Figure 27. They can arise from contaminating proteins, which co-purified during the isolation procedure. The basal Hsc70 ATPase activity was about 0.2 min^{-1} (Figure 27, Hsc70), and was stimulated about 3-fold by the classical co-chaperone Hsp40 (Figure 27, Hsc70/Hsp40). Equal amounts of Tpr2 were adequately able to stimulate Hsc70 at least to the same extent (Figure 27, Hsc70/Tpr2). The double clamp mutant (Figure 27 Hsc70/dT12) had the same effect as the wild type protein, whereas the mutation in the J-domain reduced the stimulation of the Hsc70 ATPase activity almost to background levels (Figure 27 Hsc70/dJ). The data demonstrate that the stimulatory J-domain effect of Tpr2 on the Hsc70 ATPase is comparable to the classical co-chaperone Hsp40 and is not influenced by affinity changes of the TPR-clamp contacts.

Next, the correlation of the stimulation of the Hsc70 ATPase activity with the transition to a stable chaperone substrate complex was tested. The Ligand-binding domain (LBD) of the GR was chosen as a model substrate since the GR also served as the respective *in vivo* substrate and release assays to monitor chaperone-substrate interactions have already been established for this domain (Young and Hartl 2000; Sondermann et al. 2001). The LBD is sufficient to be recognized as an Hsc70 substrate and can also form complexes with the complete multichaperone machinery. The LBD was purified as a myc-his tagged protein under mildly denaturing conditions. The *in vitro* experiment contained only purified proteins. The LBD was denatured and pre-bound to Ni-NTA-agarose beads. After washing off the denaturant, the pellet was incubated for 10 min with 5 μM Hsc70 and equimolar amounts of the indicated proteins (Figure 28) in the presence of ATP at room temperature. The beads were recovered and washed with ATP-free buffer. Bound proteins were eluted with Laemmli buffer and resolved on SDS-PAGE together with the supernatant (Figure 28, pellet left panel, supernatant right panel).
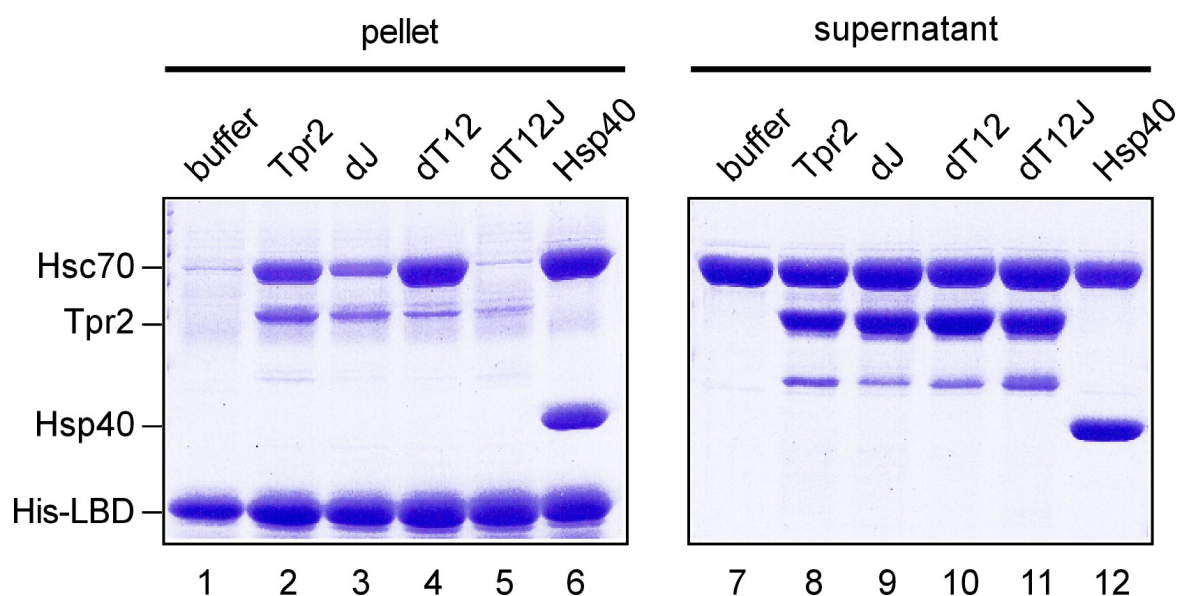

Figure 28   **Cofactor-dependent binding of Hsp70 to partially unfolded substrate.**

Tight Hsp70-substrate interaction is dependent on the J domain of Tpr2. The recombinant his-tagged ligand binding domain (LBD) of the GR was denatured and partially refolded in detergent. It was then allowed to bind to Ni-NTA beads. The beads were further incubated for 10 min at room temperature with 5 μM Hsc70 or additional 5 μM Tpr2, the J mutant (dJ), the double-clamp mutant (dT12), the triple mutant (dT12J) or Hsp40 in the presence of ATP. The beads were recovered and bound proteins were eluted with Laemmli/EDTA buffer (pellet). Proteins in the supernatant were precipitated and also subjected to SDS-PAGE (supernatant).

When no cofactor was present, Hsc70 did not co-precipitate with the LBD (Figure 28, lane 1 and 7). In the presence of the classical J-domain co-chaperone Hsp40, a significant amount of the chaperone was pulled down (Figure 28, lane 6 and 12). Moreover, a noticeable amount of Hsp40 appeared in the pellet fraction, which was probably due to direct binding of the co-chaperone to the partially denatured substrate (Szabo et al. 1996). The presence of Tpr2 induced Hsc70 binding to substrate equally effectively as Hsp40 (Figure 28, lane 2 and 8). The double clamp mutation had no negative influence on the chaperone-substrate complex formation (Figure 28, lane 3 and 10). This corresponded with the result from the ATPase assay (Figure 27, Hsc70/dT12) where the double clamp mutant did not inhibit the J-domain dependent stimulation of the Hsc70 ATPase. In analogy to the result from the ATPase stimulation experiment, the point-mutation in the J-domain of Tpr2 (dJ) was ineffective in stimulating a tight binding of Hsc70 to the model substrate (Figure 28, lane 3 and 9). In combination with the double clamp mutant (dT12J) the chaperone binding was completely abolished (Figure 28, lane 5 and 11). Together, the level of Hsc70 binding induced by Tpr2 was in the same range as that caused by Hsp40. As predicted from the sequence alignment, the experiments with the Tpr2 mutants demonstrate that it is the J-domain that triggers Hsc70-dependent nucleotide hydrolysis and thereby induces the transition to a tight substrate complex. The TPR domains of Tpr2 may slightly stabilise Hsc70 binding to substrate in the absence of a functional J-domain, but this stabilisation is not required for substrate binding by Hsc70 (Figure 28, lane 3 and 4). Notably the association of Tpr2 with the LBD was much weaker than that detected for Hsc70 and was abolished by mutation of the TPR-clamps and the Hsc70 interacting J-domain (Figure 28, lane 2 and 5). This suggests that Tpr2 does not bind to unfolded substrates directly, but only through Hsc70 or in a further step via Hsp90 and that any effect of Tpr2 on protein folding must be mediated by its interaction with the chaperones. This is different from the direct polypeptide interaction seen with Hsp40 (Figure 28, lane 6). The results obtained from the co-precipitation experiments reflect the observations from the ATPase activity assay (Figure 27) and identify Tpr2 as a functional J-domain cofactor of Hsc70.

To show that the function of Tpr2 is productive in terms of Hsp70-mediated protein folding, the refolding of luciferase was tested in an *in vitro* experiment. Recombinantly produced luciferase was chemically denatured in 6 M guanidinium hydrochloride for 15 minutes. The protein solution was diluted 1:100 into samples containing the indicated proteins (Figure 29, right of graph). The dilution was sufficient to eliminate the denaturing effect and

allow chaperone-mediated protein refolding. The buffer system was supplemented with 3% desalted RL to obtain a good refolding rate. This amount of RL yielded refolding rates in the presence of Hsc70 and cofactors, which were comparable to the maximum refolding yields obtained in 50 % RL. It was not possible to get significant folding kinetics without the additional RL. This makes the results more difficult to interpret, since it remains unknown which factors in the RL help to increase the refolding efficiency. In addition to the indicated proteins the samples contained ATP/Mg and the experiment was carried out at 37°C.
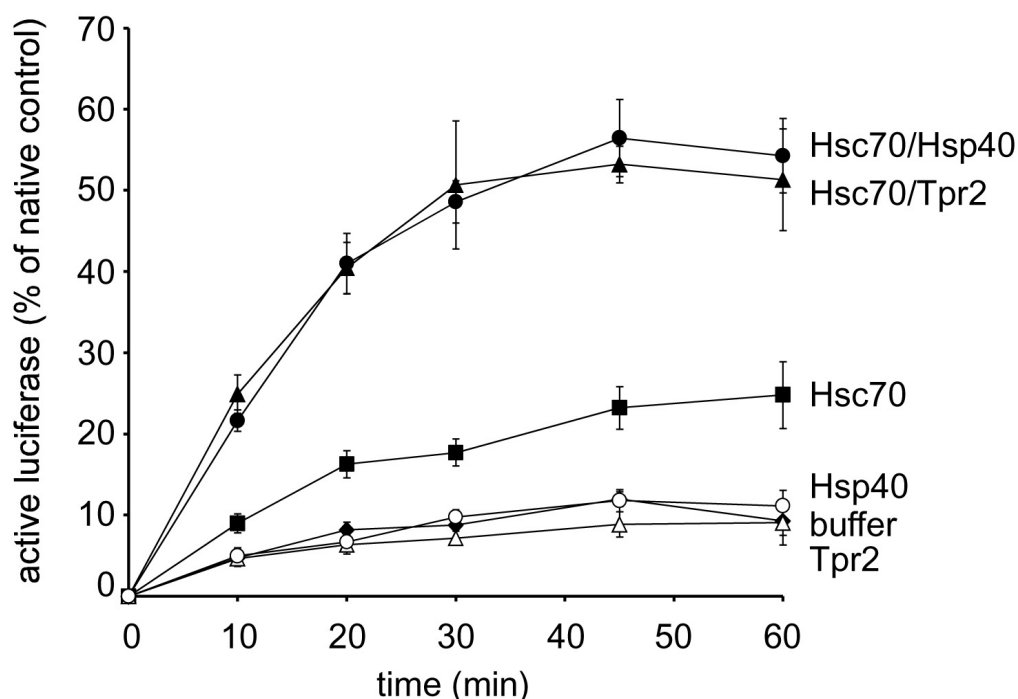

Figure 29   Hsc70 dependent luciferase refolding.

Tpr2 efficiently stimulates Hsp70-dependent substrate refolding. Myc-tagged luciferase was chemically denatured in 6M guanidinium-HCl for 15 min. It was then diluted 1:100 into reactions containing 3 % desalted RL and ATP supplemented with buffer only or 1 μM Hsc70 alone or in combination with 2 μM Hsp40 or Tpr2. The reactions had been preheated to 30 °C and were kept at this temperature for the time of the assay. The increase of luciferase activity over time was monitored by testing aliquots of the samples with the Promega luciferase assay system. The activity is plotted as percentage of the activity of the native control.

The refolding of luciferase over time was determined by a luminometer assay (Promega) and normalised to luciferase levels measured under non-denaturing control conditions (Figure 29). The samples which contained luciferase alone or in combination with either 2 μM Hsp40 or 2 μM Tpr2 (Figure 29, buffer, Hsp40, Tpr2), showed an equal basal level of luciferase activity, which was about 10 % of control at the end of the time course. Thus, none of the

cofactors themselves can increase the low, spontaneous refolding of the substrate above background. In the presence of 1 μM Hsc70 the measured activity increased about two-fold over background (Figure 29, Hsc70), which corresponds with the property of Hsc70 to refold luciferase at its low basal ATPase activity. In combination with 2 μM Hsp40 a maximal luciferase activity of about 60 % is reached after 45 minutes (Figure 29, Hsc70/Hsp40). 2 μM Tpr2 together with 1 μM Hsc70 (Figure 29, Hsc70/Tpr2) yielded equal amounts and showed the same initial kinetics as the combination of chaperone and Hsp40. This shows that Tpr2 stimulates Hsc70 in a functionally relevant manner, which leads to effective refolding of the chaperone-dependent substrate. Different ratios between Hsc70 and Hsp40 in the range of 1:0.5 to 1:8 and Hsc70 in combination with Tpr2 (1:1 to 1:4) showed equal refolding yields.

In the preceding section it was demonstrated that the J-domain in Tpr2 fulfils the three criteria, which are hallmarks of the classical co-chaperone Hsp40. It stimulates Hsp70 ATPase activity, induces substrate binding and accelerates Hsp70-mediated protein refolding. Together, this identifies a TPR-clamp independent functional contribution of Tpr2 on Hsp70 and tags it as a new J-domain cofactor.

3.3.5 Contributions of Tpr2 to the chaperone complex composition

So far, the Tpr2 domains were biochemically analysed for their predicted effects on isolated chaperones. The next set of experiments examined the effects of Tpr2 on Hsp70 and Hsp90 simultaneously and allowed to detect possible rearrangements in the multichaperone complex. For this purpose, the LBD release assay described by Young (Young and Hartl 2000) was used. A schematical overview of the experiment is given in Figure 30.
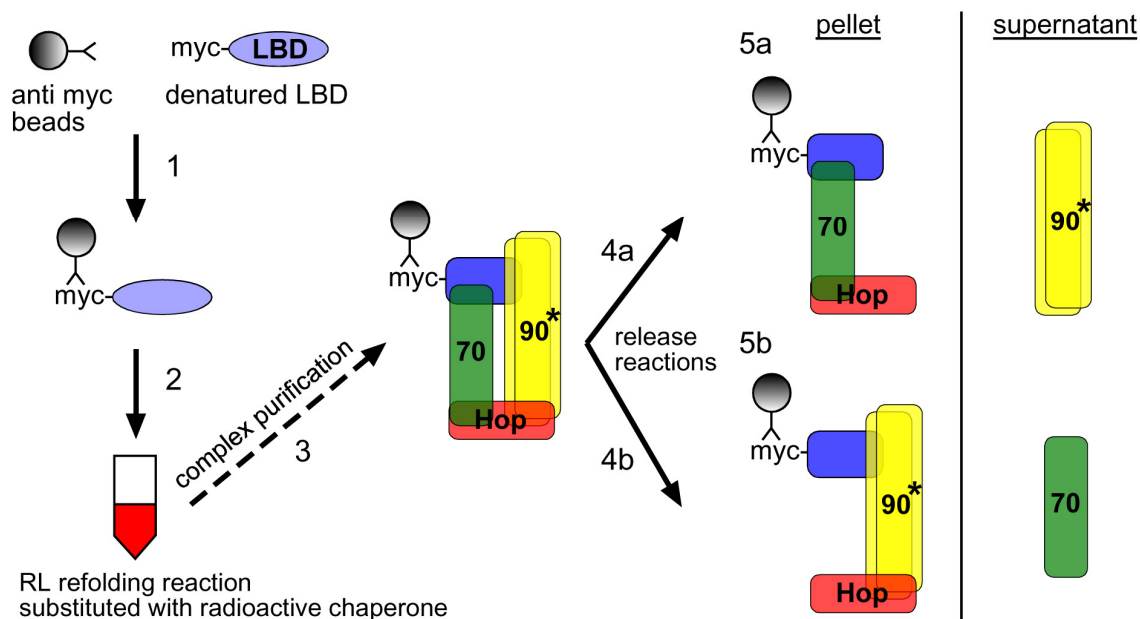
Figure 30   Diagram of the LBD release assay.

The myc-tagged LBD was chemically denatured followed by a partial refolding in detergent and binding to αmyc coupled protein G-beads (1). The complex was added to desalted RL substituted with a radiolabelled chaperone (2). The substrate and bound chaperones were recovered (3) and subjected to different release conditions, containing the proteins of interest (4). Finally supernatant and pellet were separated (5) and resolved on SDS-PAGE. The gels were evaluated with a Phosphorimager system

A monoclonal anti-myc antibody was covalently coupled to protein G-beads. The myc-tagged LBD was denatured in a separate reaction and the denaturant was removed before it was added to the antibody beads (Figure 30, step 1). The binding was allowed to occur for 5 minutes before excess amounts of LBD were removed by washing the beads twice. The antibody-antigen complex was then added to desalted RL, which was supplemented with ATP/Mg and radiolabelled chaperone (Figure 30, step 2). The labelling of the chaperone had been carried out in a parallel transcription-translation coupled reaction (TNT, Promega). The advantage of this method is that the radiolabel can be quantitatively measured in the final analysis of the experiment. The chaperones were allowed to interact with the substrate for 10 minutes before the complex was purified (Figure 30, step 3). This was done by splitting the reaction into 10 separate samples before washing the pellet to obtain about equal amounts of beads in every tube. The samples were then subjected to a set of release conditions (Figure 30, step 4, a and b) to test the effect of the protein of interest on the complex composition. This step of the experiment was carried out with purified proteins in a buffer solution. The dilute environment favours the release of proteins from the complex into the supernatant fraction

and reduces the backward assembly tendency of the complex. In the last part of the experiment supernatant and pellet fraction are separated after 10 minutes (Figure 30, step 5, a and b). The proteins in the pellet were eluted with Laemmli buffer. The supernatant was precipitated with chloroform/methanol (Wessel and Flugge 1984) and the proteins were resuspended in gel loading buffer. All samples were then analysed by SDS-PAGE. The gels were dried and exposed on a Phosphorimager plate. The radioactive signal was measured and the amount of released chaperone was calculated in percent of radioactivity in the supernatant in relation to the sum of supernatant and pellet fractions.

In the first panel of experiments the release of wild type Hsp90 was followed. The assay was carried out in the presence or absence of ATP/Mg during the release reaction (Figure 31, black bars without ATP, grey bars with ATP).
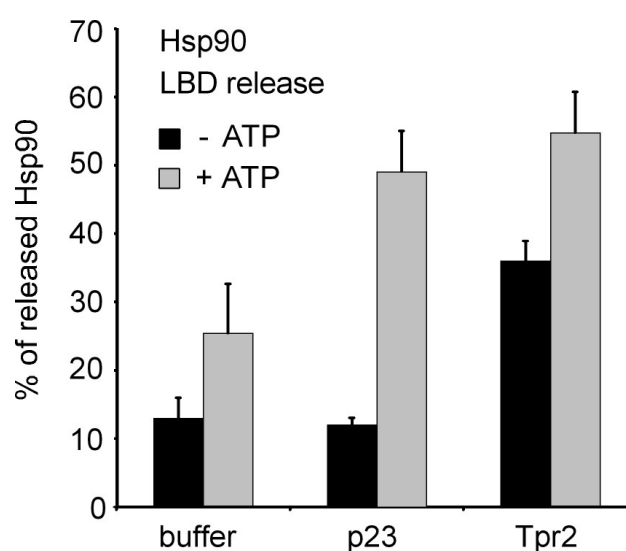

Figure 31   Hsp90 release from LBD.

Tpr2 dissociates Hsp90 from substrate complexes. The recombinant myc-tagged LBD was denatured for 10 min in 1% SDS, 50 mM Tris-HCl pH 7.5 at room temperature before diluting it 10-fold into buffer C (20 mM HEPES-KOH pH 7.5, 100 mM KAc, 1 % NP40, 1 % Na-deoxycholate, 0.1 % SDS), containing α-myc coupled protein-G beads. After 30 min the beads were recovered and added to RL desalted in buffer B, substituted with radiolabelled Hsp90 from a TNT reaction (Promega). After 10 min the reaction was stopped by addition of 10 units apyrase (Sigma), the immuneprecipitants were re-isolated and added to the release reactions. These contained buffer B alone or supplemented with 5 μM p23 or Tpr2. After 10 min supernatant and pellet were separated. Proteins in the pellet were released from the beads by boiling in Laemmli buffer. The supernatant was precipitated and the proteins were dissolved in Laemmli buffer. All fractions were resolved on SDS-PAGE and the radiolabelled chaperone was detected by Phosphorimager analysis. The fraction of released radiolabelled chaperone was plotted as a percentage of the totally recovered radioactivity.

A basal fraction of about 12 % Hsp90 was released when the complex was incubated in buffer alone (Figure 31, buffer black bar). This amount was about doubled in the presence of ATP (Figure 31, buffer grey bar) as previously reported (Young and Hartl 2000). In the presence of the regulatory cofactor p23 the amount of released Hsp90 increased up to 50 % only when ATP was present. p23 alone was insufficient to stimulate Hsp90 release above the basal level of the control in the absence of nucleotide (Figure 31, p23). Interestingly, Tpr2 also caused a discharge of the chaperone to a similar extent as p23 in the presence of ATP (Figure 31, compare p23 and Tpr2 grey bars). Intriguingly, this effect was also clearly measurable when nucleotide was omitted during the release reaction (Figure 31, Tpr2 black bar). This result was different from p23 and suggests a release mechanism of Tpr2 on Hsp90, which is independent of the chaperone's ATPase activity. To verify this effect a titration series was performed (Figure 32).
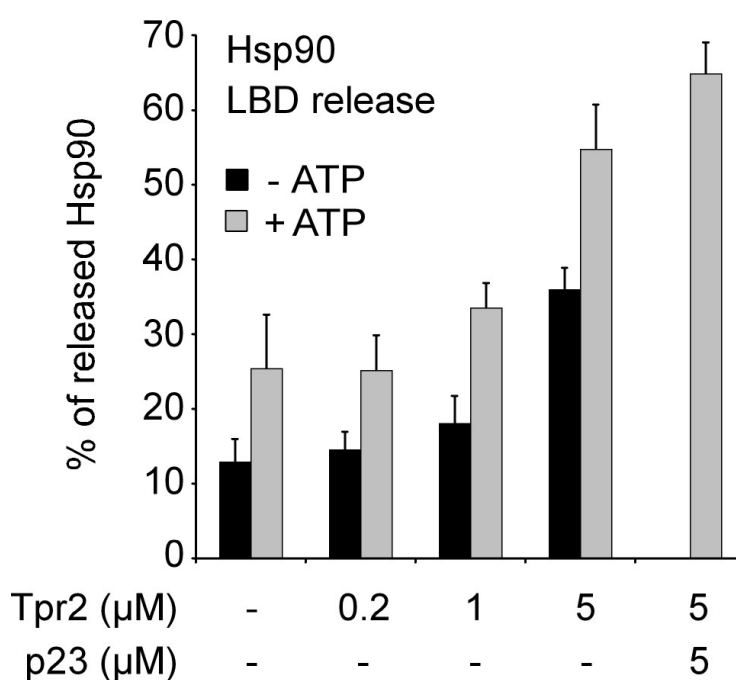

Figure 32   Tpr2 titration of Hsp90 release.

The release of Hsp90 from LBD-chaperone complexes is dependent on the amount of Tpr2. The LBD-release assay was carried out as described. Hsp90 was added in its radiolabelled form and its release from the substrate-chaperone complex is given as percentage of total recovered radioactivity in the presence (black columns) or absence (grey columns) of nucleotide. The release was measured in the presence of buffer alone, with increasing amounts of Tpr2 (0.2, 1 and 5 μM) or where indicated in combination with p23 (5 μM). The error bars are standard deviations from at least three independent experiments.

The control sample without additional proteins is identical to the control shown in the previous experiment (Figure 31, buffer). The amounts of released Hsp90 increased in line with increasing amounts of Tpr2 (Figure 32, Tpr2 concentration 0.2 to 5 µM). This was observed both in the presence and absence of ATP (Figure 32, compare black and grey bars). Although the cellular levels of Tpr2 are substochiometric compared to Hsp90, these concentrations are insufficient to obtain a measurable effect under the *in vitro* conditions. The release of Hsp90 starts to exceed the background threshold only when Tpr2 is present in about equimolar amounts (Figure 32, Tpr2 1 µM). A maximum release is reached when Tpr2 is present at a concentration of 5 µM during the release reaction (Figure 32, Tpr2 5 µM). This cannot be significantly exceeded in the presence of additional p23 (Figure 32, Tpr2 5 µM, p23 5 µM). On the other hand, the presence of both cofactors did not have any negative or adverse effects on Hsp90 release.

The ATPase activity of yeast Hsp90 (Hsp82) was measured to demonstrate that the effect of Tpr2 in the LBD release assay was not evoked by influencing the nucleotide hydrolysis rate of the chaperone. Since the recombinantly expressed yeast homolog is clearly more active in its ATP turnover as compared to the human isoforms, Hsp82 was used in the following experiments. Hsp82 and Hsp90 are highly homologous and can functionally substitute for each other (Obermann et al. 1998).
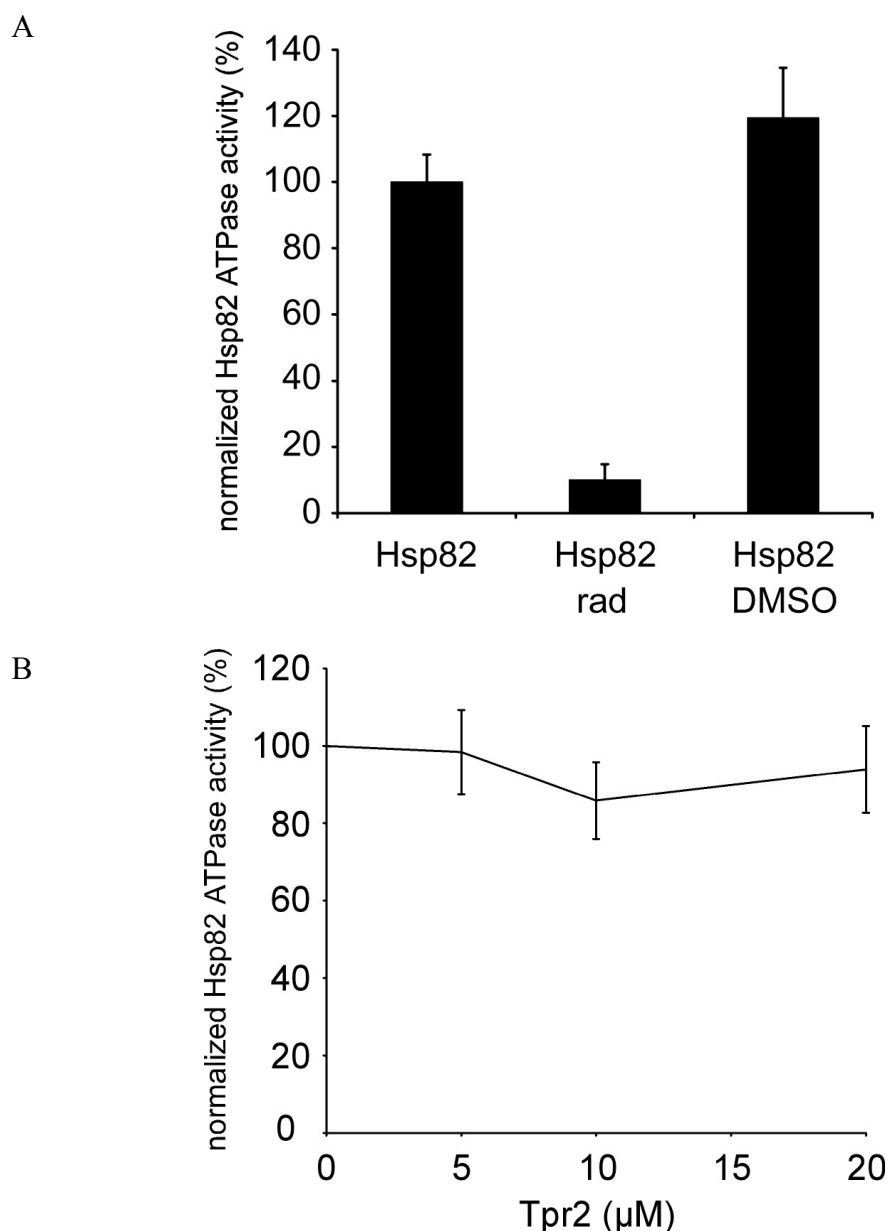
A

B

Figure 33   Influence of Tpr2 on Hsp82 ATPase activity.

Tpr2 does not diminish the ATPase activity of Hsp82. The yeast Hsp90 homolog Hsp82 was expressed in *E. coli* and purified. 2 μM Hsp82 were incubated at 30°C in the presence of 100 μM ATP, substituted with 1 μC [α–^{32}P]ATP. Samples were taken at different time points and analysed by thin layer chromatography. The ATPase activity was calculated from the linear range of the experiment and normalised for better comparison. (A) Hsp82 was incubated alone or in presence of the Hsp90 specific inhibitor Radicicol (rad). The solvent DMSO was applied as a control. (B) The ATPase activity of Hsp82 was measured in the presence of increasing amounts of Tpr2 (5, 10, 20 μM) and plotted as a percentage of untreated control.

To ensure that ATP hydrolysis was dependent on the ATPase activity of Hsp82 and not due to contaminations with co-purified ATPases, the inhibitory effect of Radicicol (rad) was used to discriminate between these cases. Radicicol competes for binding to the ATP pocket of Hsp82, similar to the benzoquinone ansamycin drugs. This in turn leads to an inactivation of the chaperone. These antibiotics have been shown to be highly specific and effective in targeting Hsp90 and they do not inhibit other ATPases. Thus hydrolysis rates measured after Radicicol treatment are likely to be caused by contaminations. The ATPase assay was carried out in analogy to the Hsc70 experiment. A preparation of Hsp82 was effectively inhibited by Radicicol in its ATPase activity, down to a background level of 10 % as compared to the untreated control (Figure 33 A, Hsp82, Hsp82/rad). When the Radicicol solvent DMSO was added to the assay, no inhibitory effect was observed (Figure 33 A, Hsp82/DMSO). This demonstrates that the Hsp82 preparation is highly pure and is ATPase active.

The steady-state activity of Hsp82 was then measured in the presence of increasing amounts of Tpr2 (Figure 33 B). No significant reduction or stimulation in the ATPase activity was detected up to a 10-fold molar excess of Tpr2 over Hsp82 (Figure 33 B, Tpr2 20 µM). In contrast, Sti1 the yeast homolog of Hop was reported to abolish chaperone-dependent ATP hydrolysis almost completely at a 8.5 fold molar excess (Prodromou et al. 1999). This means that the release of Hsp90 from the multichaperone complex is not due to an effect of Tpr2 on the chaperone's ATPase activity.

In the light of the previous experiments, it can be speculated that the release of Hsp90 would also occur when the ATPase activity of the chaperone itself was eliminated. To test this assumption, a mutant version of Hsp90 was radiolabelled in a TNT reaction and tested for release. The mutant contained a single amino acid exchange in the N-terminal ATPase domain (D93N), which rendered it incapable of even binding to nucleotide (Obermann et al. 1998). The results obtained with this mutant are summarised in Figure 34.
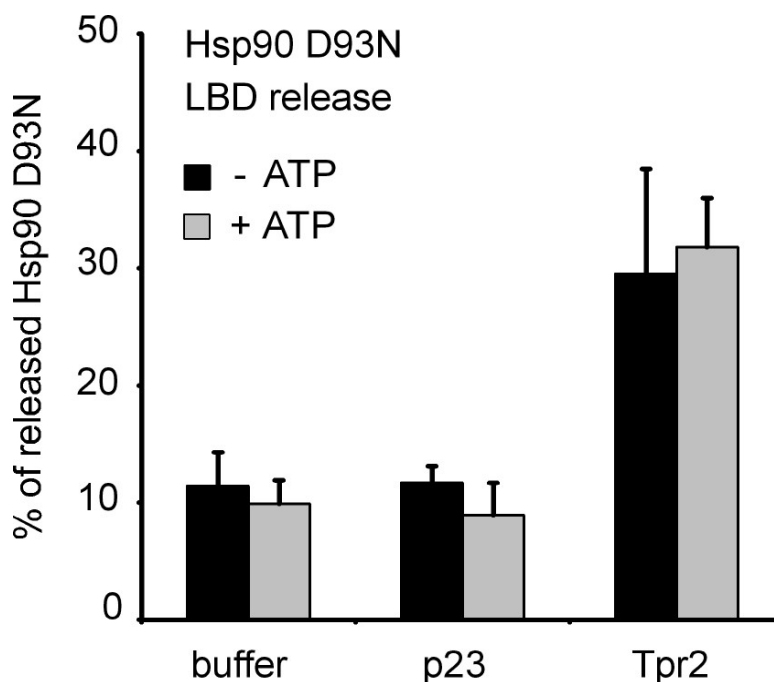
Figure 34   Cofactor-dependent release of Hsp90 D93N.

Tpr2 releases the ATPase-defective mutant of Hsp90 (Hsp90 D93N) from substrate complexes. The LBD release assay was carried out as described. A mutated form of Hsp90 (Hsp90 D93N) was radiolabelled in a separate TNT reaction before being added to the complex formation. This mutant carries a single amino acid exchange, which renders it incapable of binding and hydrolysing ATP. The release reactions were carried out with (grey columns) or without ATP (black columns). Where indicated, the buffer was substituted with 5 µM p23 or Tpr2. The error bars are standard deviations from at least three independent experiments.

The mutant Hsp90 cannot be released by the cofactor p23, even in the presence of nucleotide. This corresponds with the data published by Young and Hartl 2000. p23, which couples the ATPase activity to the peptide dissociation, is functionally dependent on a ATPase active chaperone. In contrast, Tpr2 still releases mutant Hsp90 from the complex, independent of the presence of nucleotide (Figure 34). In combination with the ATPase data (Figure 33) this suggests a release mechanism which is unconnected to the ATPase activity of Hsp90.

Independent of its contribution to the folding of a specific subset of proteins, Hsp90 is thought to bind to a broad range of denatured substrates under stress conditions. This holding mechanism allows a transient stabilisation of denatured proteins until the environmental conditions permit their refolding. However, their folding is normally not stringently dependent on Hsp90. It was tested if Tpr2 can also liberate Hsp90 from such non-stringent substrates. Firefly luciferase has been shown to fulfil the criteria for a holding-substrate

(Schneider et al. 1996). It can bind to Hsp90 in its partially denatured form, but this alone is insufficient to accomplish its refolding. A myc-his-tagged luciferase was used to isolate multichaperone complexes from RL in the same manner as described in the LBD-assay. To eliminate a nucleotide effect, the ATPase-negative mutant Hsp90 D93N was used in this experiment (Figure 35).
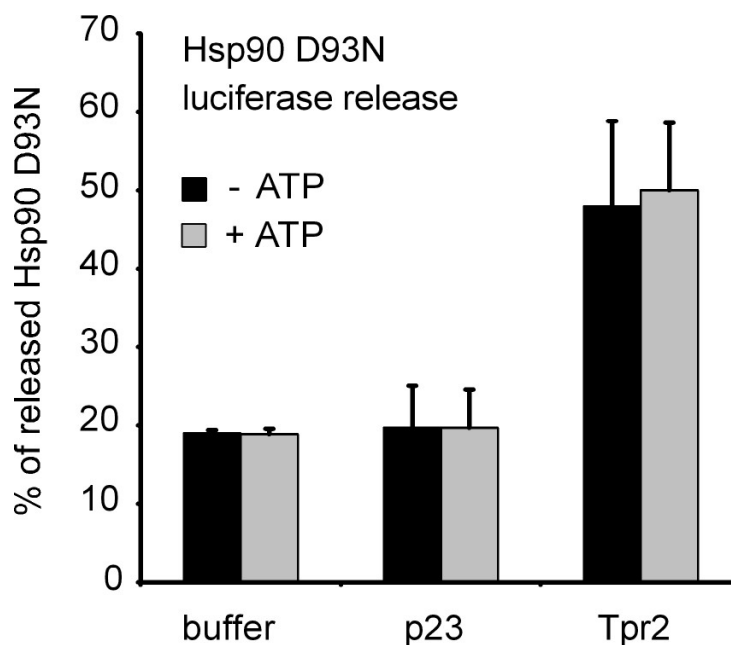

Figure 35   Hsp90 D93N release from luciferase.

Tpr2 causes release of Hsp90 D93N from luciferase, an Hsp90-folding independent substrate. The release assay was carried out as described, with the exception that myc-tagged luciferase was bound to the antibody beads. The ATPase negative Hsp90 D93N was radiolabelled and its release is given as a percentage of total recovered radioactivity. The release reactions contained no ATP (black columns) or 2 mM ATP (grey bars) in combination with 5 μM p23, or 5 μM Tpr2 or no additional protein.

The buffer control showed a background release of Hsp90 D93N, which was independent of nucleotide and slightly higher as compared to the LBD experiment. Again p23 cannot actively liberate the ATPase negative form of Hsp90 from the complex and the release was comparable to the buffer control. The presence of Tpr2 led to a release of Hsp90, independent of nucleotide. This demonstrates that the release effect of Tpr2 follows a more general mechanism and works independently of the chaperone-mediated folding activity.

To identify the structural elements of Tpr2, which are responsible for the dissociation, the mutants were tested in the LBD release assay. The averaged data of at least three independent experiments are summarised in Figure 36.
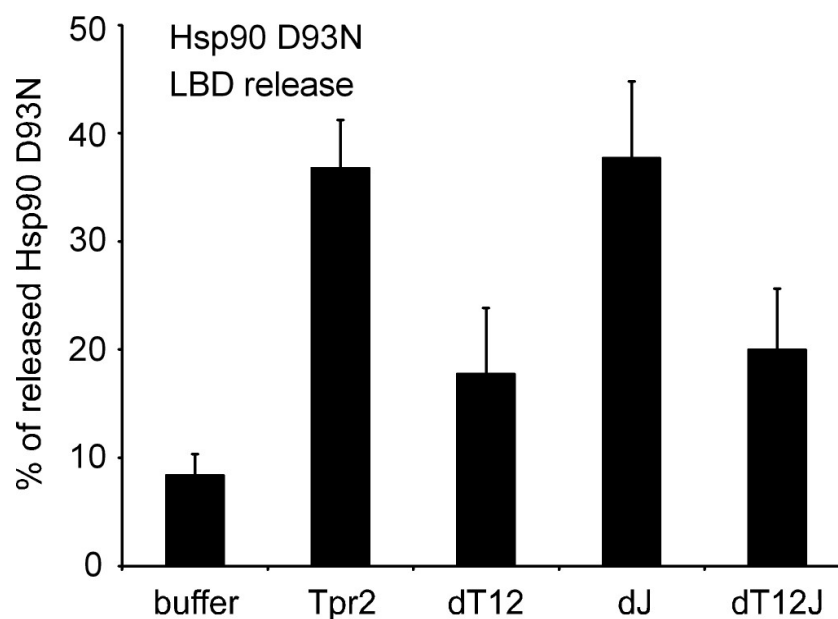
Figure 36   Hsp90 D93N release from LBD with Tpr2 mutants.

The Hsp90-substrate dissociation is dependent on the TPR-clamps of Tpr2. The release assay was carried out as described. The myc-tagged LBD was used as an Hsp90-dependent folding substrate. The ATPase negative D93N mutant of Hsp90 was radiolabelled and its release is given as a percentage of the total recovered radioactivity. The release reactions contained no nucleotide. In addition to the buffer control 5 μM of Tpr2, the double clamp mutant (dT12), the J domain mutant (dJ) or the triple mutant (dT12J) was present in the release reactions. The error bars give the standard deviation from at least three independent experiments.

Buffer control and Tpr2 wild-type protein behaved similarly to previous experiments. When the double-clamp mutants (dT12, dT12J) were used, the release efficiency significantly dropped to about 18-20 % (Figure 36). This is still above background level (8 %) and there is no significant difference between the mutants, indicating no contribution to the release from the J-domain. In agreement with this, the single J-domain mutant (dJ) was as efficient in releasing Hsp90 D93N as well as the wild-type protein. The residual activity of the clamp-mutants matches the low, but measurable binding affinities, as described by SPR analysis (Figure 24). Since both the high cofactor to chaperone ratio and the dilute environment favour the release effect, the weak affinity of the mutants is probably enough to yield a low release rate. In summary, the release of Hsp90 from the multichaperone complex is nucleotide-independent but connected to intact TPR-clamp interactions. This would indicate a steric regulation of the chaperone-substrate interaction independent of the chaperone's nucleotide status.

Next, it was tested if Tpr2 has any influence on the release of Hsp70 from isolated complexes. In the presence of nucleotide, the basal level of release increased from 8 to 22 %. When BAG-1 was used as a positive control (Sondermann et al. 2002) about 60 % of Hsp70 was released in the presence of ATP compared to 6 % in the absence of nucleotide (Figure 37).
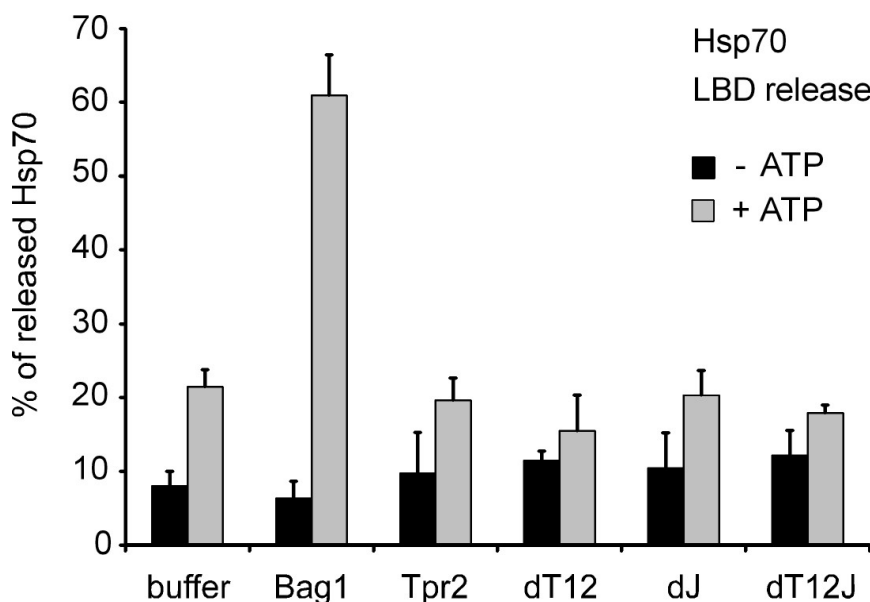

Figure 37   Cofactor-dependent release of Hsp70.

Tpr2 does not release Hsp70 from the multichaperone complex. The complex isolation was carried out as described, using the LBD as the bait-substrate. Hsp70 was separately radiolabelled in a TNT reaction and the release efficiency is indicated as a percentage of total recovered radioactivity under the given conditions. The release reaction was carried out in the presence (grey columns) or absence (black columns) of 2 mM ATP and 10 mM Mg. Where indicated, additional proteins were added at a concentration of 5 μM each. Those were the Hsp70 nucleotide exchange factor BAG-1, Tpr2, the clamp mutant (dT12), the J mutant (dJ) or the combined triple mutant (dT12J).

In contrast to its effect on Hsp90, Tpr2 did not cause a release of Hsp70 that was distinguishable from the buffer control, either in the presence or in the absence of ATP. In accordance with this, the mutants also lacked the ability to liberate the chaperone (Figure 37).

In summary, the assay identifies Tpr2 as an Hsp90-specific release factor. Its mode of operation is dependent on intact TPR-clamp domains, but does not require the presence of ATP. Since the release affects Hsp90 dependent substrates (LBD), as well as non-stringent substrates (luciferase), it is likely that Tpr2 has a general mode of action on Hsp90, which is independent of the type of polypeptide bound.

3.3.6 *In vitro* reconstitution of the GR refolding

The previous paragraphs describe the contributions of the separate domains of Tpr2 to different effects on either Hsp70 or Hsp90. The respective experiments were designed to specifically look at isolated aspects in the folding process of the chaperones. In order to further understand the physiologic role of the Tpr2 domains it was important to show how the individual functions of Tpr2 contribute to the activity of the whole protein. To assess this, the Tpr2 mutants were tested in the context of the folding of the GR as a stringent substrate of the multichaperone complex.
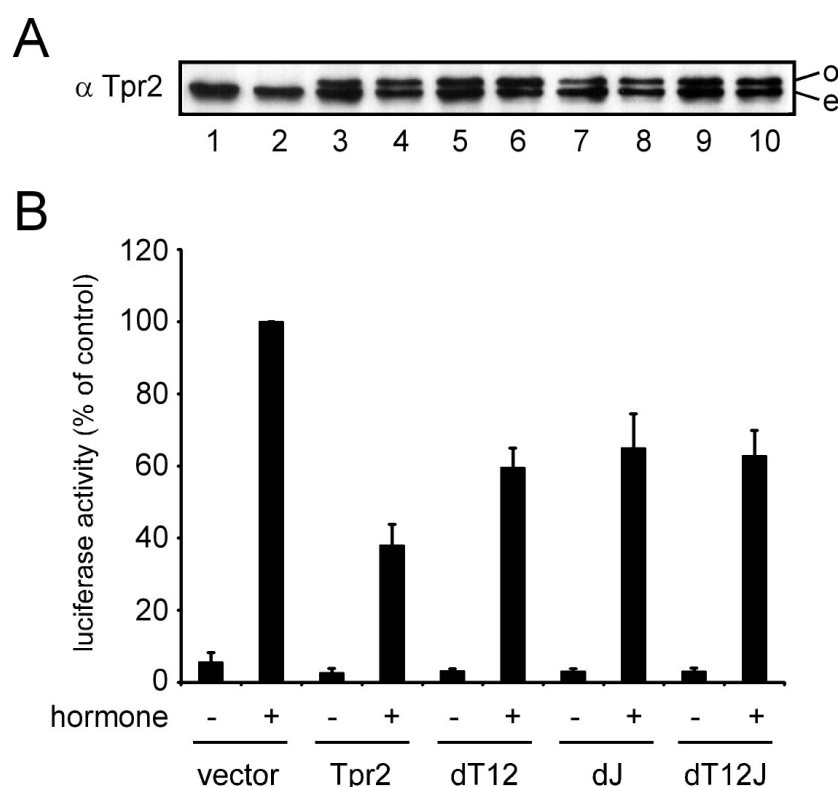

Figure 38   Overexpression of Tpr2 mutants *in vivo*.

Tpr2 mutants have a reduced effect on the GR folding in N2a cells. The GR dependent activation of luciferase transcription in N2a cells was monitored in the presence or absence of hormone induction as described in Figure 14. The cells were cotransfected with an empty vector, or expression vectors for Tpr2 (Tpr2), the double-clamp mutant (dT12), the J domain mutant (dJ) or the triple mutant (dT12J) in combination with the luciferase reporter and the β-galactosidase control vector. (A) Immunoblot detected with a polyclonal antibody against Tpr2 (α-Tpr2). Endogenous protein is marked with (e) the overexpressed, myc-tagged protein is labelled with (o). (B) The columns represent normalised luciferase levels standardized for the hormone induced vector control. Error bars are standard deviations from at least three independent experiments. The lanes in (A) correspond to the columns in (B).

For this purpose, the Tpr2 mutants were subcloned into the mammalian expression vector pcDNA3.1, which was already used to identify the *in vivo* phenotype of the wild-type protein. The transient transfection of N2a cells and the detection of GR folding was carried out as described under 3.2.1.

All Tpr2 variants expressed about equally well in N2a cells as estimated by immunoblotting and the recombinant proteins were detected as slower migrating bands, due to the additional myc-his tag (Figure 38 A). Since the transformation efficiency was incomplete, the transfected cells are estimated to contain about equal amounts of endogenous and overexpressed Tpr2. The normalised empty vector control, in the presence of hormone, was set to 100% luciferase activity. The presence of Tpr2 resulted in reduced luciferase activity after hormone treatment, down to 40% of control (Figure 38, Tpr2). The double clamp mutant (dT12), which has a reduced activity in releasing Hsp90 from the multichaperone complex, also has a reduced influence on the inhibition of GR dependent luciferase activation *in vivo*. The J-domain mutant (dJ), defective in stimulating the Hsp70 ATPase/refolding activity, caused about a similar reduced level of GR inhibition. This suggests that both the J-domain and the TPR-clamps are required for the full activity of Tpr2. Surprisingly, the dT12J mutant, which is defective in all three domains was also partially inhibitory. The remaining activity of the mutant might originate from the residual binding affinity of the TPR-clamps (Figure 24), which is enhanced in the cellular environment due to high chaperone concentrations and molecular crowding effects, or could point towards an additional activity of Tpr2. To test this possibility *in vitro* assays were developed with which the refolding of the GR under more controllable conditions can be monitored. Since the influence of Tpr2 has been shown to be exclusively on the folding of the receptor and not on downstream signalling events (Figure 19) it was sufficient to test for changes in the hormone binding affinity of the GR.

In a first approach, an *in vitro* set-up was chosen which allowed the monitoring of the chaperone-dependent folding of GR by following its migration state on a size-exclusion column. Full length GR was produced as a radioactively labelled protein in a TNT translation system. After translation, the reaction was incubated with additional hormone and/or Tpr2 for 15 min where indicated, before being transferred to ice. The sample was then loaded on a Superose 6 column and the collected fractions were analysed by scintillation counting.
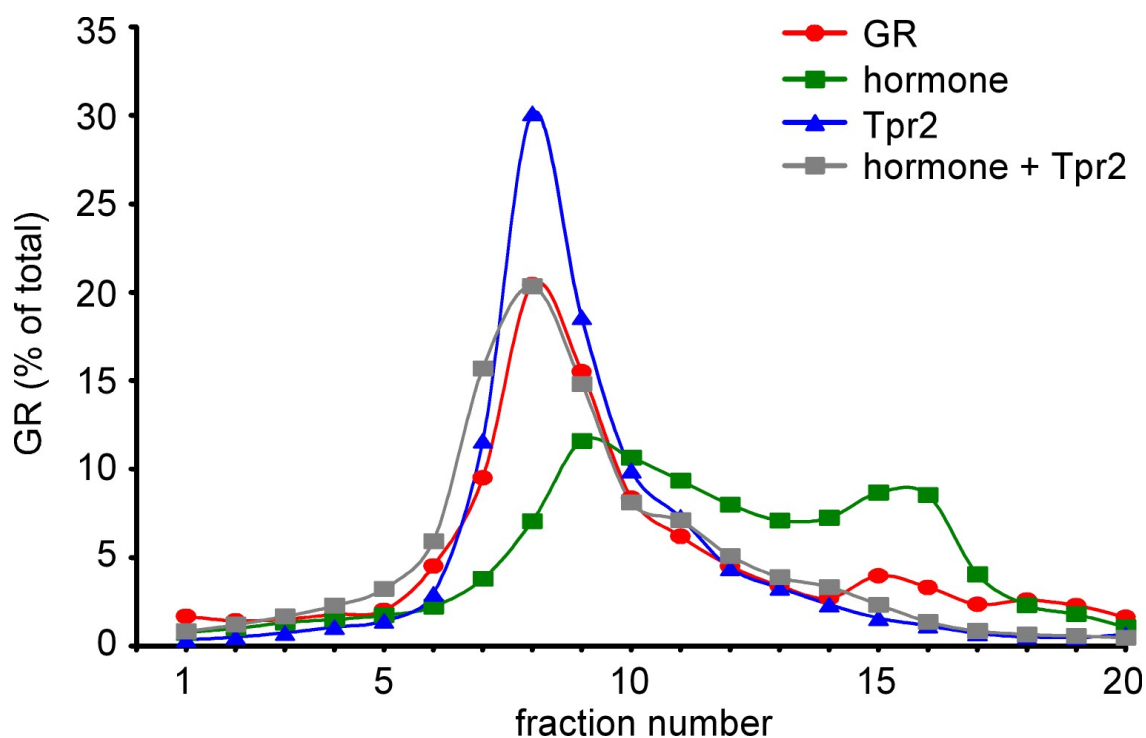
Figure 39   GR gel-filtration

The hormone binding ability of GR is lost in the presence of Tpr2. GR was radiolabelled in a TNT system (Promega). Where indicated 50 µM hormone, 10 µM Tpr2 or a combination of both were added after the translation reaction. The reactions were incubated at room temperature for 15 minutes and then transferred on ice for additional 30 minutes. Samples were analysed by size exclusion at 4°C and fractions were resolved by SDS-PAGE. The amount of radioactive receptor was determined by Phosphorimager analysis and plotted as a percentage of all collected fractions.

In the absence of additional components, the GR is mostly found around fraction 8 (Figure 39, red line), which corresponds to a size of about 450-500 kDa. This is the expected range for the multichaperone machinery. A smaller second peak is around fractions 15 to 16 and corresponds in size with the monomeric receptor. In the presence of hormone (Figure 39, green line), the monomeric peak increases, indicating that the free receptor is correctly folded and able to bind to its ligand. In accordance with this observation, the level of GR in the multichaperone peak is diminished. The separation of the two peaks becomes less defined, indicating the presence of more intermediate complexes. When Tpr2 was added to the incubation (Figure 39, blue line), the free receptor portion is lost and the fraction in the multichaperone peak increases. This suggests that an excess of Tpr2 causes a folding-unproductive trapping of the GR in the multichaperone machinery. This assumption is supported by the fact that addition of hormone (Figure 39, grey line) does not yield a monomeric receptor peak. This experiment strengthens the view that only moderate levels of

Tpr2 help the folding of GR, whereas its excess disturbs this process. Additionally, the gel-filtration experiment gives no indication for aggregated material, indicating that the receptor is rather kept in the multichaperone-complex than exposed to the environment.

The major drawback of the gel-filtration assay is the inaccurate quantification of the receptor hormone interaction, due to spreading of the peaks. This makes it unreliable in answering the question if additional functional domains of Tpr2 exist and contribute to the activity of the mutants *in vivo*. Therefore, a new experimental set-up was established, which allowed an exact measurement of the hormone-bound receptor fraction.

In this experiment, partially purified recombinant human GR was used to monitor hormone binding. The GR was added to a 50% RL mixture, which contained the proteins of interest and nucleotide. Since a percentage of the receptor was already folded and interfered with the detection of additionally folded receptor, it had to be completely denatured by a heat shock at 42°C for 5 min. The reactions were transferred to 30°C and allowed to equilibrate for 5 min. The radiolabelled hormone was subsequently added and permitted to bind. After an additional 10 minutes the samples were transferred to 4°C to stabilize the receptor ligand interaction. Free hormone was removed by passing the samples over fast-desalting columns and the flow-through, containing the receptor-bound radioactivity, was assayed by scintillation counting. The counts measured for refolded GR in the absence of additional constituents were set to 100%. This corresponds to a refolding efficiency of about 55%, when directly compared to non-denatured GR.
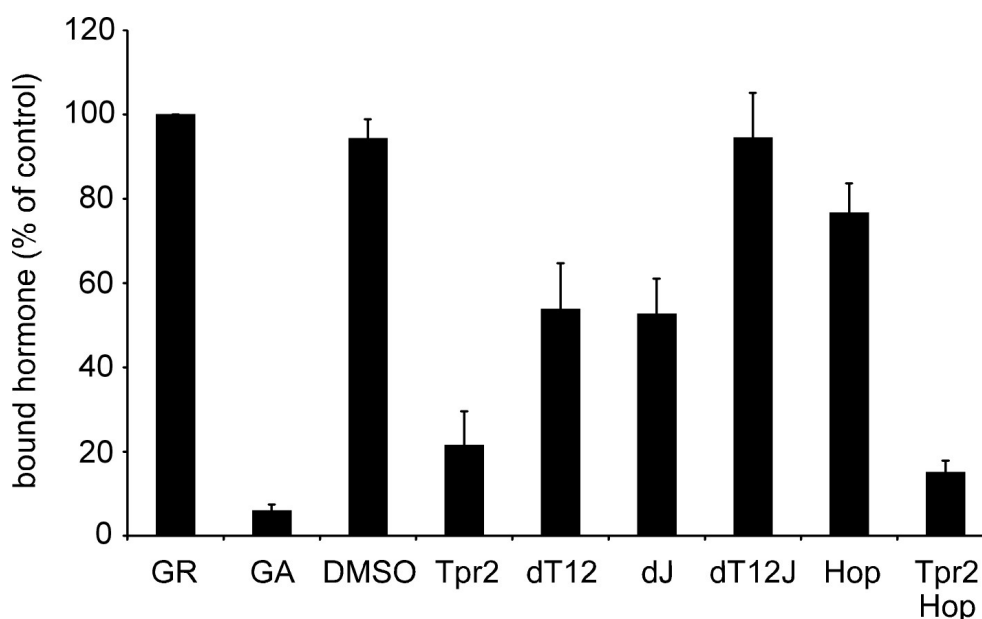
Figure 40   Hormone binding to *in vitro* refolded GR.

All domains of Tpr2 contribute to the regulation of the Hsp70/Hsp90 multichaperone machinery. Partially purified GR (4.7 nM) was added to desalted 50 % RL in buffer B, supplemented with 2 mM ATP and 5 mM Mg (GR). As a control 40 μM of the Hsp90 inhibitor Geldanamycin (GA) or equal volumes of DMSO solvent reagent (DMSO) were added to the reaction. Where indicated, 2 μM of the respective proteins were added, alone or in combination. The reactions were incubated at 42°C for 5 min to unfold the GR and then transferred to 30°C to allow chaperone-mediated refolding. After 5 min radiolabelled hormone ([1,2,4,5,7-^{3}H] dexamethasone) was added and refolding continued for 10 min. The reactions were transferred to 4°C to stabilize receptor-substrate interaction. Free hormone was removed by fast gel-filtration and the bound hormone was quantified by scintillation counting. Hormone binding to GR in the absence of additional factors (GR) was set to 100 % and other samples were normalised to this. The error bars are standard deviations from at least three independent experiments.

To demonstrate that GR refolding in this assay is dependent on Hsp90, the chaperone was selectively inhibited by Geldanamycin (GA). This almost completely abolished the presence of hormone in the flow-through fraction (Figure 40). In contrast, when the GA solvent, DMSO, was used, the hormone bound fraction was equal to the control reaction. Tpr2 diminished hormone binding to approximately 20%, which is in accordance with the *in vivo* experiments. Addition of the cofactor Hop also resulted in a moderate reduction of GR activation and this effect was not additive with the effect of Tpr2 (Figure 40, Tpr2, Hop). Thus the *in vitro* assay clearly reproduces the inhibitory effect of Tpr2 as seen after overexpression *in vivo* (Figure 14). To analyse the functional contributions of the Tpr2 domains, the purified mutants were tested. Mutations in the TPR-clamps (dT12) and in the J-domain (dJ) reduced the ability of Tpr2 to inhibit GR refolding to about 50%. In agreement

with the *in vivo* data, both domains contribute independently to the folding efficiency. When the triple mutant was tested (dT12J), the inhibitory effect was almost completely eliminated in this assay, whereas it is still measurable *in vivo*. Although a precise measurement of the affinity was not possible, the K_D of binding between dT12J and the chaperones was estimated to be around 50 µM (Figure 24). In the cytosol of live cells where chaperone concentrations are also approximately 50-150 µM (Scheibel et al. 1997; Nollen and Morimoto 2002), weak interactions with the Tpr2 mutants will still occur, whereas the lower concentrations of chaperones in the *in vitro* experiments amplify the effects of the point mutations. Thus, both the stimulation of the Hsp70 ATPase and the dissociation of Hsp90 are required for the full function of the cofactor and no additional activity of Tpr2 can be observed on the GR folding.

As has been shown in the *in vivo* experiments, a relatively small change in the abundance of Tpr2 leads to a significant drop in GR activation. Since the *in vitro* system faithfully reproduced the cell-culture experiment, it was used to titrate the effect of Tpr2 by adding increasing amounts of the cofactor.
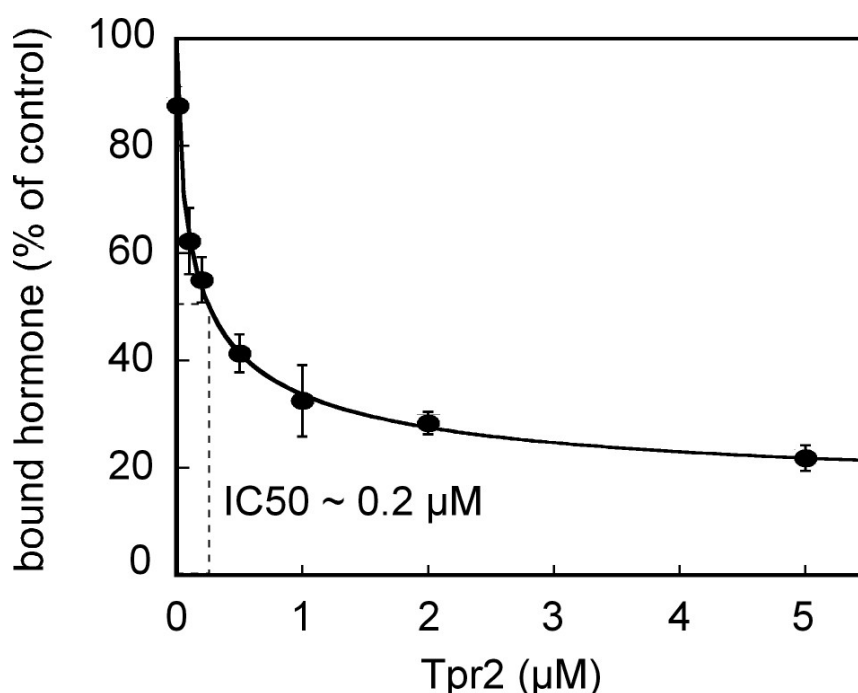
Figure 41   Titration of the Tpr2 effect on the *in vitro* refolding of GR.

The chaperone mediated *in vitro* refolding yield of GR is dependent on the concentration of Tpr2. The GR refolding assay was carried out as described in Figure 40. The reactions were supplemented with increasing concentrations of Tpr2 (0.01, 0.1, 0.2, 0.5, 1, 2, 5 µM). The normalised results were plotted against the Tpr2 concentration. The IC_{50} value was estimated to be around 0.2 µM.

The amount of added Tpr2 was in the range between 0.01 to 5 µM (Figure 41). Hormone binding was very efficiently inhibited even at low ratios of the cofactor and reached a 50% inhibition (IC_{50}) at about 0.25 µM. At this concentration Tpr2 is substochiometric to Hsp90 and Hsp70 in the RL, which are estimated to range around 2-5 µM. In agreement with the low *in vivo* abundance of Tpr2, an equally low dose of Tpr2 is sufficient in the *in vitro* assay to cause an inhibitory effect. This result supports the view that Tpr2 plays a regulatory role in the multichaperone complex rather than being a central component.

4 Discussion

The following discussion will consider how the interactions of Tpr2 with Hsp70 and Hsp90 compare with other co-chaperones, and the broader implications of Tpr2 function for the chaperone machinery in cells.

4.1 Working model for Tpr2 function

In this study Tpr2 has been identified as a new member of the regulatory cofactor group of Hsp70 and Hsp90. Its role in interacting with both Hsp70 and Hsp90 via TPR-clamp domains has been established and connected to a functional relevant activity in the folding of a stringent multichaperone substrate. Moreover the rare protein domain architecture of Tpr2 combines the TPR-clamp chaperone binding sites with a J-domain that can stimulate the Hsp70 folding cycle and by that contributes to the overall efficiency of multichaperone mediated substrate folding. The activity of Tpr2 is novel since this is the first cofactor, which provides the means for a backward transfer of substrates from Hsp90 to Hsp70. After Tpr2 has docked through its TPR-clamps the substrate is released from Hsp90 in an ATP independent manner. At the same time the substrate can be tightly bound to Hsp70 by stimulating its ATP-hydrolysis rate via the J-domain of Tpr2, shifting the chaperone to a stable, high affinity, low dynamic state.

The expression level of Tpr2 in cells appears to be finely tuned for optimum efficiency of the Hsp70/Hsp90 machinery, as an increase or decrease in Tpr2 levels reduces the yield of native protein. The correct amount of backwards transfer caused by Tpr2 most likely aids the folding of proteins which require more than one passage through Hsp70 and Hsp90.

4.1.1 Effects of Tpr2 on the substrate passage through the Hsp70/Hsp90 system

As described above, Tpr2 appears to favour the backwards transfer of substrate from Hsp90 to Hsp70. Because Hsp90 binds SHR, at both the intermediate and late stage of

maturation, it is not clear at which stage the fate of the substrate is affected. Nethertheless, the possible implications of Tpr2 interaction at each of the stages can be extrapolated from their known characteristics.

In the intermediate complex both Hsp70 and Hsp90 are usually held in close spatial proximity by the scaffold protein Hop. This stage is particularly of interest since it is assumed to mediate the passage of substrate from Hsp70 to Hsp90. *In vitro* studies with purified proteins have tried to answer the question which cofactors are actually essential to obtain a native substrate. The assay allowed monitoring of the assembly of steroid receptor/chaperone complexes in a minimal system reconstituted of Hsp70, Hsp90, Hop, Hsp40, p23 and substrate (Dittmar et al. 1998; Kosano et al. 1998). Although these proteins were sufficient for complete assembly it remained to be shown which of them contribute to the actual folding of the substrate. When monitoring the hormone binding activity of GR as a criterion for productive folding, it was demonstrated that a combination of Hsp70 and Hsp90 is sufficient to fold the receptor (Morishima et al. 2000). Although none of the chaperones alone is sufficient, there is no strict requirement for one of the other three proteins of the minimal assembly system. This finding is further strengthened by *in vivo* experiments, in which the activity of p23, Hop and Hsp40 was eliminated. After deletion of SBA1, the yeast homolog of p23, the dexamethasone induced transcription activation was not influenced (Bohen 1998; Fang et al. 1998). The yeast homolog of Hop (STI1) was deleted in another experiment and this led to a reduction of GR activity but did not eliminate it (Chang et al. 1997). Similarly a mutation in YDJ1, the yeast Hsp40 homolog, still allowed steroid response via the glucocorticoid receptor, although to a reduced level (Kimura et al. 1995). While these results add *in vivo* evidence for the nonessential role of the cofactors in GR folding, it must be emphasised that the addition of Hsp40 and Hop to the *in vitro* system contributes to a substantial increase in the yield of the steroid-binding activity of the receptor, whereas p23 is needed for the stable heterocomplex assembly (Dittmar et al. 1998; Kosano et al. 1998). Under cellular conditions, where off-pathway reactions are favored over productive folding, the effects of the cofactors on chaperone mediated folding become even more important for the fitness of the whole organism.

According to the multichaperone machine model, substrate is loaded onto Hsp70 via an initial interaction with Hsp40 as depicted as the early complex state (Figure 42). Hsp70 oscillates in its nucleotide state as it undergoes repetitive interaction cycles (Morishima et al.

2001). This fluctuation creates enough plasticity in the substrate interaction that it allows the passage onto Hsp90. Hsp90 is kept in its substrate acceptor state by Hop, which prevents ATP binding to the chaperone. In the intermediate complex Hsp70, Hsp90, Hsp40 and Hop are present at the same time and stimulate the forward transition of substrate onto Hsp90. Since Tpr2 competes with Hop for TPR-clamp binding and can substitute for the stimulating activity of Hsp40 on Hsp70, this stage probably is the main switch for substrate fate (Figure 42, intermediate complex). After replacing Hop on the Hsp90 dimer, several possible scenarios can occur.

One mode of action is the transfer of substrate within the intermediate complex. After Tpr2 breaks the Hsp90-substrate contact and stimulates the binding of Hsp70 by triggering its ATPase activity, the substrate can reenter the folding cycle right at the intermediate-complex step (Figure 42, pathway 1). This avoids the release of non-native substrates into the bulk cytosol, where they would encounter an aggregation prone situation. Such release events would be highly unproductive for the cell or could even be harmful (Hartl and Hayer-Hartl 2002). Multiple rounds of successive Hsp70-, Hsp90-interactions could actually be needed for the complete maturation of some substrates. Although the mechanism by which Hsp90 dependent substrates are recognised is still under discussion, it was suggested that a crucial event in the recognition is the partial opening of collapsed protein pockets during the priming step via Hsp70 (Pratt and Toft 2003). This would expose otherwise buried hydrophobic patches, like in the steroid binding pocket of hormone receptors, which are then in turn recognised by Hsp90. As previously mentioned, this process seems to include multiple rounds of Hsp70 binding and release cycles. In extension of this finding it seems logical that a single binding event of Hsp90 is not in every case sufficient to promote a transition of the substrate into its native conformation. Instead of releasing the substrate into the bulk solution or keeping it bound to Hsp90 in a pre-mature form it is necessary for the completion of the folding process that the substrate is recycled. The coordination of Hsp70 activity together with the release from Hsp90 could be a way to maintain an intermediate conformation and promote protein maturation through repetitive chaperone binding cycles.
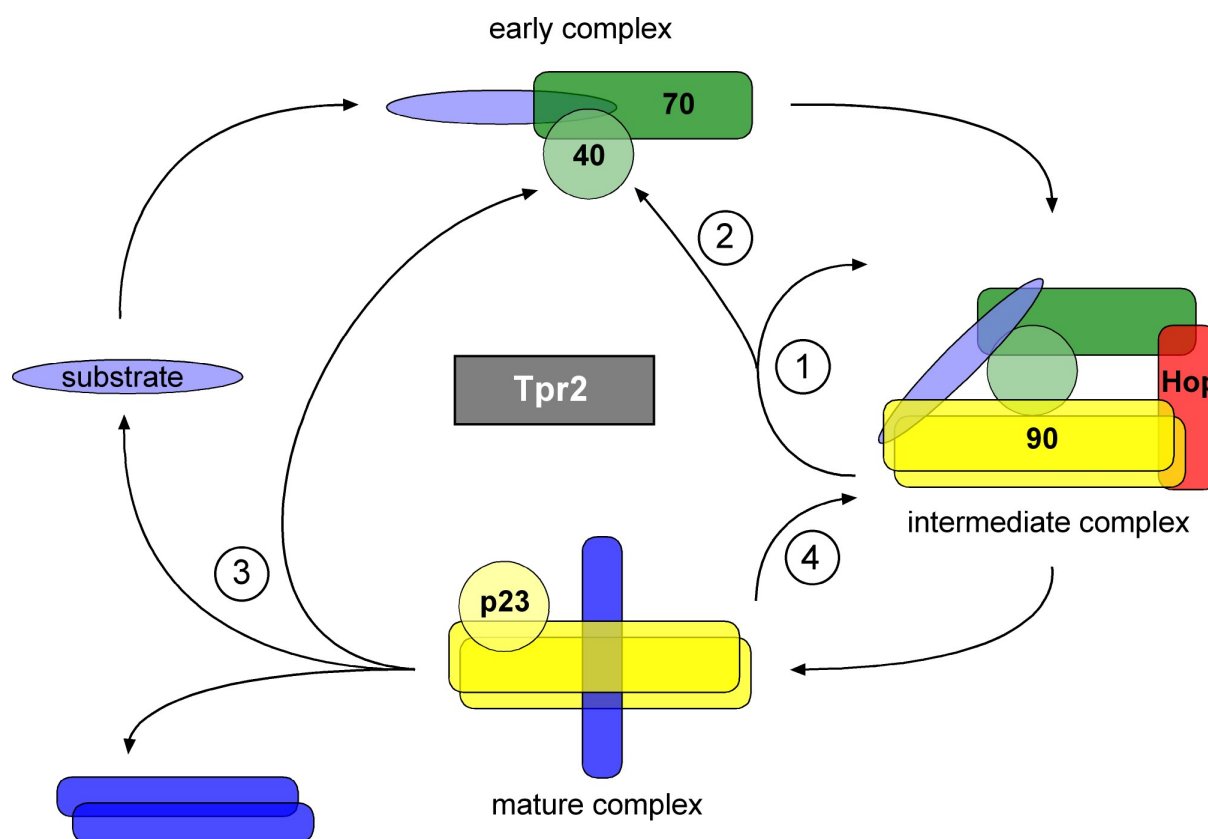
Figure 42   Tuning of the multichaperone machinery by Tpr2.

Tpr2 can influence the passage of substrates through the multichaperone machinery at different steps. Substrate can fluctuate between Hsp70 and Hsp90 within the intermediate complex (1). Substrate/Hsp90 contact is abrogated and the substrate reenters the folding cycle at the early complex state (2). Substrates which interact with the mature complex can either be recycled for folding by transfer to the early complex (3) or to the intermediate complex (4).

It is unclear how tight the Hsp70/Hsp90 interaction needs to be in terms of spatial coordination or time resolution to allow substrate maturation. Experiments have shown that the intermediate complex forms quickly after the early complex (Smith 1993). This means that even if Tpr2 would lead to a dissociation of the multichaperone complex after uncoupling Hsp90-substrate interactions (Figure 42, pathway 2), a reintegration of the complete system can be achieved in a reasonable short time span.

At the stage of the mature complex a similar decision on the folding pathway could be necessary to complete or extend the passage of the substrate through the Hsp machinery. By definition the transition to the mature complex includes replacement of Hsp40, Hsp70 and Hop by other cofactors. This also involves final modifications on the folding of the substrate towards its native structure. Before this ultimate step, the plasticity introduced by Tpr2 could allow alternative pathways. Substrate could be rebound to Hsp70 while the contact to Hsp90

is completely lost (Figure 42, pathway 3), or the multichaperone complex might directly reassemble into the intermediate state, providing the complete folding machinery on site (Figure 42, pathway 4), as suggested by the gel filtration experiment (Figure 39).

The proposed regulatory mechanism of Tpr2 is in agreement with the *in vivo* data. The experiments confirm that a well-balanced cellular level of the cofactor contributes to the folding of GR and disturbance of this balance results in a loss of effectiveness of the maturation process. In the case of excess Tpr2 the stimulated unloading of substrate from Hsp90 would not allow its complete maturation and sends it into unproductive folding cycles. The gel filtration experiment is supportive of this explanation, because GR accumulates in the Hsp90/multichaperone peak and does not form high molecular weight aggregates. In a cellular context, with temporarily increased levels of Tpr2, one can observed that GR levels are not significantly changed (Figure 18). Again this indicates that only the folding is impaired but the pathway decision towards aggregation or degradation is untouched. This point is strengthened by the observation that the response to a constitutive active GR mutant is not changed after Tpr2 overexpression (Figure 19).

4.1.2 Effects of chaperone cofactors on substrate maturation

Although the Hsp70 and Hsp90 cofactors are functionally and structural quite different the published data indicate that a productive interplay can only arise at a defined balance of the players. Imbalances in the expression levels affect the folding of stringent Hsp90 substrates in most cases negatively.

Similar to Tpr2, Hop, or its yeast homolog Sti1, was also originally identified as a general factor in the maturation pathway of Hsp90 target proteins (Chang et al. 1997). Besides its putative role in mediating the heat shock response of some Hsp70 genes (Nicolet and Craig 1989), little is reported on Hop overexpression effects. As the working model for Hop suggests that it stimulates the forward flow of substrates in the multichaperone complex, it could theoretically act as a functional antagonist of Tpr2. However, the *in vivo* and *in vitro* data shown in this study consistently demonstrate that excessive Hop does have a negative impact on chaperone mediated GR folding and this effect cannot be countered by the presence of Tpr2 (Figure 14, Figure 40). Although an antagonistic principle of the two cofactors cannot

be completely dismissed, the experimental setup does not allow its detection. Instead, the idea that the cellular concentrations of chaperone cofactors are tightly tuned for optimal activity can also be extended to Hop. The means by which excess Hop down-regulates GR folding could be related to its inhibition of the ATPase activity of Hsp90. That would hold the chaperone dimer in an open conformation incapable of undergoing conformational changes or completion of its folding cycle. This is different from Tpr2, which has a comparatively more active role by unloading substrates from Hsp90.

An interference with the folding efficiency of the multichaperone complex can also occur at a very early stage. For example BAG-1, which was identified as an inhibitor of cell death, binds to the ATPase domain of Hsp70 and stimulates its ATP hydrolysis rate up to 40 fold in combination with Hsp40. This is achieved by accelerating the release of ADP (Hohfeld and Jentsch 1997). In vitro experiments show that excess BAG-1 inhibits the refolding of an unfolded Hsp70 substrate, dependent on its ability to bind to the chaperone (Takayama et al. 1997). The direct interaction with Hsp70 explains why BAG-1 has been implicated to interact with a number of proteins, including c-Jun, Raf-1 and steroid hormone receptors. Different to Tpr2 the negative effect of BAG-1 on the regulation of GR is only partially due to the inhibition of the hormone binding activity. It also exerts a more direct function at the level of transactivation in the nucleus by repressing DNA binding of the GR. Again this requires the interaction with Hsp70 and substrate (Schneikert et al. 2000; Cato and Mink 2001; Schmidt et al. 2003). This is in contrast to Tpr2, which does not change its cellular distribution after hormone treatment (Figure 43).
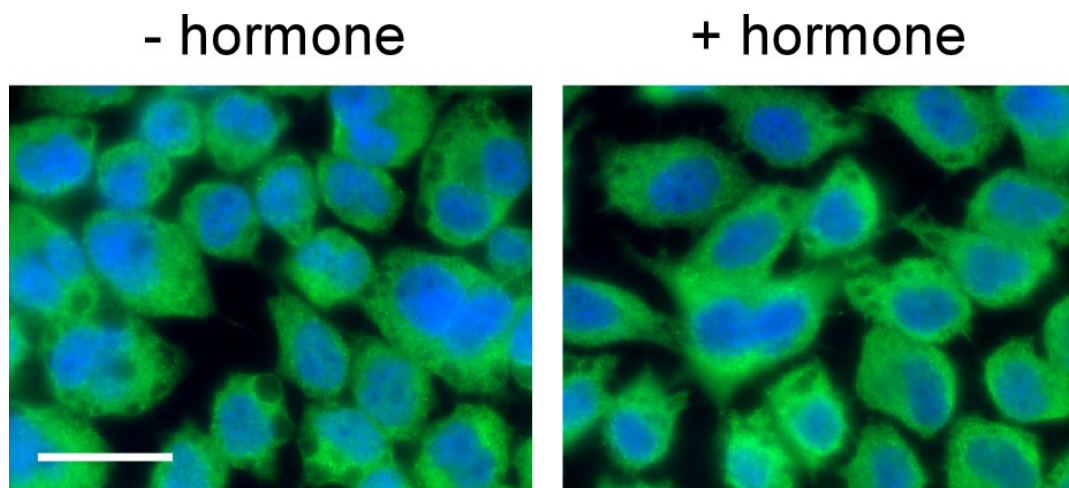
Figure 43   IF of Tpr2 in the presence or absence of hormone.

Immunofluorescence of HeLa cells after PFA fixation and Saponin treatment. Nuclei were stained with DAPI (blue) and Tpr2 was detected with an affinity purified Tpr2 antibody (α Tpr2) and visualized with a FITC conjugated secondary antibody (green). The cells were treated with 1μM Dexamethasone (+ hormone) or the respective volume of ethanol solvent (- hormone) for 24 hours. The pictures were taken at a 63 fold magnification. The scale bar represents 25 μm

The co-chaperone p23 also follows a two-way strategy in regulating chaperone dependent events by influencing receptor activation as well as transactivation. An early hint for p23 function came from a yeast screen, following the activation of the Hsp90 dependent estrogen receptor (ER). Here, p23 overexpression resulted in increased hormone binding. This effect vanished with increasing concentrations of the receptor or the hormone, indicating an important cofactor for p23 at physiological relevant concentrations. The authors also reported a redistribution of p23 to the nucleus after coexpression of the ER, suggesting that downstream events in the activation cascade might also be influenced by the co-chaperone (Knoblauch and Garabedian 1999). This is different from Tpr2, which acts only at the stage of protein folding and has no influence on transactivation events of the glucocorticoid receptor, demonstrated by the expression of a constitutive active variant of the receptor (Figure 19). In contrast, p23 shows localisation to genomic response elements dependent on the hormone activation state of intracellular receptors (Freeman and Yamamoto 2002). In combination with Hsp90 it efficiently disrupts receptor-mediated transactivation by stimulating the disassembly of the regulatory complex.

4.2 Structural comparison of multichaperone cofactors

The cofactor/co-chaperone group is quite different in terms of domain composition. In general the members of this group can be divided on the basis of the presence or absence of TPR-clamps. The cluster of non TPR-clamp proteins contains e.g. the Hsp70 interacting protein Hsp40, BAG-1 and the Hsp90 interactors Cdc37, Aha1 and p23. Cofactors of this group have divergent chaperone binding sites. In contrast, the group of TPR-clamp proteins competes for binding to a single docking site. They can be further subdivided into proteins which interact with both Hsp70 and Hsp90, like Hop or CHIP, or which exclusively bind to Hsp90, like the immunophilins of the FK506 class or which only target Hsp70, like SGT (small glutamine-rich TPR-containing protein). The specificity of this interaction is dependent on the selectivity of the TPR-clamp domain, which will be explained in more detail in the upcoming paragraphs.

4.2.1 Tpr2 domain composition

The combination of two chaperone binding sites and an Hsp70 regulatory domain makes Tpr2 unique amongst the known chaperone cofactors. A database screen for proteins containing both, TPR- and DnaJ-domains, lists 42 proteins. Many of them are identified as homologs of Tpr2. A second prominent member with this domain combination is the protein kinase inhibitor p58. Unlike Tpr2 the TPR-domains of p58 do not have the conserved clamp-anchor residues. In agreement with this finding, a TPR-dependent interaction with chaperones has not been reported for p58 in the literature. Any other protein in this list is either marked as hypothetical/unknown function or does not contain a TPR-clamp. In addition, the known homologs of Tpr2 can only be found in the superkingdom of Eukarya. Together with the fact that yeast (*Saccharomyces cerevisiae*) does not contain a homolog, one can assume that Tpr2 has a more specialised but nonessential function in the cell. The data presented in this work confirms this hypothesis and outlines a rather regulatory role of Tpr2 in the control of the multichaperone machinery.

4.2.2 Comparison of TPR-clamp cofactors

As mentioned earlier, the group of TPR-clamp containing cofactors varies in its chaperone specificity. Additionally there are also differences in the structural organisation and the occurrence of functional domains. Figure 44 gives a domain overview of a selection of members from this cofactor class.
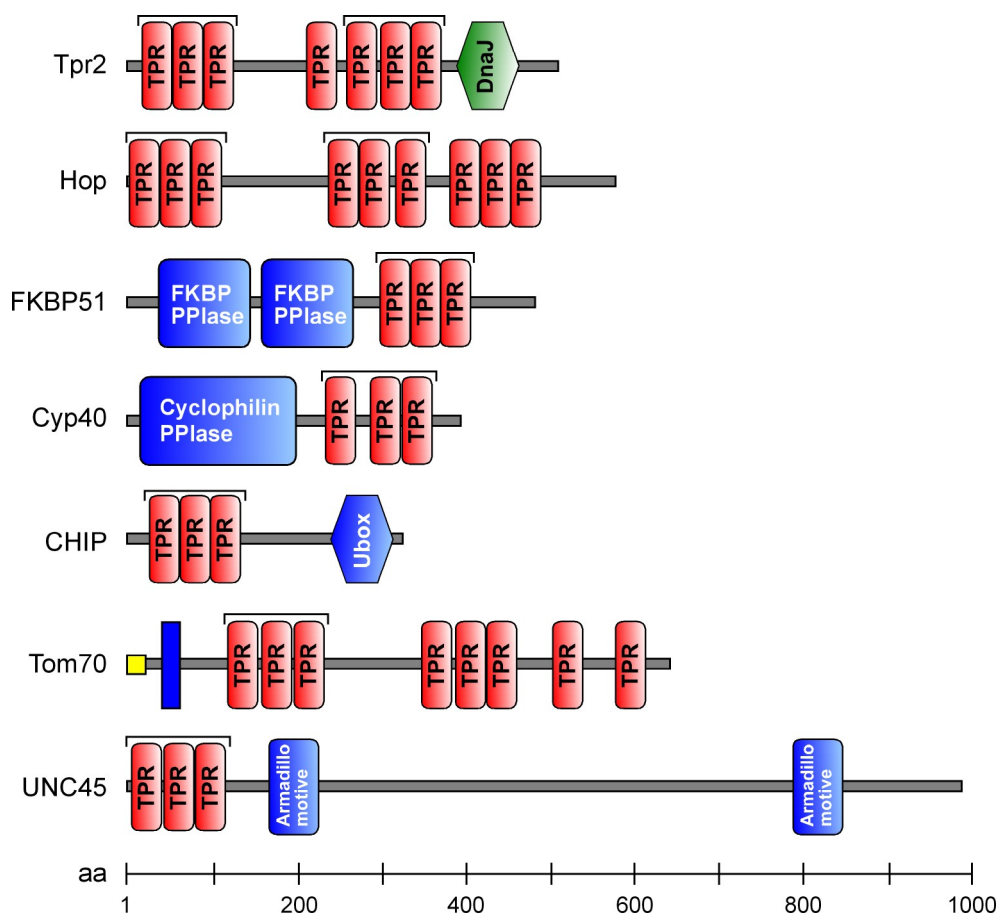
Figure 44   TPR-clamp cofactors domain organisation.

A selection of established TPR-clamp containing cofactors of Hsp70 and Hsp90 are presented in a schematic domain overview. All sequences represent the human homolog of the respective protein. The TPR-repeats (in red, TPR), which harbour a TPR-clamp domain are framed. The Tom70 sequence harbours a signal peptide (yellow box) and a transmembrane region (blue box). The protein sequences can be retrieved from the date base with the following accession codes: Tpr2: NP_003306, Hop: NP_006810, FKBP51: NP_004108, Cyp40: Q08752, CHIP: AAD33400, Tom70: NP_055635, UNC45: NP_775259.

The localisation of the TPR-clamps does not follow an obvious rule and varies from a position at the N-terminus, like in the case of CHIP, to a C-terminal appearance, for example in the case of FKBP51, or is somewhere in between, like the T2-domain of Tpr2. A similar picture emerges from the location of additional functional domains. For example the peptidyl-prolyl cis-trans isomerase domain of Cyp40 is N-terminally located, whereas the DnaJ domain of Tpr2 resides at the C-terminus of the protein, just like the Ubox of CHIP.

A common feature for all these cofactors is that the TPR-clamp domains consist of 3 sequential TPR-motifs, which are in close proximity to each other. It has not been reported that a TPR-motif within such a triplet is distally located in the primary sequence, with intervening protein domains. This means that TPR-clamps usually have a very tight domain architecture and should therefore be easily detectable in a database search.

Interestingly the proposed conserved residues, which participate in the formation the two-carboxylate clamp anchor, are not absolutely conserved (Figure 45, highlighted letters). A comparison of several known mammalian Hsp70/Hsp90 cofactors shows that in 4 cases an amino acid exchange in one of these residues can be observed (Figure 45, letters highlighted in blue). In the case of Tpr2 a conserved exchange from the expected lysine to arginine can be detected at position 4 in the first TPR-clamp (T1). The basic side chains of both amino acids and a similar steric structure can explain why this clamp is still active. Quite different to that, the exchange of asparagine by threonine in FKBP51 and FKBP52 and the exchange of arginine to phenylalanine in the case of CHIP means a much more drastic change in the charge state of the respective position. Nonetheless a chaperone specific interaction has been shown for these proteins through biochemical analysis (Chen et al. 1998; Ballinger et al. 1999).

```
Hop TPR1     VNELKEKGNKALSVGNIDDALQCYSEAIKLDP---------------HN
Hop TPR2A    ALKEKELGNDAYKKKDFDTALKHYDKAKELD---------------PTN
Tpr2 T1      AETFKEQGNAYYAKKDYNEAYNYYTKAIDMC---------------PKN
Tpr2 T2      LKAKKEDGNKAFKEGNYKLAYELYTEALGIDPN-----------NIKTN
FKBP51 TPR   AAIVKEKGTVYFKGGKYMQAVIQYGKIVSWLEME-YGLSEKESKASESFL
FKBP52 TPR   STIVKERGTVYFKEGKYKQALLQYKKIVSWLEYE-SSFSNEEAQKAQALR
Cyp40 TPR    TEDLKNIGNTFFKSQNWEMAIKKYAEVLRYVDSSKAVIETADRAKLQPIA
PP5 TPR      AEELKTQANDYFKAKDYENAIKFYSQAIELN---------------PSN
CHIP TPR     AQELKEQGNRLFVGRKYPEAAACYGRVIT-------------R--NPLV
UNC45 TPR    AVQLKEEGNRHFQLQDYKAATNSYSQALK------------LTKDKALL
Tom70 TPR    AQAAKNKGNKYFKAGKYEQAIQCYTEAISLCP----------TEKNVDL
```

```
Hop TPR1     HVLYSNRSAAYAKKGDYQKAYEDGCKTVDLKP-------DWGKGYSRKAA
Hop TPR2A    MTYITNQAAVYFEKGDYNKCRELCEKAIEVGRENREDYRQIAKAYARIGN
Tpr2 T1      ASYYGNRAATLMMLGRFREALGDAQQSVRLDD-------SFVRGHLREGK
Tpr2 T2      AKLYCNRGTVNSKLRKLDDAIEDCTNAVKLDD-------TYIKAYLRRAQ
FKBP51 TPR   LAAFLNLAMCYLKLREYTKAVECCDKALGLDS-------ANEKGLYRRGE
FKBP52 TPR   LASHLNLAMCHLKLQAFSAAIESCNKALELDS-------NNEKGLFRRGE
Cyp40 TPR    LSCVLNIGACKLKMSNWQGAIDSCLEALELDP-------SNTKALYRRAQ
PP5 TPR      AIYYGNRSLAYLRTECYGYALGDATRAIELDK-------KYIKGYYRRAA
CHIP TPR     AVYYTNRALCYLKMQQHEQALADCRRALELDG-------QSVKAHFFLGQ
UNC45 TPR    ATLYRNRAACGLKTESYVQAASDASRAIDINS-------SDIKALYRRCQ
Tom70 TPR    STFYQNRAAAFEQLQKWKEVAQDCTKAVELNP-------KYVKALFRRAK

Hop TPR1     ALEFLNRFEEAKRTYEEGLKHEANN
Hop TPR2A    SYFKEEKYKDAIHFYNKSLAEHRTP
Tpr2 T1      CHLSLGNAMAACRSFQRALELDHKN
Tpr2 T2      CYMDTEQYEEAVRDYEKVYQTEKTK
FKBP51 TPR   AQLLMNEFESAKGDFEKVLEVNPQN
FKBP52 TPR   AHLAVNDFELARADFQKVLQLYPNN
Cyp40 TPR    GWQGLKEYDQALADLKKAQGIAPED
PP5 TPR      SNMALGKFRAALRDYETVVKVKPHD
CHIP TPR     CQLEMESYDEAIANLQRAYSLAKEQ
UNC45 TPR    ALEHLGKLDQAFKDVQRCATLEPRN
Tom70 TPR    AHEKLDNKKECLEDVTAVCILEGFQ
```

Figure 45   Comparison of human TPR-clamp domains

Some TPR-clamp cofactors of Hsp70 and Hsp90 contain amino-acid exchanges in the conserved clamp-residues, which differ from Hop. All sequences represent the human homolog of the respective protein. The conserved TPR-clamp residues are marked in red. Amino-acids which differ from the respective Hop residues are marked in blue. Residues which are implicated in conferring Hsp-class specificity are represented in bold.

The prediction profile for TPR-clamp interactions becomes even less uniform when comparing the residues which have been implicated in conferring chaperone-class specificity for Hsp70 or Hsp90 through hydrophobic and van der Waals contacts (Figure 45, letters in bold) (Scheufler et al. 2000). A mutation screen with a truncated version of the yeast Hop homolog Sti1, incapable of binding to Hsp90, shows that substitution of some of these residues result in a loss of Hsp70 binding, accompanied by a novel Hsp90 interaction with the TPR1 domain. In contrast equivalent substitutions in TPR2 did not confer Hsp70 specificity (Odunuga et al. 2003). This variety of the TPR-motif in general and the clamp residues in particular makes a data base search for chaperone-specific TPR-clamp cofactors more inaccurate and must therefore always be backed up by biochemical methods. It was also suggest that the first and second clamp residues constitute the minimum interaction sites (Odunuga et al. 2003). In the present study the fifth conserved clamp residue was mutated and this resulted in a significant, but incomplete loss of TPR binding activity. Corresponding mutations in the TPR-domains of Hop or Tom70 were described to disrupt Hsp70 and Hsp90 binding (Brinker et al. 2002; Young et al. 2003). The low but measurable residual affinity of

the Tpr2 mutants (Figure 24) was probably enough to result in a partial phenotype in the *in vivo* experiments (Figure 38), where the cellular environment would favour such interactions. To completely abrogate TPR-clamp dependent binding it could be necessary to mutate more of the conserved clamp-residues. Since the reconstituted *in vitro* GR folding system shows that under more dilute conditions the Tpr2 triple mutant (dT12J) is almost inactive (Figure 40), it can be assumed that additional protein-protein interaction sites are absent or play a negligible role for the function of Tpr2. This is strengthened by the co-precipitation experiments, where chaperone binding is abolished with the dT12J mutant (Figure 22).

4.3 Regulation of chaperone function

Although the question of how Hsp70 and Hsp90 actually fold proteins has not been answered in detail yet, but a growing insight into the functional principles of how cofactors regulate Hsps has been gained in the recent years. These results provide a basic picture of how substrates are passaged through the chaperone network, which has been summarised in the introduction chapter of this work. It becomes clear that the single steps of this pathway are dependent on the coordinated action of different chaperone classes either alone or in a multiprotein structure. For the maintenance of this pathway, some cofactors regulate only one type of chaperones, others control both Hsp70 and Hsp90 or confer further functions. In this study Tpr2 was identified as a cofactor, which not only binds to Hsp70 and Hsp90, but also modulates their activity.

4.3.1 Cofactor dependent regulation of Hsp70

The substrate binding and release cycle of Hsp70 is critically dependent on its ATPase activity. J-domain containing proteins like Hsp40 stimulate the hydrolysis step in this process. By comparing wild-type Tpr2 with its J-domain mutant (dJ) it was shown that the Hsp70-activation domain is functionally active (Figure 27). Moreover, binding of Tpr2 with its TPR-clamps to the C-terminus of Hsp70 is not crucial for this function. This has also been observed for Hsp40, which can contact the chaperone at the C-terminal domain, but nucleotide turnover is not dependent on this interaction, although the efficiency profits from the binding. The NMR structure of DnaJ/Hsp40 shows that the J-domain consists of 3 alpha-helixes. Chemical shift mapping identified helix 2 and the adjacent loop region, which

contains the HPD motif, as the contact site for the ATPase domain. Recent data suggest additional contacts in the loop region and in helix 3. This part of the protein is proposed to undergo conformational changes after binding to Hsp70 (Landry 2003). Interestingly Tpr2 does contain an additional stretch of six amino-acids within this region (Figure 12). When the isolated J-domains of Hsp40 and Tpr2 were tested for their efficiency in stimulating the Hsp70 ATPase activity, the J-domain of Tpr2 was as efficient as the full-length protein, whereas the J-domain of Hsp40 retained only 50 % activity of the full-length protein (data not shown). In view of the putative expanded contact site between the J-domain and Hsp70, one could assume that the additional amino-acids in the loop region of Tpr2 might contribute to a higher affinity and as a consequence thereof to a more effective stimulation of Hsp70 in the absence of additional protein contacts. This finding was not further investigated since this study concentrated on the overall function of Tpr2. Full-length Tpr2 and Hsp40 have the same effect on Hsp70 mediated protein refolding (Figure 29), which suggests that under more relevant conditions, using the full-length proteins, the effect of the additional amino-acids is negligible.

Co-precipitation of Tpr2 with Hsp70 was abolished when the TPR-clamp mutants (dT12, dT12J) were used, suggesting that the small portion of Tpr2 in the pellet fraction is due to a chaperone interaction and not due to a formation of Tpr2/substrate complexes (Figure 28). This is different from Hsp40, which directly binds to unfolded substrates before loading them onto Hsp70. This feature of the co-chaperone is reflected in the significant amount of Hsp40 seen in the pellet fraction of the experiment.

In most cases, J-domain containing proteins are identified as homologs of Hsp40, directly engaged in the general pathway of Hsp70 mediated protein folding. In contrast, Tpr2 also contains binding sites which can direct Hsp70 into the multichaperone complex by interaction with Hsp90 through its TPR-clamps. A similar strategy of chaperone recruitment can be found in some other proteins, which also combine a J-domain with additional functions. Amongst them are the cystein string protein (CSP), implicated in exocytosis of synaptic vesicles, or auxilin, which acts in uncoating of clathrin coated vesicles (Ungewickell et al. 1995; Chamberlain and Burgoyne 2000). The common functional principle of proteins with such domain compositions is to provide Hsp70 activation at a specific cellular localisation, coupling it to protein disassembly, vesicle fusion or protein folding in the case of Tpr2, in a relevant functional context.

4.3.2 Regulation of Hsp90 function by Tpr2

The function of Hsp90 under normal growth conditions is that of an "acceptor" chaperone, which receives almost native substrates late in the folding pathway. The time course of the assembly of the multichaperone complex clearly shows that Hsp90 enters the folding-pathway after Hsp70 and guides the substrate to its mature state. Contrary to this pathway, Tpr2 is the first protein which appears to reverse the Hsp90/substrate interaction. This effect is independent of its J-domain but requires functional TPR-clamps (Figure 36). Interestingly, the release reaction does not require ATP hydrolysis by Hsp90 (Figure 34), nor does Tpr2 change the steady-state ATP turnover of Hsp90 (Figure 33). This could mean that substrate displacement after Tpr2 binding occurs as a result of a passive sterical hindrance event between Tpr2 and the substrate contact regions on Hsp90, rather than involving an active mechanism. Although such a mechanism has not been demonstrated in the case of cofactor-substrate competition before, a similar steric competition for co-chaperone binding to neighbouring regions on Hsp90 was shown for combinations of Sti1 and Aha1 in yeast (Lotz et al. 2003) and Cdc37 in combination with Hop (Owens-Grillo et al. 1996; Silverstein et al. 1998). The Tpr2 double-clamp mutants dT12 and dT12J show only a residual release activity (Figure 36), indicating that the TPR-clamp contact is the specificity conferring step for the release of substrate from Hsp90.

Since the C-terminus of Hsp90 is a common binding site for TPR-clamp cofactors, Tpr2 must compete with a multitude of these cofactors to exert its function. The actual number of TPR-acceptor sites per Hsp90 dimer is still controversially discussed. FKBP52 for example was shown to have a binding ratio of one protein per Hsp90 dimer by cross-linking experiments (Silverstein et al. 1999) and of two proteins per Hsp90 dimer as determined by isothermal calorimetry (Pirkl and Buchner 2001). An internal deletion mutant of Hsp90 (delta aa 661-677), incapable of forming dimers, interacts only weakly with FKBP52 (Chen et al. 1998). Moreover, the immunophilins Cyp40 and FKBP52 have not been found in the same heterocomplexes (Owens-Grillo et al. 1995). Together, a model for Hsp90 in which a functionally active Hsp90 dimer provides only one high affinity TPR-contact site is most consistent with all observations (Pratt and Toft 2003). The individual integration of TPR-clamp cofactors into diverse Hsp90 heterocomplexes can either be based on different

affinities, the respective local abundances of the cofactors, or on additional direct substrate interactions. Tpr2 was shown to cause release of a stringent Hsp90 substrate (Figure 31) as well as of luciferase, which cannot be folded by Hsp90 and rather utilises the chaperone as a holding compartment (Figure 35). This argues for an affinity-based recruitment of Tpr2. Either substrate specific recruitment events, e.g. between Cdc37 and cyclin-dependent kinases (Kimura et al. 1997), or the sheer number of other cofactors will compete for the interaction of Hsp90 with Tpr2 in the cell and only a small subpopulation of multichaperone complexes will contain Tpr2 as a cofactor at one time. However all TPR-clamp cofactors have fast on- and off-rates for Hsp90 (Brinker et al. 2002) and Tpr2 also shows this property (Figure 23, A and B). Thus, a small number of Tpr2 molecules may have a large effect by transiently regulating a larger number of Hsp90 dimers. The structural mechanism used by Tpr2 for substrate release from Hsp90 is still to be determined.

4.4 Cellular role of Tpr2

Similar to other chaperone cofactors, Tpr2 contributes to the overall efficiency of protein folding. It is part of a functionally divergent pool of Hsp70/Hsp90 interacting proteins, which help chaperones to adapt their activity to a wide variety of client proteins. Although a time course of substrate passage has been laid down and the basic components in this process have been identified, it remains unclear how cells tune the precise cofactor composition in relation to the particular substrate. Contrary to some other co-chaperones which can directly interact with substrates, and thus are incorporated into the multichaperone machinery, the function of Tpr2 seems to follow a more general strategy.

In the present study, Tpr2 was shown to unload substrates from Hsp90, which are either stringent (LBD) or non-stringent (luciferase). Preliminary experiments extend this function of Tpr2 to other Hsp90 dependent interactors. Overexpression of Tpr2 in a heterologous *S. cerevisiae* system inhibits the Hsp90 dependent activation of the oncoprotein v-src (Obermann, unpublished data). However, Tpr2 does not have a homolog in *S. cerevisiae* and it is unclear if it regulates yeast Hsp82 in the same manner as mammalian Hsp90. Tom70, an import receptor of the outer mitochondrial membrane, contains a TPR-clamp docking site for Hsp70 and Hsp90, which is crucial for preprotein import (Young et al. 2003). When Tpr2 is present during an import reaction, it inhibits the translocation of the substrate (Young,

unpublished data). It is not yet clear if this effect depends on substrate unloading or is due to competitive binding of excess Tpr2 to the C-termini of Hsp70 and Hsp90. However, both results widen the contributions of Tpr2 to a broader spectrum of Hsp90 interacting proteins. This further consolidates a more general role of Tpr2 in the multichaperone complex.

The data presented in this work support the view that under normal growth conditions Tpr2-induced recycling of substrates can aid the folding of a fraction of substrates, which have not reached their native fold after a single round through the multichaperone system. Mistakes during protein folding *in vivo* could occasionally lead to misfolded proteins, which are energetically trapped and cannot easily be removed from Hsp90 by completing the folding cycle. Under such conditions, when the progression through the Hsp70/Hsp90 system is blocked, Tpr2 could help to "clean" the multichaperone complex of unproductive interactions and recycles the chaperones for protein folding. In a way Tpr2 could add a proofreading function for substrate folding to the Hsp-complex. Even if the unproductive binding of substrates occur at a low frequency, such substrates would accumulate on Hsp90 during the life span of an organism and reduce the number of active chaperones over time, unless countered.

During heat-stress cells face an even more unproductive environment and react by overexpression of chaperones to counter the effects of protein unfolding. During this phase Hsp90 is utilised as a general holding compartment, which stores misfolded proteins until they can be refolded with the help of other chaperones.
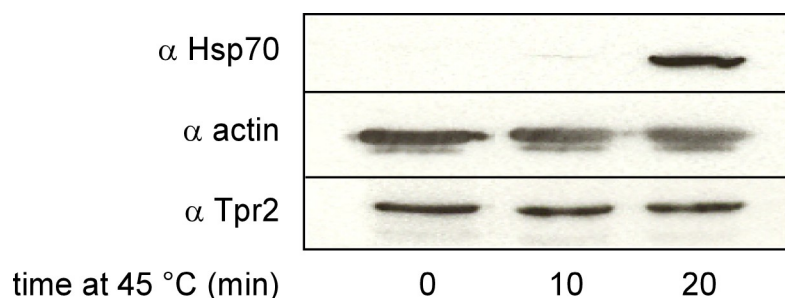

Figure 46   Heat shock with N2a cells.

The heat shock response in N2a cells does not cause induction of Tpr2. N2a cells were incubated for 10 or 20 minutes 45°C to induce a heat shock response. 24 hours after the heat shock cells were harvested and analysed by immunoblotting. Antibodies against Hsp70 (α Hsp70) were used to demonstrate the heat shock response. Actin served as a loading control (α actin) and the expression of Tpr2 was detected with a polyclonal antibody (α Tpr2).

Interestingly, Tpr2 levels in cells are not elevated after heat shock (Figure 46). Such an expression profile is in agreement with the role of Tpr2 in fine-tuning the substrate flow through the Hsp-system. Elevated levels of Tpr2 during the stress situation would abolish the holding effect of Hsp90. Otherwise secured proteins would run an increased risk of being released from the multichaperone system since the available pool of Hsp70 would be depleted due to an excess of substrates. In this situation the folding cycle could not be re-entered and the released, partially unfolded proteins would irreversibly aggregate.

Under optimised laboratory growth conditions, perturbation in the cellular levels of Tpr2 change the folding efficiency of some substrates such as GR, but the overall fitness of the mammalian cells does not seem to be altered. In other words, cells can progress through the cell cycle without obvious growth defects. This is particularly of interest, because some cell cycle regulatory kinases are known Hsp90 substrates, and therefore should also be negatively influenced by perturbed Tpr2 levels. It is possible that Tpr2 has less of an effect on kinase maturation than on GR folding, due to the Hsp90 independent chaperone activity of the kinase specific co-chaperone Cdc37 (Kimura et al. 1997). Cdc37 may have the added effect of sterically hindering TPR-clamp proteins like Tpr2 from binding to Hsp90 (Silverstein et al. 1998). This observation supports the view that the Hsp70/Hsp90 system is able to finely tune its activity by selective interactions with cofactors. In addition, a reduced population of native kinases may be compensated for by increased kinase activation through normal signalling pathways. Chaperone mediated protein folding is clearly important for the viability of the cell, and furthermore, it is integrated into the many complex processes which converge to regulate the life of any organism.

5 Summary

In the eukaryotic cytosol the abundant chaperones Hsp70 and Hsp90 cooperate together with a cohort of co-chaperones and cofactors to facilitate the folding of a growing set of substrate proteins. Amongst them are medically relevant signal transduction molecules like steroid hormone receptors or protooncogenic kinases. In this work Tpr2 was identified as a new cofactor, which modulates the passage of substrates through the Hsp70/Hsp90 multichaperone machinery in a novel manner.

- The Tpr2 protein sequence contains two separate TPR-clamp domains and an additional DnaJ-like J-domain, which is located towards the C-terminus.

- The main interaction partners of Tpr2, as determined by co-precipitation experiments, are Hsp70 and Hsp90.

- Both chaperone classes are bound to Tpr2 via TPR-clamp domain interactions. The binding affinities are in the same range as determined for the Hsp70/Hsp90 scaffold protein Hop. Different from Hop, the TPR-clamps of Tpr2 are not specific for one or the other chaperone class. Point mutations in the conserved TPR-clamp residues reduce the efficiency of this interaction.

- Intact TPR-clamps in Tpr2 are important to stimulate release of stringent or non-stringent substrates from Hsp90 but not from Hsp70. This process occurs in an ATP independent manner.

- The J-domain of Tpr2 efficiently stimulates the chaperone activity of Hsp70. It increases the intrinsic ATPase activity of Hsp70 at least to the same level as the classical co-chaperone Hsp40. Tpr2 stimulates binding of the chaperone to a partially denatured substrate and facilitates the refolding of a stringent Hsp70 substrate to the same extent as observed with Hsp40.

- The stimulation of the Hsp70 chaperone activity is dependent on the J-domain of Tpr2 but not on TPR-clamp interactions. A point mutation in the essential HPD tripeptide motif of the Tpr2 J-domain abolishes its function as an Hsp70 cofactor.

- Tpr2 inhibits the refolding of glucocorticoid receptor (GR) in a rabbit reticulocyte lysate *in vitro* system. Mutations in either the TPR-clamps or the J-domain show moderate effects, whereas the combined mutations almost completely inhibit the action of Tpr2.

- Perturbation of Tpr2 levels in live cells, either by overexpression or siRNA mediated knock-down of Tpr2, inhibit the folding of GR *in vivo*. This effect does not interfere with degradation of the receptor or downstream events in the activation cascade.

Tpr2 provides a novel regulatory function for the Hsp70/Hsp90 chaperone machinery. It facilitates the backwards transfer of substrates from Hsp90 onto Hsp70 while avoiding the risk of releasing the substrates into the bulk solution. This most likely helps to increase the folding efficiency for a subset of Hsp70/Hsp90 dependent substrates, which require repetitive passages through the multichaperone machinery to achieve their native conformation.

6 Zusammenfassung

Im eukaryotischen Zytosol kooperieren die abundanten Chaperone Hsp70 und Hsp90 mit einer Vielzahl von Ko-Chaperonen und Kofaktoren, um die Faltung einer ständig wachsende Zahl von Substraten zu ermöglichen. Unter den Substraten befinden sich medizinisch relevante Signaltransduktionsmoleküle und proto-onkogene Kinasen. Die vorliegende Arbeit identifiziert Tpr2 als neuen Kofaktor, der die Passage von Substraten durch die Hsp70/Hsp90 Multichaperon Maschinerie in neuartiger Weise moduliert.

- Die Tpr2 Proteinsequenz zeigt zwei separate TPR-Klammer Domänen und eine zusätzliche DnaJ ähnliche J-Domäne, die nahe dem C-terminalen Ende platziert ist.

- Durch Koprezipitations Experimente wurden Hsp70 und Hsp90 als die Hauptinteraktionspartner von Tpr2 identifiziert.

- Beide Chaperon Klassen binden an Tpr2 durch Interaktion mit den TPR-Klammer Domänen. Die Bindungsaffinitäten sind ähnlich denen des Hsp70/Hsp90 Gerüstproteins Hop. Im Gegensatz dazu sind die TPR-Klammern von Tpr2 aber nicht spezifisch für die eine oder die andere Chaperonklasse. Eine Punktmutation in einem der konservierten Aminosäurereste der TPR-Klammer reduziert die Effizienz dieser Interaktion.

- Die Integrität der TPR-Klammern in Tpr2 ist eine Vorraussetzung um sowohl stringente als auch nicht-stringente Substrate von Hsp90, aber nicht von Hsp70, zu dissoziieren. Dieser Vorgang ist ATP unabhängig.

- Die J-Domäne von Tpr2 stimuliert die Chaperonaktivität von Hsp70. Sie erhöht die intrinsische ATPase Aktivität von Hsp70 mindestens genauso effizient wie das klassische Ko-Chaperon Hsp40. Darüber hinaus stimuliert Tpr2 die Bindung des Chaperons an teilweise denaturierte Substrate und unterstützt die Rückfaltung eines Hsp70 abhängigen Substrats im gleichen Ausmaß wie Hsp40.

- Die Stimulation der Chaperonaktivität von Hsp70 ist abhängig von der J-Domäne von Tpr2, aber nicht von TPR-Klammer Interaktionen. Die Einführung einer Punktmutation im essentiellen HPD Motive der Tpr2 J-Domäne führt zum Verlust der Hsp70 relevanten Kofaktor Eigenschaft von Tpr2.

- Tpr2 inhibiert die Rückfaltung des Glukokortikoid Rezeptors (GR) *in vitro* in einem Kaninchen Retikulozyten Lysat. Mutationen in den TPR-Klammern oder der J-Domäne zeigen einen verringerten Effekt, während eine Kombination aus diesen Mutanten die Aktivität von Tpr2 fast komplett aufhebt.

- Modulation der Tpr2 Konzentration in Zellen, entweder durch Überexpression, oder durch siRNA vermittelte Abregulierung, hemmen die Faltung von GR *in vivo*. Dieser Effekt ist ohne Einfluss auf den proteolytischen Abbau des Rezeptors und hat auch keinen Einfluss auf Abläufe in der Aktivierungskaskade.

Tpr2 ermöglicht eine neuartige Regulation der Hsp70/Hsp90 Chaperonmaschinerie. Es fördert den Rücktransfer von Substraten von Hsp90 auf Hsp70, ohne dass die Substrate dem Risiko ausgesetzt werden, in die umgebende Lösung abgegeben zu werden. Höchstwahrscheinlich fördert dies die Faltungsproduktivität von einigen Hsp70/Hsp90 abhängigen Substraten, die mehrere Passagen durch das Multichaperonsystem benötigen, um ihre native Faltungskonformation zu erlangen.

7 References

Adam, Z. and A. K. Clarke (2002). "Cutting edge of chloroplast proteolysis." Trends Plant Sci **7**(10): 451-6.

Agashe, V. R. and F. U. Hartl (2000). "Roles of molecular chaperones in cytoplasmic protein folding." Semin Cell Dev Biol **11**(1): 15-25.

Alberti, S., J. Demand, C. Esser, N. Emmerich, H. Schild and J. Hohfeld (2002). "Ubiquitylation of BAG-1 suggests a novel regulatory mechanism during the sorting of chaperone substrates to the proteasome." J Biol Chem **277**(48): 45920-7.

Albrecht, R., C. Scheufler, A. Brinker, J. C. Young and I. Moarefi "Structural basis for the interaction of Hsp90 with the kinase chaperone Cdc37." Manuscript in preparation.

Aligue, R., H. Akhavan-Niak and P. Russell (1994). "A role for Hsp90 in cell cycle control: Wee1 tyrosine kinase activity requires interaction with Hsp90." Embo J **13**(24): 6099-106.

Anfinsen, C. B. (1972). "The formation and stabilization of protein structure." Biochem J **128**(4): 737-49.

Anfinsen, C. B. (1973). "Principles that govern the folding of protein chains." Science **181**(96): 223-30.

Argon, Y. and B. B. Simen (1999). "GRP94, an ER chaperone with protein and peptide binding properties." Semin Cell Dev Biol **10**(5): 495-505.

Ballinger, C. A., P. Connell, Y. Wu, Z. Hu, L. J. Thompson, L. Y. Yin and C. Patterson (1999). "Identification of CHIP, a novel tetratricopeptide repeat-containing protein that interacts with heat shock proteins and negatively regulates chaperone functions." Mol Cell Biol **19**(6): 4535-45.

Ban, C., M. Junop and W. Yang (1999). "Transformation of MutL by ATP binding and hydrolysis: a switch in DNA mismatch repair." Cell **97**(1): 85-97.

Bardwell, J. C. and E. A. Craig (1988). "Ancient heat shock gene is dispensable." J Bacteriol **170**(7): 2977-83.

Beissinger, M. and J. Buchner (1998). "How chaperones fold proteins." Biol Chem **379**(3): 245-59.

Berger, J. M., S. J. Gamblin, S. C. Harrison and J. C. Wang (1996). "Structure and mechanism of DNA topoisomerase II." Nature **379**(6562): 225-32.

Bergerat, A., B. de Massy, D. Gadelle, P. C. Varoutas, A. Nicolas and P. Forterre (1997). "An atypical topoisomerase II from Archaea with implications for meiotic recombination." Nature **386**(6623): 414-7.

Bimston, D., J. Song, D. Winchester, S. Takayama, J. C. Reed and R. I. Morimoto (1998). "BAG-1, a negative regulator of Hsp70 chaperone activity, uncouples nucleotide hydrolysis from substrate release." Embo J **17**(23): 6871-8.

Blond-Elguindi, S., S. E. Cwirla, W. J. Dower, R. J. Lipshutz, S. R. Sprang, J. F. Sambrook and M. J. Gething (1993). "Affinity panning of a library of peptides displayed on bacteriophages reveals the binding specificity of BiP." Cell **75**(4): 717-28.

Bohen, S. P. (1998). "Genetic and biochemical analysis of p23 and ansamycin antibiotics in the function of Hsp90-dependent signaling proteins." Mol Cell Biol **18**(6): 3330-9.

Borkovich, K. A., F. W. Farrelly, D. B. Finkelstein, J. Taulien and S. Lindquist (1989). "hsp82 is an essential protein that is required in higher concentrations for growth of cells at higher temperatures." Mol Cell Biol **9**(9): 3919-30.

Bose, S., T. Weikl, H. Bugl and J. Buchner (1996). "Chaperone function of Hsp90-associated proteins." Science **274**(5293): 1715-7.

Braig, K., Z. Otwinowski, R. Hegde, D. C. Boisvert, A. Joachimiak, A. L. Horwich and P. B. Sigler (1994). "The crystal structure of the bacterial chaperonin GroEL at 2.8 A." Nature **371**(6498): 578-86.

Brinker, A., C. Scheufler, F. Von Der Mulbe, B. Fleckenstein, C. Herrmann, G. Jung, I. Moarefi and F. U. Hartl (2002). "Ligand discrimination by TPR domains. Relevance and selectivity of EEVD-recognition in Hsp70 x Hop x Hsp90 complexes." J Biol Chem **277**(22): 19265-75.

Brychzy, A., T. Rein, K. F. Winklhofer, F. U. Hartl, J. C. Young and W. M. Obermann (2003). "Cofactor Tpr2 combines two TPR domains and a J domain to regulate the Hsp70/Hsp90 chaperone system." Embo J **22**(14): 3613-3623.

Buchberger, A., A. Valencia, R. McMacken, C. Sander and B. Bukau (1994). "The chaperone function of DnaK requires the coupling of ATPase activity with substrate binding through residue E171." Embo J **13**(7): 1687-95.

Buchner, J. (1999). "Hsp90 & Co. - a holding for folding." Trends Biochem Sci **24**(4): 136-41.

Bukau, B., E. Deuerling, C. Pfund and E. A. Craig (2000). "Getting newly synthesized proteins into shape." Cell **101**(2): 119-22.

Bukau, B. and A. L. Horwich (1998). "The Hsp70 and Hsp60 chaperone machines." Cell **92**(3): 351-66.

Cato, A. C. and S. Mink (2001). "BAG-1 family of cochaperones in the modulation of nuclear receptor action." J Steroid Biochem Mol Biol **78**(5): 379-388.

Cayley, S., B. A. Lewis, H. J. Guttman and M. T. Record, Jr. (1991). "Characterization of the cytoplasm of Escherichia coli K-12 as a function of external osmolarity. Implications for protein-DNA interactions in vivo." J Mol Biol **222**(2): 281-300.

Chamberlain, L. H. and R. D. Burgoyne (2000). "Cysteine-string protein: the chaperone at the synapse." J Neurochem **74**(5): 1781-9.

Chang, H. C. and S. Lindquist (1994). "Conservation of Hsp90 macromolecular complexes in Saccharomyces cerevisiae." J Biol Chem **269**(40): 24983-8.

Chang, H. C., D. F. Nathan and S. Lindquist (1997). "In vivo analysis of the Hsp90 cochaperone Sti1 (p60)." Mol Cell Biol **17**(1): 318-25.

Chen, M. S., A. M. Silverstein, W. B. Pratt and M. Chinkers (1996). "The tetratricopeptide repeat domain of protein phosphatase 5 mediates binding to glucocorticoid receptor heterocomplexes and acts as a dominant negative mutant." J Biol Chem **271**(50): 32315-20.

Chen, S. and D. F. Smith (1998). "Hop as an adaptor in the heat shock protein 70 (Hsp70) and hsp90 chaperone machinery." J Biol Chem **273**(52): 35194-200.

Chen, S., W. P. Sullivan, D. O. Toft and D. F. Smith (1998). "Differential interactions of p23 and the TPR-containing proteins Hop, Cyp40, FKBP52 and FKBP51 with Hsp90 mutants." Cell Stress Chaperones **3**(2): 118-29.

Clark, J. I. and P. J. Muchowski (2000). "Small heat-shock proteins and their potential role in human disease." Curr Opin Struct Biol **10**(1): 52-9.

Cloney, L. P., D. R. Bekkaoui, M. G. Wood and S. M. Hemmingsen (1992). "Assessment of plant chaperonin-60 gene function in Escherichia coli." J Biol Chem **267**(32): 23333-6.

Connell, P., C. A. Ballinger, J. Jiang, Y. Wu, L. J. Thompson, J. Hohfeld and C. Patterson (2001). "The co-chaperone CHIP regulates protein triage decisions mediated by heat-shock proteins." Nat Cell Biol **3**(1): 93-6.

Cupp-Vickery, J. R. and L. E. Vickery (2000). "Crystal structure of Hsc20, a J-type Co-chaperone from Escherichia coli." J Mol Biol **304**(5): 835-45.

Dai, K., R. Kobayashi and D. Beach (1996). "Physical interaction of mammalian CDC37 with CDK4." J Biol Chem **271**(36): 22030-4.

Demand, J., S. Alberti, C. Patterson and J. Hohfeld (2001). "Cooperation of a ubiquitin domain protein and an E3 ubiquitin ligase during chaperone/proteasome coupling." Curr Biol **11**(20): 1569-77.

Dinner, A. R., A. Sali, L. J. Smith, C. M. Dobson and M. Karplus (2000). "Understanding protein folding via free-energy surfaces from theory and experiment." Trends Biochem Sci **25**(7): 331-9.

Dittmar, K. D., M. Banach, M. D. Galigniana and W. B. Pratt (1998). "The role of DnaJ-like proteins in glucocorticoid receptor.hsp90 heterocomplex assembly by the reconstituted hsp90.p60.hsp70 foldosome complex." J Biol Chem **273**(13): 7358-66.

Ditzel, L., J. Lowe, D. Stock, K. O. Stetter, H. Huber, R. Huber and S. Steinbacher (1998). "Crystal structure of the thermosome, the archaeal chaperonin and homolog of CCT." Cell **93**(1): 125-38.

Dobson, C. M. and M. Karplus (1999). "The fundamentals of protein folding: bringing together theory and experiment." Curr Opin Struct Biol **9**(1): 92-101.

Dobson, C. M., A. Sali and M. Karplus (1998). Proteinfaltung aus theoretischer und experimenteller Sicht. Angewandte Chemie. **110:** 908-935.

Dougan, D. A., A. Mogk and B. Bukau (2002). "Protein folding and degradation in bacteria: to degrade or not to degrade? That is the question." Cell Mol Life Sci **59**(10): 1607-16.

Dutta, R. and M. Inouye (2000). "GHKL, an emergent ATPase/kinase superfamily." Trends Biochem Sci **25**(1): 24-8.

Elbashir, S. M., J. Harborth, W. Lendeckel, A. Yalcin, K. Weber and T. Tuschl (2001). "Duplexes of 21-nucleotide RNAs mediate RNA interference in cultured mammalian cells." Nature **411**(6836): 494-8.

Ellis, R. J. and F. U. Hartl (1999). "Principles of protein folding in the cellular environment." Curr Opin Struct Biol **9**(1): 102-10.

Ewalt, K. L., J. P. Hendrick, W. A. Houry and F. U. Hartl (1997). "In vivo observation of polypeptide flux through the bacterial chaperonin system." Cell **90**(3): 491-500.

Fang, Y., A. E. Fliss, J. Rao and A. J. Caplan (1998). "SBA1 encodes a yeast hsp90 cochaperone that is homologous to vertebrate p23 proteins." Mol Cell Biol **18**(7): 3727-34.

Feldman, D. E. and J. Frydman (2000). "Protein folding in vivo: the importance of molecular chaperones." Curr Opin Struct Biol **10**(1): 26-33.

Feldman, D. E., V. Thulasiraman, R. G. Ferreyra and J. Frydman (1999). "Formation of the VHL-elongin BC tumor suppressor complex is mediated by the chaperonin TRiC." Mol Cell **4**(6): 1051-61.

Felts, S. J., B. A. Owen, P. Nguyen, J. Trepel, D. B. Donner and D. O. Toft (2000). "The hsp90-related protein TRAP1 is a mitochondrial protein with distinct functional properties." J Biol Chem **275**(5): 3305-12.

Fenton, W. A. and A. L. Horwich (1997). "GroEL-mediated protein folding." Protein Sci **6**(4): 743-60.

Fenton, W. A., Y. Kashi, K. Furtak and A. L. Horwich (1994). "Residues in chaperonin GroEL required for polypeptide binding and release." Nature **371**(6498): 614-9.

Fernandez-Funez, P., M. L. Nino-Rosales, B. de Gouyon, W. C. She, J. M. Luchak, P. Martinez, E. Turiegano, J. Benito, M. Capovilla, P. J. Skinner, A. McCall, I. Canal, H. T. Orr, H. Y. Zoghbi and J. Botas (2000). "Identification of genes that modify ataxin-1-induced neurodegeneration." Nature **408**(6808): 101-6.

Flaherty, K. M., D. B. McKay, W. Kabsch and K. C. Holmes (1991). "Similarity of the three-dimensional structures of actin and the ATPase fragment of a 70-kDa heat shock cognate protein." Proc Natl Acad Sci U S A **88**(11): 5041-5.

Flynn, G. C., T. G. Chappell and J. E. Rothman (1989). "Peptide binding and release by proteins implicated as catalysts of protein assembly." Science **245**(4916): 385-90.

Fontana, J., D. Fulton, Y. Chen, T. A. Fairchild, T. J. McCabe, N. Fujita, T. Tsuruo and W. C. Sessa (2002). "Domain mapping studies reveal that the M domain of hsp90 serves as a molecular scaffold to regulate Akt-dependent phosphorylation of endothelial nitric oxide synthase and NO release." Circ Res **90**(8): 866-73.

Freedman, L. P. (1999). "Increasing the complexity of coactivation in nuclear receptor signaling." Cell **97**(1): 5-8.

Freeman, B. C., S. J. Felts, D. O. Toft and K. R. Yamamoto (2000). "The p23 molecular chaperones act at a late step in intracellular receptor action to differentially affect ligand efficacies." Genes Dev **14**(4): 422-34.

Freeman, B. C. and R. I. Morimoto (1996). "The human cytosolic molecular chaperones hsp90, hsp70 (hsc70) and hdj-1 have distinct roles in recognition of a non-native protein and protein refolding." Embo J **15**(12): 2969-79.

Freeman, B. C., D. O. Toft and R. I. Morimoto (1996). "Molecular chaperone machines: chaperone activities of the cyclophilin Cyp-40 and the steroid aporeceptor-associated protein p23." Science **274**(5293): 1718-20.

Freeman, B. C. and K. R. Yamamoto (2002). "Disassembly of transcriptional regulatory complexes by molecular chaperones." Science **296**(5576): 2232-5.

Frydman, J. (2001). "Folding of newly translated proteins in vivo: the role of molecular chaperones." Annu Rev Biochem **70**: 603-47.

Frydman, J. and J. Hohfeld (1997). "Chaperones get in touch: the Hip-Hop connection." Trends Biochem Sci **22**(3): 87-92.

Frydman, J., E. Nimmesgern, K. Ohtsuka and F. U. Hartl (1994). "Folding of nascent polypeptide chains in a high molecular mass assembly with molecular chaperones." Nature **370**(6485): 111-7.

Gao, B., Y. Emoto, L. Greene and E. Eisenberg (1993). "Nucleotide binding properties of bovine brain uncoating ATPase." J Biol Chem **268**(12): 8507-13.

Gao, Y., J. O. Thomas, R. L. Chow, G. H. Lee and N. J. Cowan (1992). "A cytoplasmic chaperonin that catalyzes beta-actin folding." Cell **69**(6): 1043-50.

Gitler, A. D., Y. Zhu, F. A. Ismat, M. M. Lu, Y. Yamauchi, L. F. Parada and J. A. Epstein (2003). "Nf1 has an essential role in endothelial cells." Nat Genet **33**(1): 75-9.

Glover, J. R. and S. Lindquist (1998). "Hsp104, Hsp70, and Hsp40: a novel chaperone system that rescues previously aggregated proteins." Cell **94**(1): 73-82.

Glover, J. R. and J. M. Tkach (2001). "Crowbars and ratchets: hsp100 chaperones as tools in reversing protein aggregation." Biochem Cell Biol **79**(5): 557-68.

Gupta, R. S. and G. B. Golding (1996). "The origin of the eukaryotic cell." Trends Biochem Sci **21**(5): 166-71.

Ha, J. H. and D. B. McKay (1994). "ATPase kinetics of recombinant bovine 70 kDa heat shock cognate protein and its amino-terminal ATPase domain." Biochemistry **33**(48): 14625-35.

Haas, I. G. and M. Wabl (1983). "Immunoglobulin heavy chain binding protein." Nature **306**(5941): 387-9.

Hanahan, D. (1983). "Studies on transformation of Escherichia coli with plasmids." J Mol Biol **166**(4): 557-80.

Hansen, W. J., N. J. Cowan and W. J. Welch (1999). "Prefoldin-nascent chain complexes in the folding of cytoskeletal proteins." J Cell Biol **145**(2): 265-77.

Hartl, F. U. (1996). "Molecular chaperones in cellular protein folding." Nature **381**(6583): 571-9.

Hartl, F. U. and M. Hayer-Hartl (2002). "Molecular chaperones in the cytosol: from nascent chain to folded protein." Science **295**(5561): 1852-8.

Haslbeck, M., S. Walke, T. Stromer, M. Ehrnsperger, H. E. White, S. Chen, H. R. Saibil and J. Buchner (1999). "Hsp26: a temperature-regulated chaperone." Embo J **18**(23): 6744-51.

Hayer-Hartl, M. K., J. J. Ewbank, T. E. Creighton and F. U. Hartl (1994). "Conformational specificity of the chaperonin GroEL for the compact folding intermediates of alpha-lactalbumin." Embo J **13**(13): 3192-202.

Hayer-Hartl, M. K., J. Martin and F. U. Hartl (1995). "Asymmetrical interaction of GroEL and GroES in the ATPase cycle of assisted protein folding." Science **269**(5225): 836-41.

Hemmingsen, S. M., C. Woolford, S. M. van der Vies, K. Tilly, D. T. Dennis, C. P. Georgopoulos, R. W. Hendrix and R. J. Ellis (1988). "Homologous plant and bacterial proteins chaperone oligomeric protein assembly." Nature **333**(6171): 330-4.

Hohfeld, J. (1998). "Regulation of the heat shock conjugate Hsc70 in the mammalian cell: the characterization of the anti-apoptotic protein BAG-1 provides novel insights." Biol Chem **379**(3): 269-74.

Hohfeld, J. and S. Jentsch (1997). "GrpE-like regulation of the hsc70 chaperone by the anti-apoptotic protein BAG-1." Embo J **16**(20): 6209-16.

Hohfeld, J., Y. Minami and F. U. Hartl (1995). "Hip, a novel cochaperone involved in the eukaryotic Hsc70/Hsp40 reaction cycle." Cell **83**(4): 589-98.

Hollenberg, S. M., V. Giguere, P. Segui and R. M. Evans (1987). "Colocalization of DNA-binding and transcriptional activation functions in the human glucocorticoid receptor." Cell **49**(1): 39-46.

Horwich, A. L., K. B. Low, W. A. Fenton, I. N. Hirshfield and K. Furtak (1993). "Folding in vivo of bacterial cytoplasmic proteins: role of GroEL." Cell **74**(5): 909-17.

Houry, W. A., D. Frishman, C. Eckerskorn, F. Lottspeich and F. U. Hartl (1999). "Identification of in vivo substrates of the chaperonin GroEL." Nature **402**(6758): 147-54.

Huang, K., R. Ghose, J. M. Flanagan and J. H. Prestegard (1999). "Backbone dynamics of the N-terminal domain in E. coli DnaJ determined by 15N- and 13CO-relaxation measurements." Biochemistry **38**(32): 10567-77.

Hutchison, K. A., K. D. Dittmar, M. J. Czar and W. B. Pratt (1994). "Proof that hsp70 is required for assembly of the glucocorticoid receptor into a heterocomplex with hsp90." J Biol Chem **269**(7): 5043-9.

Hutchison, K. A., K. D. Dittmar and W. B. Pratt (1994). "All of the factors required for assembly of the glucocorticoid receptor into a functional heterocomplex with heat shock protein 90 are preassociated in a self-sufficient protein folding structure, a "foldosome"." J Biol Chem **269**(45): 27894-9.

Jakob, U., H. Lilie, I. Meyer and J. Buchner (1995). "Transient interaction of Hsp90 with early unfolding intermediates of citrate synthase. Implications for heat shock in vivo." J Biol Chem **270**(13): 7288-94.

Johnson, B. D., R. J. Schumacher, E. D. Ross and D. O. Toft (1998). "Hop modulates Hsp70/Hsp90 interactions in protein folding." J Biol Chem **273**(6): 3679-86.

Johnson, J. L. and E. A. Craig (1997). "Protein folding in vivo: unraveling complex pathways." Cell **90**(2): 201-4.

Johnson, J. L. and D. O. Toft (1994). "A novel chaperone complex for steroid receptors involving heat shock proteins, immunophilins, and p23." J Biol Chem **269**(40): 24989-93.

Johnson, M. R., J. E. DeClue, S. Felzmann, W. C. Vass, G. Xu, R. White and D. R. Lowy (1994). "Neurofibromin can inhibit Ras-dependent growth by a mechanism independent of its GTPase-accelerating function." Mol Cell Biol **14**(1): 641-5.

Kanelakis, K. C., D. S. Shewach and W. B. Pratt (2002). "Nucleotide binding states of hsp70 and hsp90 during sequential steps in the process of glucocorticoid receptor.hsp90 heterocomplex assembly." J Biol Chem **277**(37): 33698-703.

Karzai, A. W. and R. McMacken (1996). "A bipartite signaling mechanism involved in DnaJ-mediated activation of the Escherichia coli DnaK protein." J Biol Chem **271**(19): 11236-46.

Kazemi-Esfarjani, P. and S. Benzer (2002). "Suppression of polyglutamine toxicity by a Drosophila homolog of myeloid leukemia factor 1." Hum Mol Genet **11**(21): 2657-72.

Kim, T. W. and R. E. Tanzi (1998). "Neuronal intranuclear inclusions in polyglutamine diseases: nuclear weapons or nuclear fallout?" Neuron **21**(4): 657-9.

Kimura, Y., S. L. Rutherford, Y. Miyata, I. Yahara, B. C. Freeman, L. Yue, R. I. Morimoto and S. Lindquist (1997). "Cdc37 is a molecular chaperone with specific functions in signal transduction." Genes Dev **11**(14): 1775-85.

Kimura, Y., I. Yahara and S. Lindquist (1995). "Role of the protein chaperone YDJ1 in establishing Hsp90-mediated signal transduction pathways." Science **268**(5215): 1362-5.

Klumpp, M., W. Baumeister and L. O. Essen (1997). "Structure of the substrate binding domain of the thermosome, an archaeal group II chaperonin." Cell **91**(2): 263-70.

Knoblauch, R. and M. J. Garabedian (1999). "Role for Hsp90-associated cochaperone p23 in estrogen receptor signal transduction." Mol Cell Biol **19**(5): 3748-59.

Kosano, H., B. Stensgard, M. C. Charlesworth, N. McMahon and D. Toft (1998). "The assembly of progesterone receptor-hsp90 complexes using purified proteins." J Biol Chem **273**(49): 32973-9.

Kramer, G., T. Rauch, W. Rist, S. Vorderwulbecke, H. Patzelt, A. Schulze-Specking, N. Ban, E. Deuerling and B. Bukau (2002). "L23 protein functions as a chaperone docking site on the ribosome." Nature **419**(6903): 171-4.

Krobitsch, S. and S. Lindquist (2000). "Aggregation of huntingtin in yeast varies with the length of the polyglutamine expansion and the expression of chaperone proteins." Proc Natl Acad Sci U S A **97**(4): 1589-94.

Laemmli, U. K. (1970). "Cleavage of structural proteins during the assembly of the head of bacteriophage T4." Nature **227**(259): 680-5.

Landry, S. J. (2003). "Structure and energetics of an allele-specific genetic interaction between dnaJ and dnaK: correlation of nuclear magnetic resonance chemical shift perturbations in the J-domain of Hsp40/DnaJ with binding affinity for the ATPase domain of Hsp70/DnaK." Biochemistry **42**(17): 4926-36.

Langer, T., C. Lu, H. Echols, J. Flanagan, M. K. Hayer and F. U. Hartl (1992). "Successive action of DnaK, DnaJ and GroEL along the pathway of chaperone-mediated protein folding." Nature **356**(6371): 683-9.

Leroux, M. R. and F. U. Hartl (2000). "Protein folding: versatility of the cytosolic chaperonin TRiC/CCT." Curr Biol **10**(7): R260-4.

Lewis, V. A., G. M. Hynes, D. Zheng, H. Saibil and K. Willison (1992). "T-complex polypeptide-1 is a subunit of a heteromeric particle in the eukaryotic cytosol." Nature **358**(6383): 249-52.

Liberek, K., J. Marszalek, D. Ang, C. Georgopoulos and M. Zylicz (1991). "Escherichia coli DnaJ and GrpE heat shock proteins jointly stimulate ATPase activity of DnaK." Proc Natl Acad Sci U S A **88**(7): 2874-8.

Lindquist, S. (1986). "The heat-shock response." Annu Rev Biochem **55**: 1151-91.

Lindquist, S. and E. A. Craig (1988). "The heat-shock proteins." Annu Rev Genet **22**: 631-77.

Little, E., M. Ramakrishnan, B. Roy, G. Gazit and A. S. Lee (1994). "The glucose-regulated proteins (GRP78 and GRP94): functions, gene regulation, and applications." Crit Rev Eukaryot Gene Expr **4**(1): 1-18.

Liu, F. H., S. J. Wu, S. M. Hu, C. D. Hsiao and C. Wang (1999). "Specific interaction of the 70-kDa heat shock cognate protein with the tetratricopeptide repeats." J Biol Chem **274**(48): 34425-32.

Liu, X. D., K. A. Morano and D. J. Thiele (1999). "The yeast Hsp110 family member, Sse1, is an Hsp90 cochaperone." J Biol Chem **274**(38): 26654-60.

Llorca, O., J. Martin-Benito, P. Gomez-Puertas, M. Ritco-Vonsovici, K. R. Willison, J. L. Carrascosa and J. M. Valpuesta (2001). "Analysis of the interaction between the eukaryotic chaperonin CCT and its substrates actin and tubulin." J Struct Biol **135**(2): 205-18.

Lotz, G. P., H. Lin, A. Harst and W. M. Obermann (2003). "Aha1 binds to the middle domain of Hsp90, contributes to client protein activation, and stimulates the ATPase activity of the molecular chaperone." J Biol Chem **278**(19): 17228-35.

Louvion, J. F., R. Warth and D. Picard (1996). "Two eukaryote-specific regions of Hsp82 are dispensable for its viability and signal transduction functions in yeast." Proc Natl Acad Sci U S A **93**(24): 13937-42.

Lucast, L. J., R. T. Batey and J. A. Doudna (2001). "Large-scale purification of a stable form of recombinant tobacco etch virus protease." Biotechniques **30**(3): 544-6, 548, 550 passim.

Luders, J., J. Demand and J. Hohfeld (2000). "The ubiquitin-related BAG-1 provides a link between the molecular chaperones Hsc70/Hsp70 and the proteasome." J Biol Chem **275**(7): 4613-7.

Lynch, T. M. and D. H. Gutmann (2002). "Neurofibromatosis 1." Neurol Clin **20**(3): 841-65.

Martin, J., T. Langer, R. Boteva, A. Schramel, A. L. Horwich and F. U. Hartl (1991). "Chaperonin-mediated protein folding at the surface of groEL through a 'molten globule'-like intermediate." Nature **352**(6330): 36-42.

Martin, J., M. Mayhew, T. Langer and F. U. Hartl (1993). "The reaction cycle of GroEL and GroES in chaperonin-assisted protein folding." Nature **366**(6452): 228-33.

Maruya, M., M. Sameshima, T. Nemoto and I. Yahara (1999). "Monomer arrangement in HSP90 dimer as determined by decoration with N and C-terminal region specific antibodies." J Mol Biol **285**(3): 903-7.

Mayer, M. P., R. Nikolay and B. Bukau (2002). "Aha, another regulator for hsp90 chaperones." Mol Cell **10**(6): 1255-6.

Mayer, M. P., H. Schroder, S. Rudiger, K. Paal, T. Laufen and B. Bukau (2000). "Multistep mechanism of substrate binding determines chaperone activity of Hsp70." Nat Struct Biol **7**(7): 586-93.

Mayhew, M., A. C. da Silva, J. Martin, H. Erdjument-Bromage, P. Tempst and F. U. Hartl (1996). "Protein folding in the central cavity of the GroEL-GroES chaperonin complex." Nature **379**(6564): 420-6.

Mayhew, M. and F. U. Hartl (1996). "Lord of the rings: GroES structure." Science **271**(5246): 161-2.

McCarty, J. S., A. Buchberger, J. Reinstein and B. Bukau (1995). "The role of ATP in the functional cycle of the DnaK chaperone system." J Mol Biol **249**(1): 126-37.

McKenna, N. J. and B. W. O'Malley (2002). "Minireview: nuclear receptor coactivators--an update." Endocrinology **143**(7): 2461-5.

Menalled, L. B. and M. F. Chesselet (2002). "Mouse models of Huntington's disease." Trends Pharmacol Sci **23**(1): 32-9.

Meunier, L., Y. K. Usherwood, K. T. Chung and L. M. Hendershot (2002). "A subset of chaperones and folding enzymes form multiprotein complexes in endoplasmic reticulum to bind nascent proteins." Mol Biol Cell **13**(12): 4456-69.

Meyer, P., C. Prodromou, B. Hu, C. Vaughan, S. M. Roe, B. Panaretou, P. W. Piper and L. H. Pearl (2003). "Structural and functional analysis of the middle segment of hsp90: implications for ATP hydrolysis and client protein and cochaperone interactions." Mol Cell **11**(3): 647-58.

Minami, Y., J. Hohfeld, K. Ohtsuka and F. U. Hartl (1996). "Regulation of the heat-shock protein 70 reaction cycle by the mammalian DnaJ homolog, Hsp40." J Biol Chem **271**(32): 19617-24.

Minami, Y., H. Kawasaki, M. Minami, N. Tanahashi, K. Tanaka and I. Yahara (2000). "A critical role for the proteasome activator PA28 in the Hsp90-dependent protein refolding." J Biol Chem **275**(12): 9055-61.

Minami, Y., H. Kawasaki, Y. Miyata, K. Suzuki and I. Yahara (1991). "Analysis of native forms and isoform compositions of the mouse 90-kDa heat shock protein, HSP90." J Biol Chem **266**(16): 10099-103.

Minami, Y., Y. Kimura, H. Kawasaki, K. Suzuki and I. Yahara (1994). "The carboxy-terminal region of mammalian HSP90 is required for its dimerization and function in vivo." Mol Cell Biol **14**(2): 1459-64.

Minton, A. P. (1983). "The effect of volume occupancy upon the thermodynamic activity of proteins: some biochemical consequences." Mol Cell Biochem **55**(2): 119-40.

Mogk, A., T. Tomoyasu, P. Goloubinoff, S. Rudiger, D. Roder, H. Langen and B. Bukau (1999). "Identification of thermolabile Escherichia coli proteins: prevention and reversion of aggregation by DnaK and ClpB." Embo J **18**(24): 6934-49.

Morano, K. A., P. C. Liu and D. J. Thiele (1998). "Protein chaperones and the heat shock response in Saccharomyces cerevisiae." Curr Opin Microbiol **1**(2): 197-203.

Morimoto, R. I. (1998). "Regulation of the heat shock transcriptional response: cross talk between a family of heat shock factors, molecular chaperones, and negative regulators." Genes Dev **12**(24): 3788-96.

Morishima, Y., K. C. Kanelakis, P. J. Murphy, D. S. Shewach and W. B. Pratt (2001). "Evidence for iterative ratcheting of receptor-bound hsp70 between its ATP and ADP conformations during assembly of glucocorticoid receptor.hsp90 heterocomplexes." Biochemistry **40**(4): 1109-16.

Morishima, Y., K. C. Kanelakis, A. M. Silverstein, K. D. Dittmar, L. Estrada and W. B. Pratt (2000). "The Hsp organizer protein hop enhances the rate of but is not essential for glucocorticoid receptor folding by the multiprotein Hsp90-based chaperone system." J Biol Chem **275**(10): 6894-900.

Morishima, Y., P. J. Murphy, D. P. Li, E. R. Sanchez and W. B. Pratt (2000). "Stepwise assembly of a glucocorticoid receptor.hsp90 heterocomplex resolves two sequential ATP-dependent events involving first hsp70 and then hsp90 in opening of the steroid binding pocket." J Biol Chem **275**(24): 18054-60.

Motohashi, K., Y. Watanabe, M. Yohda and M. Yoshida (1999). "Heat-inactivated proteins are rescued by the DnaK.J-GrpE set and ClpB chaperones." Proc Natl Acad Sci U S A **96**(13): 7184-9.

Muchowski, P. J., G. Schaffar, A. Sittler, E. E. Wanker, M. K. Hayer-Hartl and F. U. Hartl (2000). "Hsp70 and hsp40 chaperones can inhibit self-assembly of polyglutamine proteins into amyloid-like fibrils." Proc Natl Acad Sci U S A **97**(14): 7841-6.

Murthy, A. E., A. Bernards, D. Church, J. Wasmuth and J. F. Gusella (1996). "Identification and characterization of two novel tetratricopeptide repeat-containing genes." DNA Cell Biol **15**(9): 727-35.

Nagata, H., W. J. Hansen, B. Freeman and W. J. Welch (1998). "Mammalian cytosolic DnaJ homologues affect the hsp70 chaperone-substrate reaction cycle, but do not interact directly with nascent or newly synthesized proteins." Biochemistry **37**(19): 6924-38.

Nathan, D. F., M. H. Vos and S. Lindquist (1997). "In vivo functions of the Saccharomyces cerevisiae Hsp90 chaperone." Proc Natl Acad Sci U S A **94**(24): 12949-56.

Netzer, W. J. and F. U. Hartl (1997). "Recombination of protein domains facilitated by co-translational folding in eukaryotes." Nature **388**(6640): 343-9.

Netzer, W. J. and F. U. Hartl (1998). "Protein folding in the cytosol: chaperonin-dependent and -independent mechanisms." Trends Biochem Sci **23**(2): 68-73.

Neupert, W. (1997). "Protein import into mitochondria." Annu Rev Biochem **66**: 863-917.

Nicchitta, C. V. (2000). "Role of chaperones in antigen processing." Immunol Invest **29**(2): 101-4.

Nicolet, C. M. and E. A. Craig (1989). "Isolation and characterization of STI1, a stress-inducible gene from Saccharomyces cerevisiae." Mol Cell Biol **9**(9): 3638-46.

Nollen, E. A. and R. I. Morimoto (2002). "Chaperoning signaling pathways: molecular chaperones as stress-sensing 'heat shock' proteins." J Cell Sci **115**(Pt 14): 2809-16.

Obermann, W. M., H. Sondermann, A. A. Russo, N. P. Pavletich and F. U. Hartl (1998). "In vivo function of Hsp90 is dependent on ATP binding and ATP hydrolysis." J Cell Biol **143**(4): 901-10.

Odunuga, O. O., J. A. Hornby, C. Bies, R. Zimmermann, D. J. Pugh and G. L. Blatch (2003). "Tetratricopeptide repeat motif-mediated Hsc70-mSTI1 interaction. Molecular characterization of the critical contacts for successful binding and specificity." J Biol Chem **278**(9): 6896-904.

Onuchic, J. N., Z. Luthey-Schulten and P. G. Wolynes (1997). "Theory of protein folding: the energy landscape perspective." Annu Rev Phys Chem **48**: 545-600.

Owens-Grillo, J. K., M. J. Czar, K. A. Hutchison, K. Hoffmann, G. H. Perdew and W. B. Pratt (1996). "A model of protein targeting mediated by immunophilins and other proteins that bind to hsp90 via tetratricopeptide repeat domains." J Biol Chem **271**(23): 13468-75.

Owens-Grillo, J. K., K. Hoffmann, K. A. Hutchison, A. W. Yem, M. R. Deibel, Jr., R. E. Handschumacher and W. B. Pratt (1995). "The cyclosporin A-binding immunophilin CyP-40 and the FK506-binding immunophilin hsp56 bind to a common site on hsp90 and exist in independent cytosolic heterocomplexes with the untransformed glucocorticoid receptor." J Biol Chem **270**(35): 20479-84.

Panaretou, B., C. Prodromou, S. M. Roe, R. O'Brien, J. E. Ladbury, P. W. Piper and L. H. Pearl (1998). "ATP binding and hydrolysis are essential to the function of the Hsp90 molecular chaperone in vivo." Embo J **17**(16): 4829-36.

Panaretou, B., G. Siligardi, P. Meyer, A. Maloney, J. K. Sullivan, S. Singh, S. H. Millson, P. A. Clarke, S. Naaby-Hansen, R. Stein, R. Cramer, M. Mollapour, P. Workman, P. W. Piper, L. H. Pearl and C. Prodromou (2002). "Activation of the ATPase activity of hsp90 by the stress-regulated cochaperone aha1." Mol Cell **10**(6): 1307-18.

Pande, V. S., A. Grosberg, T. Tanaka and D. S. Rokhsar (1998). "Pathways for protein folding: is a new view needed?" Curr Opin Struct Biol **8**(1): 68-79.

Pande, V. S. and D. S. Rokhsar (1999). "Folding pathway of a lattice model for proteins." Proc Natl Acad Sci U S A **96**(4): 1273-8.

Parks, T. D., K. K. Leuther, E. D. Howard, S. A. Johnston and W. G. Dougherty (1994). "Release of proteins and peptides from fusion proteins using a recombinant plant virus proteinase." Anal Biochem **216**(2): 413-7.

Parsell, D. A. and S. Lindquist (1993). "The function of heat-shock proteins in stress tolerance: degradation and reactivation of damaged proteins." Annu Rev Genet **27**: 437-96.

Pearl, L. H. and C. Prodromou (2000). "Structure and in vivo function of Hsp90." Curr Opin Struct Biol **10**(1): 46-51.

Pellecchia, M., T. Szyperski, D. Wall, C. Georgopoulos and K. Wuthrich (1996). "NMR structure of the J-domain and the Gly/Phe-rich region of the Escherichia coli DnaJ chaperone." J Mol Biol **260**(2): 236-50.

Pfund, C., N. Lopez-Hoyo, T. Ziegelhoffer, B. A. Schilke, P. Lopez-Buesa, W. A. Walter, M. Wiedmann and E. A. Craig (1998). "The molecular chaperone Ssb from Saccharomyces cerevisiae is a component of the ribosome-nascent chain complex." Embo J **17**(14): 3981-9.

Picard, D. (2002). "Heat-shock protein 90, a chaperone for folding and regulation." Cell Mol Life Sci **59**(10): 1640-8.

Pirkl, F. and J. Buchner (2001). "Functional analysis of the Hsp90-associated human peptidyl prolyl cis/trans isomerases FKBP51, FKBP52 and Cyp40." J Mol Biol **308**(4): 795-806.

Porankiewicz, J., J. Wang and A. K. Clarke (1999). "New insights into the ATP-dependent Clp protease: Escherichia coli and beyond." Mol Microbiol **32**(3): 449-58.

Pratt, W. B. (1998). "The hsp90-based chaperone system: involvement in signal transduction from a variety of hormone and growth factor receptors." Proc Soc Exp Biol Med **217**(4): 420-34.

Pratt, W. B. and D. O. Toft (2003). "Regulation of Signaling Protein Function and Trafficking by the hsp90/hsp70-Based Chaperone Machinery." Exp Biol Med (Maywood) **228**(2): 111-33.

Prodromou, C., S. M. Roe, R. O'Brien, J. E. Ladbury, P. W. Piper and L. H. Pearl (1997). "Identification and structural characterization of the ATP/ADP-binding site in the Hsp90 molecular chaperone." Cell **90**(1): 65-75.

Prodromou, C., G. Siligardi, R. O'Brien, D. N. Woolfson, L. Regan, B. Panaretou, J. E. Ladbury, P. W. Piper and L. H. Pearl (1999). "Regulation of Hsp90 ATPase activity by tetratricopeptide repeat (TPR)-domain co-chaperones." Embo J **18**(3): 754-62.

Reimann, B., J. Bradsher, J. Franke, E. Hartmann, M. Wiedmann, S. Prehn and B. Wiedmann (1999). "Initial characterization of the nascent polypeptide-associated complex in yeast." Yeast **15**(5): 397-407.

Robinson, C. V., M. Gross, S. J. Eyles, J. J. Ewbank, M. Mayhew, F. U. Hartl, C. M. Dobson and S. E. Radford (1994). "Conformation of GroEL-bound alpha-lactalbumin probed by mass spectrometry." Nature **372**(6507): 646-51.

Roseman, A. M., S. Chen, H. White, K. Braig and H. R. Saibil (1996). "The chaperonin ATPase cycle: mechanism of allosteric switching and movements of substrate-binding domains in GroEL." Cell **87**(2): 241-51.

Rosenhagen, M. C., J. C. Young, G. M. Wochnik, A. S. Herr, U. Schmidt, F. U. Hartl, F. Holsboer and T. Rein (2001). "Synergistic inhibition of the glucocorticoid receptor by radicicol and benzoquinone ansamycins." Biol Chem **382**(3): 499-504.

Rudiger, S., L. Germeroth, J. Schneider-Mergener and B. Bukau (1997). "Substrate specificity of the DnaK chaperone determined by screening cellulose-bound peptide libraries." Embo J **16**(7): 1501-7.

Rudiger, S., M. P. Mayer, J. Schneider-Mergener and B. Bukau (2000). "Modulation of substrate specificity of the DnaK chaperone by alteration of a hydrophobic arch." J Mol Biol **304**(3): 245-51.

Rudiger, S., J. Schneider-Mergener and B. Bukau (2001). "Its substrate specificity characterizes the DnaJ co-chaperone as a scanning factor for the DnaK chaperone." Embo J **20**(5): 1042-50.

Rye, H. S., S. G. Burston, W. A. Fenton, J. M. Beechem, Z. Xu, P. B. Sigler and A. L. Horwich (1997). "Distinct actions of cis and trans ATP within the double ring of the chaperonin GroEL." Nature **388**(6644): 792-8.

Sakahira, H., P. Breuer, M. K. Hayer-Hartl and F. U. Hartl (2002). "Molecular chaperones as modulators of polyglutamine protein aggregation and toxicity." Proc Natl Acad Sci U S A **99 Suppl 4**: 16412-8.

Sali, A., E. Shakhnovich and M. Karplus (1994). "How does a protein fold?" Nature **369**(6477): 248-51.

Schechter, A. N., R. F. Chen and C. B. Anfinsen (1970). "Kinetics of folding of staphylococcal nuclease." Science **167**(919): 886-7.

Scheibel, T., S. Neuhofen, T. Weikl, C. Mayr, J. Reinstein, P. D. Vogel and J. Buchner (1997). "ATP-binding properties of human Hsp90." J Biol Chem **272**(30): 18608-13.

Scheibel, T., T. Weikl and J. Buchner (1998). "Two chaperone sites in Hsp90 differing in substrate specificity and ATP dependence." Proc Natl Acad Sci U S A **95**(4): 1495-9.

Scheufler, C., A. Brinker, G. Bourenkov, S. Pegoraro, L. Moroder, H. Bartunik, F. U. Hartl and I. Moarefi (2000). "Structure of TPR domain-peptide complexes: critical elements in the assembly of the Hsp70-Hsp90 multichaperone machine." Cell **101**(2): 199-210.

Schmid, D., A. Baici, H. Gehring and P. Christen (1994). "Kinetics of molecular chaperone action." Science **263**(5149): 971-3.

Schmidt, U., G. M. Wochnik, M. C. Rosenhagen, J. C. Young, F. U. Hartl, F. Holsboer and T. Rein (2003). "Essential role of the unusual DNA-binding motif of BAG-1 for inhibition of the glucocorticoid receptor." J Biol Chem **278**(7): 4926-31.

Schneider, C., L. Sepp-Lorenzino, E. Nimmesgern, O. Ouerfelli, S. Danishefsky, N. Rosen and F. U. Hartl (1996). "Pharmacologic shifting of a balance between protein refolding and degradation mediated by Hsp90." Proc Natl Acad Sci U S A **93**(25): 14536-41.

Schneikert, J., S. Hubner, G. Langer, T. Petri, M. Jaattela, J. Reed and A. C. Cato (2000). "Hsp70-RAP46 interaction in downregulation of DNA binding by glucocorticoid receptor." Embo J **19**(23): 6508-16.

Schroder, H., T. Langer, F. U. Hartl and B. Bukau (1993). "DnaK, DnaJ and GrpE form a cellular chaperone machinery capable of repairing heat-induced protein damage." Embo J **12**(11): 4137-44.

Schultz, C. P. (2000). "Illuminating folding intermediates." Nat Struct Biol **7**(1): 7-10.

Schulz, A., S. Schwab, G. Homuth, S. Versteeg and W. Schumann (1997). "The htpG gene of Bacillus subtilis belongs to class III heat shock genes and is under negative control." J Bacteriol **179**(10): 3103-9.

Siegers, K., T. Waldmann, M. R. Leroux, K. Grein, A. Shevchenko, E. Schiebel and F. U. Hartl (1999). "Compartmentation of protein folding in vivo: sequestration of non-native polypeptide by the chaperonin-GimC system." Embo J **18**(1): 75-84.

Sikorski, R. S., M. S. Boguski, M. Goebl and P. Hieter (1990). "A repeating amino acid motif in CDC23 defines a family of proteins and a new relationship among genes required for mitosis and RNA synthesis." Cell **60**(2): 307-17.

Silverstein, A. M., M. D. Galigniana, K. C. Kanelakis, C. Radanyi, J. M. Renoir and W. B. Pratt (1999). "Different regions of the immunophilin FKBP52 determine its association with the glucocorticoid receptor, hsp90, and cytoplasmic dynein." J Biol Chem **274**(52): 36980-6.

Silverstein, A. M., N. Grammatikakis, B. H. Cochran, M. Chinkers and W. B. Pratt (1998). "p50(cdc37) binds directly to the catalytic domain of Raf as well as to a site on hsp90 that is topologically adjacent to the tetratricopeptide repeat binding site." J Biol Chem **273**(32): 20090-5.

Smith, D. F. (1993). "Dynamics of heat shock protein 90-progesterone receptor binding and the disactivation loop model for steroid receptor complexes." Mol Endocrinol **7**(11): 1418-29.

Smith, D. F., B. A. Stensgard, W. J. Welch and D. O. Toft (1992). "Assembly of progesterone receptor with heat shock proteins and receptor activation are ATP mediated events." J Biol Chem **267**(2): 1350-6.

Smith, D. F., L. Whitesell, S. C. Nair, S. Chen, V. Prapapanich and R. A. Rimerman (1995). "Progesterone receptor structure and function altered by geldanamycin, an hsp90-binding agent." Mol Cell Biol **15**(12): 6804-12.

Sokolenko, A., S. Lerbs-Mache, L. Altschmied and R. G. Herrmann (1998). "Clp protease complexes and their diversity in chloroplasts." Planta **207**(2): 286-95.

Sondermann, H., A. K. Ho, L. L. Listenberger, K. Siegers, I. Moarefi, S. R. Wente, F. U. Hartl and J. C. Young (2002). "Prediction of novel Bag-1 homologs based on structure/function analysis identifies Snl1p as an Hsp70 co-chaperone in Saccharomyces cerevisiae." J Biol Chem **277**(36): 33220-7.

Sondermann, H., C. Scheufler, C. Schneider, J. Hohfeld, F. U. Hartl and I. Moarefi (2001). "Structure of a Bag/Hsc70 complex: convergent functional evolution of Hsp70 nucleotide exchange factors." Science **291**(5508): 1553-7.

Song, H. Y., J. D. Dunbar, Y. X. Zhang, D. Guo and D. B. Donner (1995). "Identification of a protein with homology to hsp90 that binds the type 1 tumor necrosis factor receptor." J Biol Chem **270**(8): 3574-81.

Soti, C. and P. Csermely (2002). "Chaperones and aging: role in neurodegeneration and in other civilizational diseases." Neurochem Int **41**(6): 383-9.

Stebbins, C. E., A. A. Russo, C. Schneider, N. Rosen, F. U. Hartl and N. P. Pavletich (1997). "Crystal structure of an Hsp90-geldanamycin complex: targeting of a protein chaperone by an antitumor agent." Cell **89**(2): 239-50.

Stepanova, L., X. Leng, S. B. Parker and J. W. Harper (1996). "Mammalian p50Cdc37 is a protein kinase-targeting subunit of Hsp90 that binds and stabilizes Cdk4." Genes Dev **10**(12): 1491-502.

Sternlicht, H., G. W. Farr, M. L. Sternlicht, J. K. Driscoll, K. Willison and M. B. Yaffe (1993). "The t-complex polypeptide 1 complex is a chaperonin for tubulin and actin in vivo." Proc Natl Acad Sci U S A **90**(20): 9422-6.

Stuart, R. A., D. M. Cyr and W. Neupert (1994). "Hsp70 in mitochondrial biogenesis: from chaperoning nascent polypeptide chains to facilitation of protein degradation." Experientia **50**(11-12): 1002-11.

Sullivan, W., B. Stensgard, G. Caucutt, B. Bartha, N. McMahon, E. S. Alnemri, G. Litwack and D. Toft (1997). "Nucleotides and two functional states of hsp90." J Biol Chem **272**(12): 8007-12.

Szabo, A., R. Korszun, F. U. Hartl and J. Flanagan (1996). "A zinc finger-like domain of the molecular chaperone DnaJ is involved in binding to denatured protein substrates." Embo J **15**(2): 408-17.

Szabo, A., T. Langer, H. Schroder, J. Flanagan, B. Bukau and F. U. Hartl (1994). "The ATP hydrolysis-dependent reaction cycle of the Escherichia coli Hsp70 system DnaK, DnaJ, and GrpE." Proc Natl Acad Sci U S A **91**(22): 10345-9.

Takayama, S., D. N. Bimston, S. Matsuzawa, B. C. Freeman, C. Aime-Sempe, Z. Xie, R. I. Morimoto and J. C. Reed (1997). "BAG-1 modulates the chaperone activity of Hsp70/Hsc70." Embo J **16**(16): 4887-96.

Tanaka, N. and H. Nakamoto (1999). "HtpG is essential for the thermal stress management in cyanobacteria." FEBS Lett **458**(2): 117-23.

Taniuchi, H. and C. B. Anfinsen (1969). "An experimental approach to the study of the folding of staphylococcal nuclease." J Biol Chem **244**(14): 3864-75.

Teter, S. A., W. A. Houry, D. Ang, T. Tradler, D. Rockabrand, G. Fischer, P. Blum, C. Georgopoulos and F. U. Hartl (1999). "Polypeptide flux through bacterial Hsp70:

DnaK cooperates with trigger factor in chaperoning nascent chains." Cell **97**(6): 755-65.

Theyssen, H., H. P. Schuster, L. Packschies, B. Bukau and J. Reinstein (1996). "The second step of ATP binding to DnaK induces peptide release." J Mol Biol **263**(5): 657-70.

Trent, J. D., E. Nimmesgern, J. S. Wall, F. U. Hartl and A. L. Horwich (1991). "A molecular chaperone from a thermophilic archaebacterium is related to the eukaryotic protein t-complex polypeptide-1." Nature **354**(6353): 490-3.

Tsai, J. and M. G. Douglas (1996). "A conserved HPD sequence of the J-domain is necessary for YDJ1 stimulation of Hsp70 ATPase activity at a site distinct from substrate binding." J Biol Chem **271**(16): 9347-54.

Ungewickell, E., H. Ungewickell, S. E. Holstein, R. Lindner, K. Prasad, W. Barouch, B. Martin, L. E. Greene and E. Eisenberg (1995). "Role of auxilin in uncoating clathrin-coated vesicles." Nature **378**(6557): 632-5.

Vainberg, I. E., S. A. Lewis, H. Rommelaere, C. Ampe, J. Vandekerckhove, H. L. Klein and N. J. Cowan (1998). "Prefoldin, a chaperone that delivers unfolded proteins to cytosolic chaperonin." Cell **93**(5): 863-73.

van der Straten, A., C. Rommel, B. Dickson and E. Hafen (1997). "The heat shock protein 83 (Hsp83) is required for Raf-mediated signalling in Drosophila." Embo J **16**(8): 1961-9.

Versteeg, S., A. Mogk and W. Schumann (1999). "The Bacillus subtilis htpG gene is not involved in thermal stress management." Mol Gen Genet **261**(3): 582-8.

Vijayalakshmi, J., M. K. Mukhergee, J. Graumann, U. Jakob and M. A. Saper (2001). "The 2.2 A crystal structure of Hsp33: a heat shock protein with redox-regulated chaperone activity." Structure (Camb) **9**(5): 367-75.

Wall, D., M. Zylicz and C. Georgopoulos (1994). "The NH2-terminal 108 amino acids of the Escherichia coli DnaJ protein stimulate the ATPase activity of DnaK and are sufficient for lambda replication." J Biol Chem **269**(7): 5446-51.

Wallace, A. D. and J. A. Cidlowski (2001). "Proteasome-mediated glucocorticoid receptor degradation restricts transcriptional signaling by glucocorticoids." J Biol Chem **276**(46): 42714-21.

Warrick, J. M., H. Y. Chan, G. L. Gray-Board, Y. Chai, H. L. Paulson and N. M. Bonini (1999). "Suppression of polyglutamine-mediated neurodegeneration in Drosophila by the molecular chaperone HSP70." Nat Genet **23**(4): 425-8.

Wawrzynow, A., B. Banecki and M. Zylicz (1996). "The Clp ATPases define a novel class of molecular chaperones." Mol Microbiol **21**(5): 895-9.

Welch, W. J. and J. R. Feramisco (1982). "Purification of the major mammalian heat shock proteins." J Biol Chem **257**(24): 14949-59.

Wessel, D. and U. I. Flugge (1984). "A method for the quantitative recovery of protein in dilute solution in the presence of detergents and lipids." Anal Biochem **138**(1): 141-3.

Whitesell, L., E. G. Mimnaugh, B. De Costa, C. E. Myers and L. M. Neckers (1994). "Inhibition of heat shock protein HSP90-pp60v-src heteroprotein complex formation by benzoquinone ansamycins: essential role for stress proteins in oncogenic transformation." Proc Natl Acad Sci U S A **91**(18): 8324-8.

Wickner, R. B., K. L. Taylor, H. K. Edskes, M. L. Maddelein, H. Moriyama and B. T. Roberts (2000). "Prions of yeast as heritable amyloidoses." J Struct Biol **130**(2-3): 310-22.

Wiederkehr, T., B. Bukau and A. Buchberger (2002). "Protein turnover: a CHIP programmed for proteolysis." Curr Biol **12**(1): R26-8.

Xu, Y. and S. Lindquist (1993). "Heat-shock protein hsp90 governs the activity of pp60v-src kinase." Proc Natl Acad Sci U S A **90**(15): 7074-8.

Xu, Z., A. L. Horwich and P. B. Sigler (1997). "The crystal structure of the asymmetric GroEL-GroES-(ADP)7 chaperonin complex." Nature **388**(6644): 741-50.

Yang, X., G. Chernenko, Y. Hao, Z. Ding, M. M. Pater, A. Pater and S. C. Tang (1998). "Human BAG-1/RAP46 protein is generated as four isoforms by alternative translation initiation and overexpressed in cancer cells." Oncogene **17**(8): 981-9.

Yoshimune, K., T. Yoshimura, T. Nakayama, T. Nishino and N. Esaki (2002). "Hsc62, Hsc56, and GrpE, the third Hsp70 chaperone system of Escherichia coli." Biochem Biophys Res Commun **293**(5): 1389-95.

Young, J. C. and F. U. Hartl (2000). "Polypeptide release by Hsp90 involves ATP hydrolysis and is enhanced by the co-chaperone p23." Embo J **19**(21): 5930-40.

Young, J. C., N. J. Hoogenraad and F. U. Hartl (2003). "Molecular chaperones hsp90 and hsp70 deliver preproteins to the mitochondrial import receptor tom70." Cell **112**(1): 41-50.

Young, J. C., I. Moarefi and F. U. Hartl (2001). "Hsp90: a specialized but essential protein-folding tool." J Cell Biol **154**(2): 267-73.

Young, J. C., W. M. Obermann and F. U. Hartl (1998). "Specific binding of tetratricopeptide repeat proteins to the C-terminal 12-kDa domain of hsp90." J Biol Chem **273**(29): 18007-10.

Young, J. C., C. Schneider and F. U. Hartl (1997). "In vitro evidence that hsp90 contains two independent chaperone sites." FEBS Lett **418**(1-2): 139-43.

Zhu, X., X. Zhao, W. F. Burkholder, A. Gragerov, C. M. Ogata, M. E. Gottesman and W. A. Hendrickson (1996). "Structural analysis of substrate binding by the molecular chaperone DnaK." Science **272**(5268): 1606-14.

Zimmerman, S. B. and A. P. Minton (1993). "Macromolecular crowding: biochemical, biophysical, and physiological consequences." Annu Rev Biophys Biomol Struct **22**: 27-65.

Zimmerman, S. B. and S. O. Trach (1991). "Estimation of macromolecule concentrations and excluded volume effects for the cytoplasm of Escherichia coli." J Mol Biol **222**(3): 599-620.

Zimmermann, R. (1998). "The role of molecular chaperones in protein transport into the mammalian endoplasmic reticulum." Biol Chem **379**(3): 275-82.

Zolkiewski, M. (1999). "ClpB cooperates with DnaK, DnaJ, and GrpE in suppressing protein aggregation. A novel multi-chaperone system from Escherichia coli." J Biol Chem **274**(40): 28083-6.

Zwanzig, R., A. Szabo and B. Bagchi (1992). "Levinthal's paradox." Proc Natl Acad Sci U S A **89**(1): 20-2.

8 Abbreviations

(v/v)	volume per volume
(w/v)	weight per volume
μ	micro ($*10^{-6}$)
AA/BisAA	acrylamide / bis-acrylamide
Ac	acetate
ADP	adenosine 5'-diphosphate
APS	ammonium persulphate
ATP	adenosine 5'-triphosphate
Bag	Bcl2-associated athanogene
	eukaryotic nucleotide exchange factor for Hsp70
BIA(core)	biomolecular interaction analysis
C. elegans	*Caenorhabditis elegans*
C70 / C90	carboxyl terminal domaine of Hsp70 / Hsp90
C70-12	Hsp70 C-terminal tridecapeptide
	Ac-C-GSGSGPTIEEVD-COOH
C90-12	Hsp90 C-terminal tridecapeptide
	Ac-C-GDDDTSRMEEVD-COOH
CCT	chaperone-containing TCP-1
CHIP	carboxyl-terminus Hsc70 interacting protein
CIP	calf intestinal phosphatase
Cyp	cyclophiline
Da	dalton
dd H_2O	double destilled water
DMSO	dimethylsulfoxide
DNA	desoxyribonucleic acid
DnaJ	prokaryotic Hsp40 chaperone
DnaK	prokaryotic Hsp70 chaperone
dNTP	didesoxy-nucleoside triphosphate
ds	double strand
dTPR2	drosphila TPR2 protein
E. coli	*Escherichia coli*
EDTA	ethylenediaminetetraacetic acid
ER	endoplasmatic reticulum
EtOH	ethanol
FBS	fetal bovine serum
FKBP	FK-506 binding protein
FPLC	fast performance liquid chromatogaphy
g	gram
G protein	guaninnucleotide binding protein
GA	geldananmycin
GimC / prefoldin	genes involved in microtubule biogenesis
GroEL	procaryotic Hsp60 chaperonine
GroES	procaryotic Hsp10 chaperonine
GrpE	procaryotic nucleotide exchange factor for DnaK
Hdj2	human Hsp40 chaperone

HEPES	N-(2-hydroxyethyl)piperazine-N'-(2-ethanesulfonic acid)
Hip	Hsc70 interacting protein
Hop	heat shock protein organizing protein
Hop / p60	Hsp70-Hsp90organizing protein
Hsc	heat shock cognate protein
Hsp	heat shock protein
HtpG	procaryotic Hsp90
Tpr2	human TPR2 protein
IPTG	isopropyl-β-D-thiogalactopyranoside
J-domain	Hsp70 ATPase stimulating domain of Hsp40
k	kilo (*10^3)
K_D	thermodynamic dissociation constant
l	liter
LB	Luria-Bertani
LBD	ligand binding domain
M	molar
m	milli (*10^{-3})
MDJ1	mitochondrial Hsp40
MeOH	methanol
MgAc$_2$	magnesium acetate
min	minutes
MW	molecular weight
n	nano (*10^{-9})
OD	optical density
PAGE	polyacrylamide gelelectrophoresis
PBS	phosphate buffered saline
PCR	polymerase chain reaction
PEI	polythyleneimine
P_i	inorganic phosphate
PP5	protein-Ser/Thr-phosphatase 5
RA	radicycol
R_{eq}	SPR signal during equilibrium binding
RT	room temperature
S. pombe	*Schizosaccharomyces pombe*
S. cerevisiae	*Saccharomyces cerevisiae*
SCJ1	Hsp40 chaperone in the ER
SDS	sodium dodecylsulfate
sec	seconds
SHR	steroid hormone receptor
SPR	surface plasmon resonance
Ssa, Ssb, Ssc	Hsp70 chaperone in yeast
STI1	p60/Hop homolog in rodents
$t_{1/2}$	half time
TAE	Tris / acetate / EDTA buffer
TB	terrific broth
TCP-1	T-complex contained protein 1
TEMED	N,N,N',N'-tetramethylethylendiamine
TEV	tobacco etch virus
TF	trigger factor

TLC	thin layer chromatography
TPR	tetratrico peptide repeat
TriC / CCT	TCP-1 ring complex / chaperonin containing TCP-1 eukaryotic, cytoplasmatic Hsp60 chaperonin
Tris	Tris(hydroxymethyl)aminomethane
U	unit

Lebenslauf

Alexander Brychzy

geboren am 16.07.1970
in Hof an der Saale

Schule

1977 - 1990   **Grundschule und Gymnasium, Hof**
Abschluss: allgemeine Hochschulreife

Militärdienst

1990 - 1991   **Bundeswehr, Weiden**

Studium

10/1991 - 12/1997   **Universität Bayreuth, Studiengang Biologie Diplom**

SS 94   Vordiplom in allgemeiner Biologie, Genetik, organischer Chemie und Mathematik

WS 94/95   University of York, ERASMUS Austauschstudent
Thema: "Nuclear DNA Content and Composition in *Poa annua*"
Betreuer: Dr. Susan M. Bougourd und Dr. Richard Law

SS 95   Mitarbeiterpraktikum am Lehrstuhl Genetik
Thema: „Identifikation von Bodenbakterien mittels PCR-Fingerprinting"
Betreuerin: Dr. Sonja Selenska-Pobell

SS 96   Praktikum an der Biologischen Bundesanstalt Braunschweig
Thema: „Analyse nicht kultivierbarer Bodenbakterien"
Betreuer: Prof. Dr. Backhaus

WS 96/97   mündliche Diplomprüfung in Genetik, Mikrobiologie und ökologischer Chemie

SS 97   Diplomarbeit im Fachbereich Genetik
Thema: „Analyse pH-regulierter Gene bei *Bacillus subtilis*"
Betreuer: Prof. Dr. Wolfgang Schumann

WS 97/98   Studienabschluss: Diplom-Biologe Univ.

Promotion

04/1998 - 12/1998   MPI für Biochemie in Martinsried, AG Molekulare Onkologie
Thema: „Funktionsanalyse des CBC-VHL Komplexes im Zellzyklus"
Betreuer: Dr. Arnim Pause

01/1999 – 10/2003   MPI für Biochemie in Martinsried, Abteilung Zelluläre Biochemie
Thema: „Characterisation of Tpr2, a Novel Regulator of the Hsp70/Hsp90 Multichaperone Complex"
Betreuer: Prof. Dr. F. Ulrich Hartl

Danksagung

Mein besonderer Dank gilt Prof. Dr. F. Ulrich Hartl für seine uneingeschränkte Kollegialität, sein stetes Interesse am Fortgang der Arbeit und für die Bereitstellung der hervorragenden Arbeitsbedingungen.

Prof. Dr. Wolfgang Baumeister danke ich sehr für die Vertretung der Doktorarbeit vor der Fakultät der Technischen Universität München.

Sehr herzlich möchte ich mich bei meinem Betreuer Jason Young bedanken, der mit seiner außerordentlichen fachlichen Kompetenz und intensiven Betreuung das Gelingen der Arbeit erst ermöglichte. Er ist ein hervorragender Lehrer und ich hoffe, dass seine Talente noch vielen anderen Studenten zur Verfügung stehen werden.

Ebenfalls bedanken möchte ich mich bei Wolfgang Obermann für die Überlassung des spannenden Themas, seinen Beitrag zur Finanzierung meiner Stelle und für viele motivierende Gespräche.

Meinen Kollegen Gregor Schaffar, und Tanja Büsgen danke ich für ihre Freundschaft und für ein sehr außergewöhnliches erstes Jahr am MPI. Auch wenn wir jetzt getrennte Wege gehen, hoffe ich, dass wir uns mal wieder zum Schnitzelessen verabreden werden.

Peter Breuer danke ich für seine Bemühungen mir etwas über das Leben im allgemeinen und das Laborleben im besonderen beizubringen. Ich vermute leider, dass ich bei all den genuschelten Antworten nur die Hälfte verstanden habe.

Für die vielen Stunden, die ihr mich bei der Computerarbeit unterstützt habt und auch für die anregenden Diskussionen über D2 Techniken bedanke ich mich bei Dirk Wischnewski und Ulrich Heller. Danke auch an Michael Kerner, der immer ein offenes Ohr für meine technischen Fragen hatte.